# Uniform-Electric-Field-Approximation Based Modelling of Longitudinal Piezoelectric Transducers

Yangkun Zhang

The University of Adelaide

School of Mechanical Engineering

The University of Adelaide

Australia

A thesis submitted in fulfilment of the requirements for the degree of
Doctor of Philosophy

July 18, 2016

# Abstract

Longitudinal piezoelectric transducers (LPT), which collectively refer to piezoelectric actuators, vibrators, sensors and actuators designed for longitudinal deformations or vibrations, are the most widely used piezoelectric devices. LPT model, which can be used to predict the behavior or performance in time/frequency domain, plays a vital role in the design and optimization of these LPT-based applications. Existing models which can be used for dynamic behavior prediction, are based on the complex electro-mechanical coupled fundamentals of piezoelectricity, which involves a complex position-varying electric field. Therefore, solving these models for the design and optimization of LPT-based applications is very computationally inefficient.

After initial extensive investigations of possible effective simplifications in the complex fundamentals for modeling LPT, it is found that the electric field in LPT could be effectively approximated to be uniform (i.e. electric field is independent of its position) and this approximation could greatly simplify and facilitate the modeling of LPT-based applications. Therefore, the aim of this research is to study the uniform-electric-field approximation in simplifying the analysis, modelling and calculations of LPT for facilitating design and optimization of the LPT-based applications. LPT can, in principle, be divided into d31-mode LPT and d33-mode LPT. Both types are investigated in this thesis work.

The main contributions of this thesis work are presented in 6 chapters, with each based on an individual scientific paper.

*Paper 1* presents the rationale behind the uniform-electric-field-approximation for d33-mode LPT together with its scope and limitation. Then, based on the approximation, novel simplified fundamentals of both simple-layer-type and stack-type d33-mode LPT are formulated, which could provide a very simple analytical solution, especially for the stack-type.

To facilitate the modeling of free and loaded vibration of d33-mode LPT in a more straightforward way, a simple equivalent circuit is presented in *Paper 2*. The presented circuit is inspired by the network theory and formulated exactly based on the simplified fundamentals of d33-mode LPT presented in *Paper 1*.

In many LPT-based applications, LPT are joined with other layers, such as backing layers and propagating layers. For the calculations and analysis of a multilayer structure, a transfer matrix method is always used. Therefore, to further facilitate the calculation when LPT are joined with other layers, the simplified fundamentals of LPT in *Paper 1* is wrapped into a transfer matrix form as detailed in *Paper 3*.

When LPT are used in a complex structure, a finite element model is widely applied for computation and analysis. Based on the uniform-electric-field-approximation, two simple equivalent finite element models of LPT are presented in *Paper 4*, which can largely simplify the modeling process and reduce the computational efforts of direct finite element modeling of LPT.

Then, *Paper 5* presents the rationale behind the uniform-electric-field-approximation for d31-mode LPT, which is different in nature to those of d33-mode. Also, an equivalent mixing method is proposed to consider electrode and adhesive layers within d31-mode LPT. The related equivalent circuit and transfer matrix of d31-mode LPT are formulated.

Inspired by d33-mode, *Paper 6* presents simple equivalent finite element models of d31-mode LPT.

# Declarations

I certify that this work contains no material which has been accepted for the award of any other degree or diploma in my name, in any university or other tertiary institution and, to the best of my knowledge and belief, contains no material previously published or written by another person, except where due reference has been made in the text. In addition, I certify that no part of this work will, in the future, be used in a submission in my name, for any other degree or diploma in any university or other tertiary institution without the prior approval of the University of Adelaide and where applicable, any partner institution responsible for the joint-award of this degree.

I give consent to this copy of my thesis when deposited in the University Library, being made available for loan and photocopying, subject to the provisions of the Copyright Act 1968.

The author acknowledges that copyright of published works contained within this thesis resides with the copyright holder(s) of those works.

I also give permission for the digital version of my thesis to be made available on the web, via the University digital research repository, the Library Search and also through web search engines, unless permission has been granted by the University to restrict access for a period of time.

SIGNED: ...................... DATE: ......................

# List of Publications

This thesis is not written in the conventional narrative format but in the publication format as a portfolio of publications either published or submitted for publication by peer-reviewed journals according to the 'Academic Program Rules' of the University of Adelaide. The research outcomes of this thesis have results in the generation of 6 either published or submitted journal papers and 2 refereed conference papers which are listed below:

Journal Papers

*Paper 1* Zhang, Y., Lu, T. F., & Al-Sarawi, S. (2015). Formulation of a simple distributed-parameter model of multilayer piezoelectric actuators. *Journal of Intelligent Material Systems and Structures*, 1045389X15595294.

*Paper 2* Zhang, Y., Lu, T. F., & Peng, Y. (2015). Three-port equivalent circuit of multi-layer piezoelectric stack. *Sensors and Actuators A: Physical*, 236, 92-97.

*Paper 3* Zhang, Y., Lu, T. F., Al-Sarawi, S., Tu, Z. (2016). A Simplified Transfer Matrix of Multi-layer Piezoelectric Stack. *Journal of Intelligent Material Systems and Structures*, 1045389X16651153.

*Paper 4* Zhang, Y., & Lu, T. F. (2016). Simple Equivalent Finite Element Models of D33-Mode Multi-layer Piezoelectric Actuator, submitted to *Smart Materials and Structures*

*Paper 5* Zhang, Y., Lu, T. F., & GAO, W. (2016). Model D31-mode Longitudinal Piezoelectric Transducers. Submitted to *Sensors and Actuators A: Physical*

*Paper 6* Zhang, Y., Lu, T. F., & Al-Sarawi, S. (2016). Simple Equivalent Finite Element Models of D31-Mode Multi-Layer Piezoelectric Actuator. Submitted to *Journal of Intelligent Material Systems and Structures*

Conference Papers

Conference-1 Yangkun Zhang and Tien-Fu Lu 2014, 'Investigation on the Uniform-Electrical-Field Assumption for Modeling multi-layer piezoelectric actuators', *8th Asia International conference on Mathematical Modeling and computer simulation*, 23-25 September, Taipei, Taiwan, page 251-254

Conference-2 Yangkun Zhang and Tien-Fu Lu 2014, 'A Simple Distributed Parameter Analytical Model of Multi-layer Piezoelectric Actuator', *8th Asia International conference on Mathematical Modeling and computer simulation*, 23-25 September, Taipei, Taiwan, page 247-250

# Acknowledgements

# Table of Contents

# Chapter 1

# Introduction

# CHAPTER 1

# INTRODUCTION

## 1.1  Overview

Piezoelectricity is a fascinating property of many natural and synthetic materials that can directly transform electrical energy into mechanical energy and vice versa. The intriguing phenomenon of piezoelectricity demonstrates various ingredients to arouse inspirations and innovations of physicists and engineers, thus enabling numerous revolutionary opportunities and a huge technological development in the recent decades. In 2010, the global demand for piezoelectric devices was reported to be valued at about 14.8 billion US dollars [1].

The most widely used piezoelectric devices are longitudinal piezoelectric transducers (LPT), which collectively refer to piezoelectric actuators, vibrators, sensors and actuators associated designed for longitudinal deformation or vibrations. Compared with other types of piezoelectric transducers such as bending and shear piezoelectric transducers, LPT provides a larger stiffness, a larger operation bandwidth, more simple and compact structure and more direct energy conversion, thus enabling a large output force and fast response in actuator and vibrator applications, high transient response for sensor applications, and a high mechanical-to-electrical energy conversion efficiency for energy harvesting applications. Consequently, they cover a wide range of applications such as nano-positioning [2-4], ultrasonic cleaning [5], acoustic imaging [6,7] and non-destructive testing[8], especially in the field of automation, biotechnology, information and communication, manufacturing, and defense industry.

For these LPT-based applications, modelling of LPT, which can be used to predict the behavior or performance in time/frequency domain, plays a vital role in their design and optimization. For example, based on modelling, designers can explore possible transducer configurations prior to fabrication, thus greatly cutting down the design period and design cost. Existing models which can be used for dynamic behavior prediction, are based on the complex electro-mechanical coupled fundamentals of piezoelectricity, which involves a complex position-varying electric field. Therefore,

solving these models for design and optimization of LPT-based applications is very computationally inefficient.

## 1.2 Aims and Objectives

After initial extensive investigations of possible effective simplifications in the complex fundamentals for modeling LPT, it is found that the electric field in LPT could be effectively approximated to be uniform (i.e. electric field could be effectively approximated independent of its position) and this approximation could greatly simplify and facilitate the modeling of LPT-based applications. Therefore, the aim of this research is to study the uniform-electric-field approximation in simplifying the analysis, modelling and calculations of LPT for facilitating design and optimization of the LPT-based applications. LPT can, in principle, be divided into d31-mode LPT and d33-mode LPT. Both types are investigated in this thesis work.

The objectives of this research are:

➢ Investigate the rationales behind the uniform-electric-field approximation respectively for d33-mode LPT and d31-mode LPT together with their corresponding scopes and limitations;

➢ Derive the uniform-electric-field-approximation based simplified fundamentals of d33-mode LPT and d31-mode LPT for both sing-layer type and stack type;

➢ Develop simple equivalent circuits based on the simplified fundamentals of d31-mode LPT and d33-mode LPT to facilitate the analysis and modelling in a straightforward way;

➢ Develop simple transfer matrix formalism of d31-mode LPT and d33-mode LPT to facilitate the calculation when they are used in a multi-layer stacked structure; and

➢ Develop simple finite element models of d31-mode LPT and d33-mode LPT to facilitate their calculation when they are used in a complex structure.

## 1.3 Preview of the thesis

Chapter 2 provides a general background, literature review, and research gaps. Then, to address the identified research gaps, 6 journal papers are respectively presented from Chapter 3 to Chapter 8. Chapter 9 presents the conclusions and future work. In addition, two conference papers, which are also relevant to the present work, are included in the appendix.

## References

[1] Intelligence, A. M. (2010). Market report: World piezoelectric device market.

[2] Peng, Y., Ito, S., Sakurai, Y., Shimizu, Y., & Gao, W. (2013). Construction and verification of a linear-rotary microstage with a millimeter-scale range. *International Journal of Precision Engineering and Manufacturing*, 14(9), 1623-1628

[3] Nishimura, T., Hosaka, H., & Morita, T. (2012). Resonant-type smooth impact drive mechanism (SIDM) actuator using a bolt-clamped Langevin transducer. *Ultrasonics*, 52(1), 75-80.

[4] Goldfarb, M., & Celanovic, N. (1997). Modeling piezoelectric stack actuators for control of micromanipulation. *Control Systems, IEEE*, *17*(3), 69-79.

[5] Cook, E. G. (1985).*U.S. Patent No. 4,527,901*. Washington, DC: U.S. Patent and Trademark Office.

[6]Pfleiderer, K., Stoessel, R., & Busse, G. (2003, August). Health monitoring techniques using integrated sensors. In NDE for Health Monitoring and Diagnostics (pp. 224-231). International Society for Optics and Photonics.

[7]Tressler, J. F., Alkoy, S., & Newnham, R. E. (1998). Piezoelectric sensors and sensor materials. *Journal of Electroceramics*, *2*(4), 257-272.

[8] Guo, N., Cawley, P., & Hitchings, D. (1992). The finite element analysis of the vibration characteristics of piezoelectric discs. *Journal of sound and vibration*, *159*(1), 115-13

# Chapter 2

# BACKGROUND AND LITERATURE

# REVIEW

# CHAPTER 2

# BACKGROUND AND LITERATURE REVIEW

## 2.1 Introduction

The purpose of this chapter is to provide a general background on longitudinal piezoelectric transducers (LPT) and to review the relevant literature to modeling of LPT and its applications, all focusing on linear behaviors.

This chapter is structured around four sections. Section 2.2 provides a general background of LPT. To establish the field of knowledge, 3D fundamentals of piezoelectric material is presented in Section 2.3. Then, the relevant literature to modeling of LPT and its applications are reviewed in Section 2.4. Section 2.5 presents conclusion.

## 2.2 Background of LPT

Longitudinal piezoelectric transducers (LPT) collectively refer to piezoelectric actuators, vibrators, sensors and actuators designed for longitudinal deformations or vibrations. Compared with other types of piezoelectric transducers such as bending and shear piezoelectric transducers, LPT provides a larger stiffness, a larger operation bandwidth, more simple and compact structure and more direct energy conversion, thus enabling a large output force and fast response in actuator and vibrator applications, high transient response for sensor applications, and a high mechanical-to-electrical energy conversion efficiency for energy harvesting applications.

In principle, LPT can be divided into d33-mode LPT and d31-mode LPT. With reference to Figure 2.1, when a voltage is applied to the piezo wafer in the direction opposite to its pre-polarized direction, it will induce an expansion in the polarized direction $\Delta t$ and a contraction in the direction orthogonal to the polarized direction $\Delta L$. The former is known as d33-mode and the latter is known as d31-mode. For either d33-mode or d31-mode, the piezo wafer is often designed to be thin in the polarized direction so that it can strengthen the electric field and provide a high mechanical output.
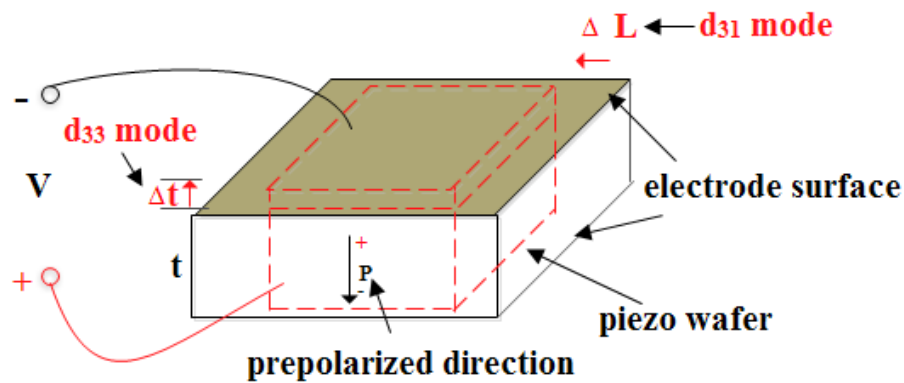
**Figure 2.1 D33-mode and d31-mode of piezoelectricity**

## 2.2.1 D33-mode LPT

With reference to Figure 2.2, d33-mode LPT is based on the operation of thin piezo layer which is thickness polarized, excited, and operated (stressed and strained). For the d33-mode LPT, the longitudinal direction refers to the thickness direction of the piezo wafer.
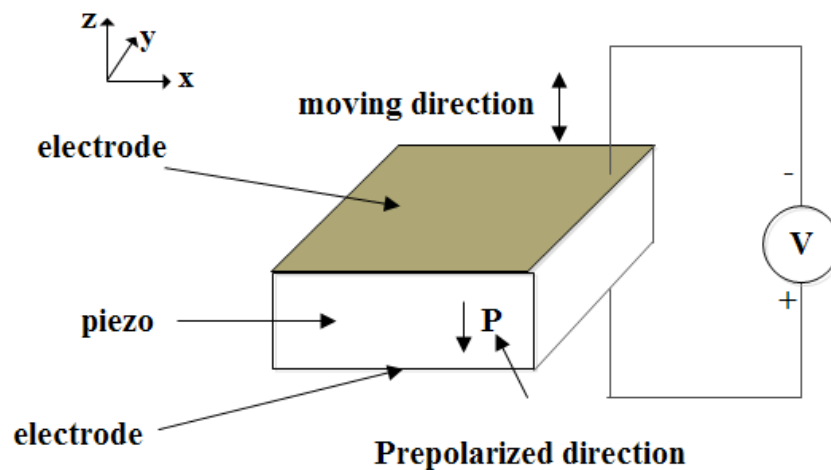


**Figure 2.2 Schematic of d33-mode LPT**

## 2.2.1.1 Single-type d33-mode LPT

Single-type d33-mode LPT refers to d33-mode LPT which use only one piezo wafer in the transducer. Note, for single-type d33-mode LPT, the piezo wafer is not a standalone element but joined by other layers in thickness direction such as additional thin piezo wafers, substrate and other propagating medium which are not shown in Figure 2.2.

They have a high stiffness and high electro-acoustic conversion efficiency and offer a high speed of operation in transmitter mode (electrical energy input, mechanical energy output) (Nishimura et al., 2012). Therefore, they can generate powerful ultrasonic

waves, thus widely applied in ultrasonic applications such as ultrasonic cleaning and ultrasonic welding. Besides, in receiver mode (mechanical energy input, electrical response output), single-type d33-mode LPT can provide a high transient response, thus widely applied in acoustic imaging (Zipparo et al., 1997, Foster et al., 1991).

### 2.2.1.2 Stack-type d33-mode LPT

With reference to Figure 2.3, the piezo wafer shown in Figure 2.2 can be used in a stack configuration along the thickness direction, known as stack-type d33-mode LPT. Each piezo layer is mechanically connected in series and electrically connected. Such a stack configurations enables a large displacement output with a low voltage input in a compact size in transmitter mode and a large charge output in receiver mode.
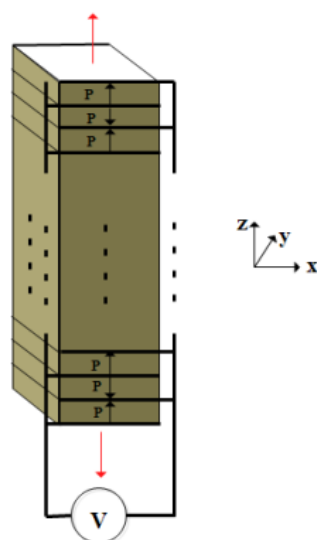


**Figure 2.3 Stack-type d33-mode LPT**

Consequently, in transmitter mode, stack-type d33-mode LPT are widely used as linear actuators, known as multi-layer piezoelectric actuators. They cover a wide range of applications from optical alignment (Peng et al., 2013) to vibrations cancellations in disc drives (Ma and Ang, 2000). In receiver mode, due to its large charge output and the desired feature that the amount of charges output generated is proportional to the applied force, they are also widely used as pressure and accelerometer sensors. Recently, stack-type d33-mode LPT are also explored as energy harvester due to their wide bandwidth and high energy conversion efficiency and large output charges (Adhikari et al., 2009, Xu et al., 2013).

### 2.2.2 D31-mode LPT

With reference to Figure 2.4, d31-mode LPT are based on the operation of thin piezo layer which is thickness polarized and excited but operated (i.e. stressed and strained) in the lateral direction (x-direction in Figure 2.4). For the d31-mode LPT, the longitudinal direction is along the operation direction ((x-direction in Figure 2.4) rather than thickness direction of the piezo wafer.
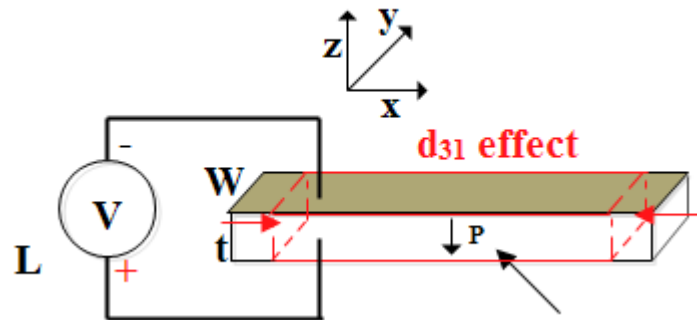


**Figure 2.4 Schematic of d31-mode LPT**

### 2.2.2.1 Single-type d31-mode LPT

Single d31-mode operated slab shown in Figure 2.4 can, in principle, be used as a single-type d31-mode LPT. However, as the piezoelectric coefficient for d33 is 2-5 times larger than that of d31-mode, they are often not preferred in practice for the longitudinal operation. Instead, it is widely applied for bending (Wood et al., 2005) and shearing operation (Morita et al., 2012), for various actuator, sensor and energy harvester applications. As this research focuses on longitudinal transducers, it will be not discussed here.

### 2.2.2.2 Stack-type d31-mode LPT

With reference to Figure 2.5, the piezo wafer shown in Figure 2.4 can be used in a stack configuration along the thickness direction and operated in longitudinal direction, known as stack-type d31-mode LPT. Compared with stack-type d33-mode LPT, the structure of stack-type d31-mode LPT is more robust to extension, as shown in Figure 2.6. Therefore, stack-type d31-mode LPT are preferred as a contracting transducers involving operation under strong tensions (Uchino and Giniewicz 2003, Xu et al., 2011).
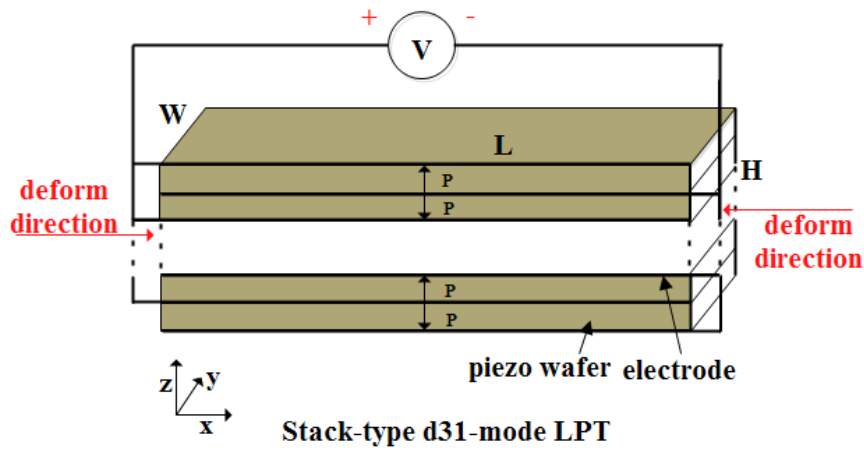
**Figure 2.5 Schematic of stack-type d31-mode LPT**
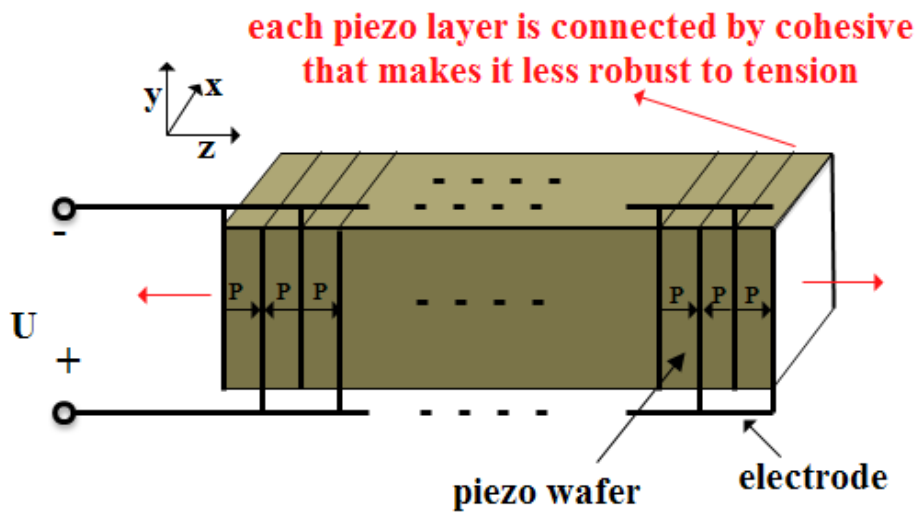
**Figure 2.6 Configurations of multi-layer d33-LPT**

## 2.3 3D fundamentals of piezoelectric material

To establish the field of knowledge, 3D electro-mechanical coupled fundamentals of piezoelectric material are presented in this section.

### 2.3.1 Constitutive equations of piezoelectricity

The 3D constitutive equations of piezoelectric material, which are adopted by the latest IEEE standard (Meitzler et al, 1988) to describe the electro-mechanical coupled behaviors of piezoelectricity, are shown in Figure 2.7.

## Piezoelectric Constitutive Equations (Matrix-vector notation )

**Hook's Law (elasticity)**

**Electrical Coupled term**

$$\{T\} = [c^E]\{S\} - [e]^T\{E\}$$

$$\{D\} = [e]\{S\} + [\varepsilon^S]\{E\}$$

**Mechanical Coupled term**

**Capacitance (dielectric permittivity)**
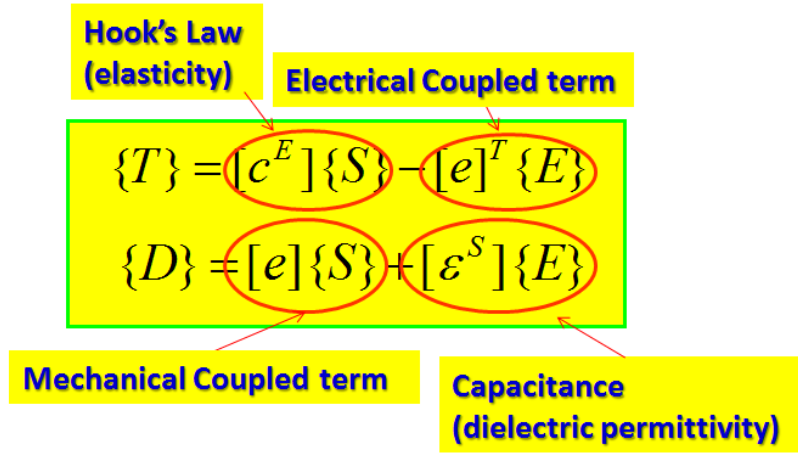
**Figure 2.7 Piezoelectric constitutive equations (matrix-vector notation)**

The full matrix form is shown in the following matrix equation:

$$
\begin{Bmatrix} T_1 \\ T_2 \\ T_3 \\ T_4 \\ T_5 \\ T_6 \end{Bmatrix} =
\begin{bmatrix}
c_{11}^E & c_{12}^E & c_{13}^E & 0 & 0 & 0 \\
c_{12}^E & c_{22}^E & c_{23}^E & 0 & 0 & 0 \\
c_{13}^E & c_{23}^E & c_{33}^E & 0 & 0 & 0 \\
0 & 0 & 0 & c_{44}^E & 0 & 0 \\
0 & 0 & 0 & 0 & c_{55}^E & 0 \\
0 & 0 & 0 & 0 & 0 & c_{66}^E
\end{bmatrix}
\begin{Bmatrix} S_1 \\ S_2 \\ S_3 \\ S_4 \\ S_5 \\ S_6 \end{Bmatrix} -
\begin{bmatrix}
0 & 0 & e_{31} \\
0 & 0 & e_{32} \\
0 & 0 & e_{33} \\
0 & e_{24} & 0 \\
e_{15} & 0 & 0 \\
0 & 0 & 0
\end{bmatrix}
\begin{Bmatrix} E_1 \\ E_2 \\ E_3 \end{Bmatrix},
\tag{2.1.a}
$$

$$
\begin{Bmatrix} D_1 \\ D_2 \\ D_3 \end{Bmatrix} =
\begin{bmatrix}
0 & 0 & 0 & 0 & e_{15} & 0 \\
0 & 0 & 0 & e_{24} & 0 & 0 \\
e_{31} & e_{32} & e_{33} & 0 & 0 & 0
\end{bmatrix}
\begin{Bmatrix} S_1 \\ S_2 \\ S_3 \\ S_4 \\ S_5 \\ S_6 \end{Bmatrix} +
\begin{bmatrix}
\varepsilon_{11}^s & 0 & 0 \\
0 & \varepsilon_{22}^s & 0 \\
0 & 0 & \varepsilon_{33}^s
\end{bmatrix}
\begin{Bmatrix} E_1 \\ E_2 \\ E_3 \end{Bmatrix}.
\tag{2.1.b}
$$

or in a more compact form as shown below:

$$T_p = c_{pq}^E S_q - e_{kp} E_k, \tag{2.2.a}$$

$$D_i = e_{iq} S_q + \varepsilon_{ik}^S E_k. \tag{2.2.b}$$

$S_q, T_p, E_k$, and $D_i$ ($q, p = 1, 2, 3, 4, 5, 6$ and $k, i = 1, 2, 3$) are respectively the components of strain tensor $S$, stress tensor $T$, electric field tensor $E$ and electric displacement tensor $D$. $c_{pq}^E$, $e_{kp}$, $\varepsilon_{ik}^S$ are respectively the components of elastic stiffness matrix $c^E$

measured at constant electric fields, piezoelectric stress matrix $e$ measured at constant strains and dielectric coefficients $\varepsilon^S$ measured at constant strains.

Note, a compressed notation is used here ($T_p = T_{ij}$, $S_q = S_{kl}$ when $k = l$ or $S_q = 2S_{kl}$ when $k \neq l$, $c_{pq}^E = c_{ijkl}^E$, $e_{kp} = e_{kij}$ where $i, j, k, l$ takes the values $1, 2, 3$ based on Figure 2.8).

| p or q | ij or kl |
|--------|----------|
| 1 | 11 |
| 2 | 22 |
| 3 | 33 |
| 4 | 23 or 32 |
| 5 | 13 or 31 |
| 6 | 12 or 21 |

x(1)

z(3)

y(2)
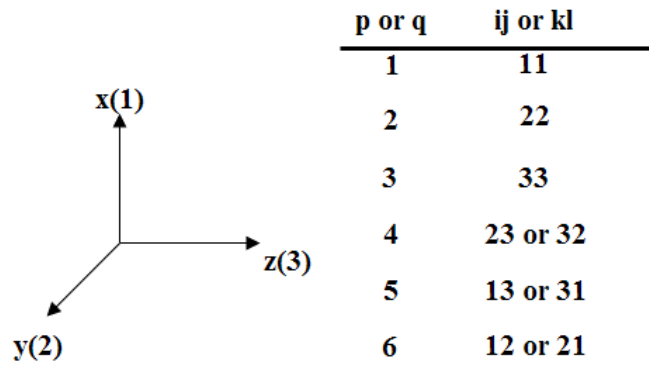
**Figure 2.8 Index notation (Meitzler et al 1988)**

The index notations follow the IEEE standard on piezoelectricity (Meitzler et al 1988) and the measurement of these piezoelectric material coefficients are also standardized there.

**2.3.2 Newton's Second Law**

By applying Newton's second law to piezoelectric material, one can derive the following stress equations of motions within a piezo body:

$$T_{ij,j} = \rho \frac{\partial^2 u_j}{\partial t^2} \text{ where } i, j = 1, 2, 3. \tag{2.3}$$

$\rho$ is the density of piezoelectric material, $t$ is the time variable, $u_j$ are the displacement of a material point.

Note, the comma ',' followed by an index denotes partial differentiation with respect to a space coordinate.

### 2.3.3 Charge balance

The charge balance within a piezo body along the direction of '1', '2' and '3' gives:

$$D_{i,i} = 0, i = 1, 2, 3. \tag{2.4}$$

The strain $S_{kl}$ and the electric field $E_k$ can be respectively expressed with mechanical displacement $u_k$ and electric potential $\varphi_k$ as follows:

$$S_{kl} = \frac{1}{2}(u_{k,l} + u_{l,k}) \text{ where } k, l = 1, 2, 3 \tag{2.5.a}$$

$$E_k = \varphi_{k,k} \text{ where } k = 1, 2, 3. \tag{2.5.b}$$

By combining the constitutive equations of piezoelectricity with Newton's Second Law and Charge balance together with boundary conditions, based on the 27 independent equations ((9 equations in Equation (2.1), 3 equations from Equation (2.3), 3 equations from Equation (2.4) and 9 equations from Equation (2.5)), 24 unknowns ($S_q$, $T_p$, $E_k$, $D_i$, $u_k$ and $\varphi_k$ ($q, p = 1, 2, 3, 4, 5, 6$ and $k, i = 1, 2, 3$)) can be theoretically solved.

However, solving the analytical solutions from these complex coupled derivative equations is extremely difficult except some simple cases. For solving a 3D problem of piezoelectricity, numerical methods such as finite element method can be performed.

In conclusion, to establish the field of knowledge, a 3D electro-mechanical coupled fundamentals of piezoelectric material are presented in this section. 1D and 2D problems can be solved based on such 3D fundamentals by applying some simplifications.

## 2.4 Existing modeling of LPT

Existing modeling of LPT in literature can be generally divided into exact models of LPT and approximate models based on a whole LPT system.

### 2.4.1 Exact modelling of LPT

### 2.4.1.1 Single-type d33-mode LPT

### Direct Analytical Method

With reference to Figure 2.9, the fundamentals of d33-mode LPT can be simplified into 1D problem along the thickness direction (z direction shown in Figure 2.9).
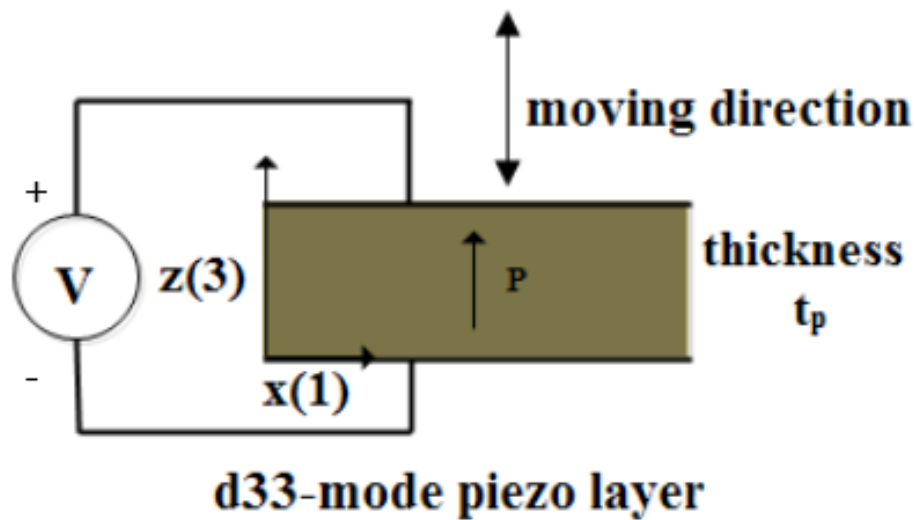


**Figure 2.9 D33-mode piezo layer for analysis**

The constitutive equations can be simplified into 1D, shown below:

$$T_3 = c'S_3 - e'E_3, \tag{2.6.a}$$

$$D_3 = e'S_3 + \varepsilon'E_3, \tag{2.6.b}$$

where $S_3$, $T_3$, $E_3$, and $D_3$ are respectively strain, stress, electric field and electric displacement along the thickness direction( $z$ direction). $c'$, $e'$, and $\varepsilon'$ are respectively the elastic, piezoelectric, dielectric coefficients for 1D constitutive equations. The mechanical strain and electric field can be also expressed with regard to displacement and electric potential along the thickness direction shown below:

$$S_3 = S(z,t) = \frac{\partial u(z,t)}{\partial z},$$
(2.7.a)

$$E_3 = E(z,t) = -\frac{\partial \varphi(z,t)}{\partial z},$$
(2.7.b)

where $z$ and $t$ are respectively position variable and time variable.

By applying Newton's second law to the thickness direction, one can derive:

$$T_{3,3} = \frac{\partial T(z,t)}{\partial z} = \rho \frac{\partial^2 u(z,t)}{\partial^2 t}.$$
(2.8)

Note, the comma ',' followed by an index denotes partial differentiation with respect to a space coordinate.

Based on charge balance along the thickness direction, one can derive:

$$D_{3,3} = \frac{\partial D(z,t)}{\partial z} = 0.$$
(2.9)

By substituting Equations (2.8) and (2.9) into Equations (2.6) with Equations (2.7), one can derive:

$$c' \frac{\partial^2 u(z,t)}{\partial^2 z} + e' \frac{\partial^2 \varphi(z,t)}{\partial^2 z} = \rho \frac{\partial^2 u(z,t)}{\partial^2 t},$$
(2.10.a)

$$\frac{\partial^2 \varphi(z,t)}{\partial^2 z} = \frac{e'}{\varepsilon'} \frac{\partial^2 u(z,t)}{\partial^2 z},$$
(2.10.b)

where $\rho$ is density of the piezoelectric material.

Solving Equations (2.10) with possible solution forms $u(z,t) = u(z)e^{jwt}$ and $\varphi(z,t) = \varphi(z)e^{jwt}$ (where $w$ is the excitation frequency) gives the general analytical solutions to $u(z,t)$, $\varphi(z,t)$, $S(z,t)$ and $E(z,t)$:

$$u(z,t) = (A_1 \sin(hz) + A_2 \cos(hz))e^{jwt},$$
(2.11.a)

$$\varphi(z,t) = (\frac{e'}{\varepsilon'}(A_1 \sin(hz) + A_2 \cos(hz)) + B_1 z + B_2)e^{jwt},$$
(2.11.b)

$$S(z,t) = (A_1 h \cos(hz) - A_2 h \sin(hz))e^{jwt}$$
(2.11.c)

$$E(z,t) = (\frac{e'}{\varepsilon'}(A_1 h \cos(hz) - A_2 h \sin(hz)) + B_1)e^{jwt},$$
(2.11.d)

$$T(z,t) = (c'(1 + \frac{e'^2}{\varepsilon' c'})(A_1 h \cos(hz) - A_2 h \sin(hz)) + e' B_1)e^{jwt},$$

(2.11.e)

$$D(z,t) = -\varepsilon' B_1,$$

(2.11.f)

where $h = w \sqrt{\dfrac{\rho}{c'(1 + \dfrac{e'^2}{\varepsilon' c'})}}$ , $A_1, A_2, B_1$ and $B_2$ are integration constants.

By solving $A_1, A_2, B_1$ from three boundary conditions of the piezo layer ( two boundary conditions from two mechanical boundaries at two ends of the piezo layer and one boundary condition from the electrical boundary condition), the specific analytical solutions to $u(z,t), \varphi(z,t), S(z,t)$ and $E(z,t)$ can be solved. Note $B_2$ is immaterial.

Although the fundamentals of single piezo layer can be solved by direct analytical methods shown above, deriving specific analytical solutions by direct analytical method for analysis and calculation of single-type d33-mode LPT are quite complex and cumbersome, as the piezo layer is joined by other medium for applications of single-type d33-mode LPT.

**Exact equivalent circuit method**

It is shown by Mason (Mason 1948, Mason 1956) that most of the difficulties in deriving the specific analytical solutions by direct analytical method can be overcome by introducing an exact equivalent circuit of the piezo layer, well known as Mason's equivalent circuit shown in Figure 2.10. By borrowing the network theory, Mason formulated the circuit exactly based on the 1D electro-mechanical fundamentals of d33-mode piezo layer. The details can be seen in literature.
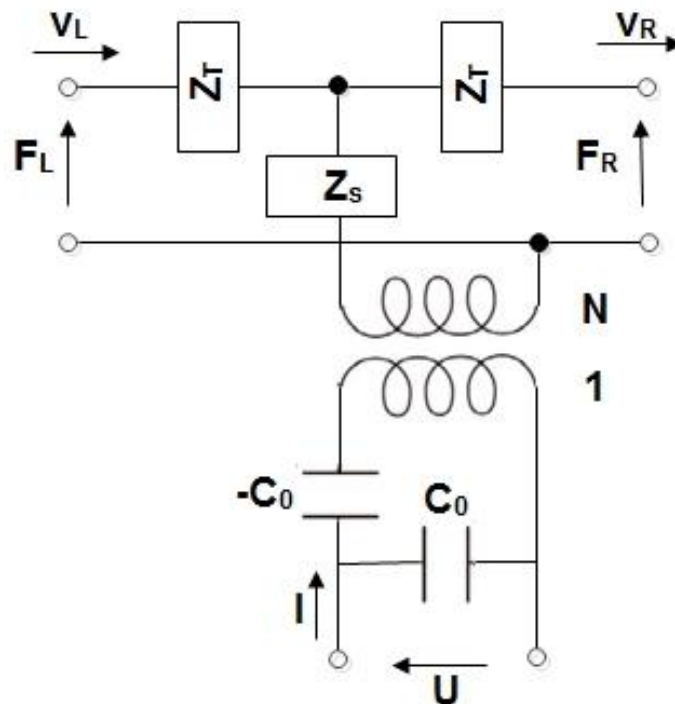
**Figure 2.8 Mason's Equivalent Circuits**

In Mason equivalent circuit, there is a negative capacitance in electrical port, which is hard to understand in physical meaning. To make the electrical circuit more physical to understand, Krimholtz, Leedom, and Matthae(1970) derived an alternative form with an exact equivalence to Mason equivalent circuit, knows as KLM equivalent circuit, shown in Figure 2.11. The details can be seen in literature.
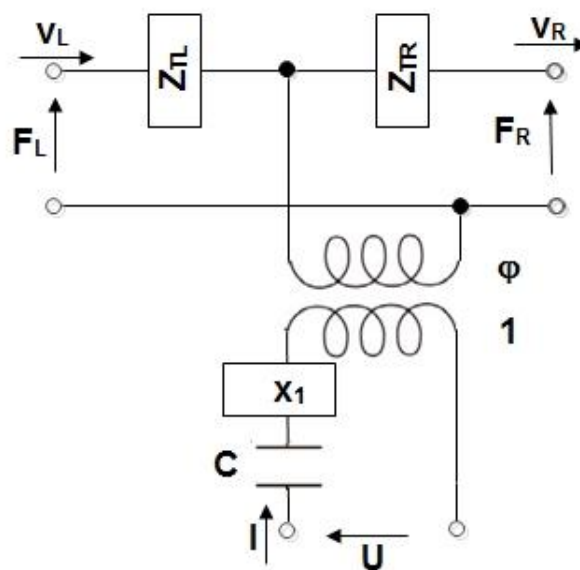


**Figure 2.9 KLM Equivalent Circuits**

The two exact equivalent circuits greatly facilitate the analysis and calculation of single-type d33-mode LPT in a straightforward way.

### 2.4.1.2 Stack-type d33-mode LPT

**Direct Analytical Method**

With reference to Figure 2.12, the operation of stack-type d33-mode LPT can be also based on the aforementioned 1D fundamentals of d33-mode piezo layer. Each piezo layer is mechanically connected in series and electrically connected in parallel. For such a stack configuration, it is theatrically possible but extremely difficult to derive specific analytical solutions by direct analytical method for analysis and calculation of stack-type d33-mode LPT.
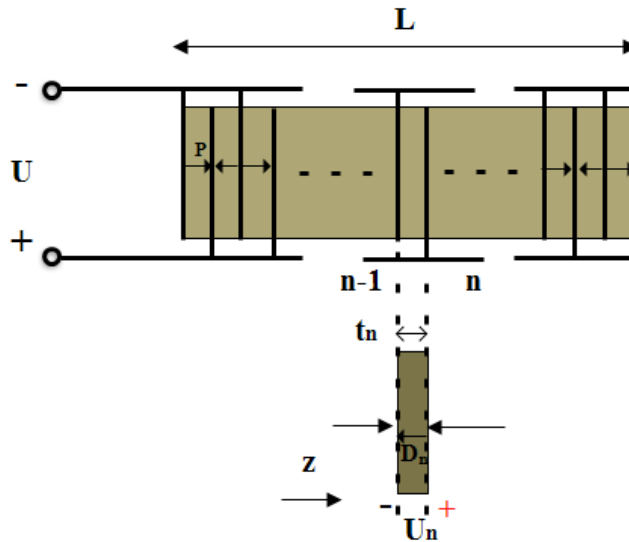


**Figure 2.10 Stack-type d33-mode LPT for analysis**

**Exact equivalent circuit method**

With reference to Figure 2.13, as stack-type d33-mode LPT connects each single-layer piezo element mechanically in series and electrically in parallel, it can be modelled by Mason's equivalent circuit or KLM equivalent circuit in the way shown in Figure 2.9.
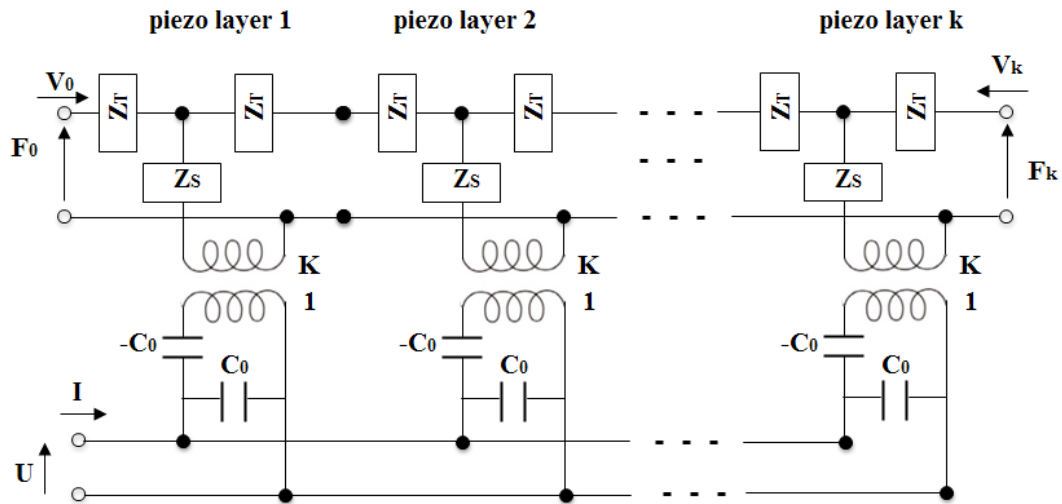
**Figure 2.11 Model stack-type d33-mode LPT based on Mason's equivalent circuit**

Although modelling is straightforward, solving such a complex electrical circuit is also very cumbersome.

**Transfer matrix method**

To facilitate the computation of the multiple-piezo-layer configuration in stack-type d33-mode LPT, transfer matrix method is proposed in literature. The transfer matrix method is based on the fact that some physical quantities follow simple continuity conditions across the boundaries from one layer to the next. Therefore, if physical quantities on one side of certain layer can be correlated to the other side of the layer in a matrix form (known as transfer matrix), the dynamics of a stack of layers then can be simply computed by multiplication of individual layer matrix in the stack.
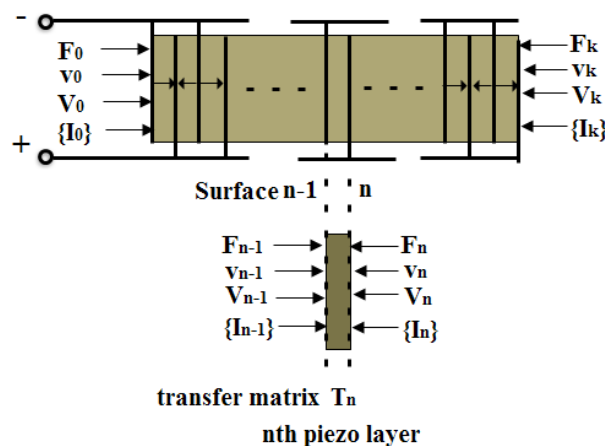
**Figure 2.12 Model d33-mode multi-layer piezoelectric transducer based on transfer matrix method**

With reference to Figure 2.14, for a stack-type d33-mode LPT composed of $k$ piezo layers, based on the aforementioned 1D fundamentals of d33-mode piezo layer, the force $F$, velocity $v$, electric potential $V$, and electrical current $\{I\}$ on one side of a piezo layer can be correlated to the other side of the layer in the matrix form(Morita et al. 2001 and Bloomfield 2002), shown below:

$$\begin{bmatrix} F_n \\ v_n \\ V_n \\ \{I_n\} \end{bmatrix} = T_{p,n} \cdot \begin{bmatrix} F_{n-1} \\ v_{n-1} \\ V_{n-1} \\ \{I_{n-1}\} \end{bmatrix},$$

(2.12)

$n = 1, 2, ..., k$

As the force, velocity, electric potential, and electrical current are connected continuously at the boundary surface between two adjacent piezo layers, the force, velocity, electric potential, and electrical current at two ends of the whole piezo stack can be easily computed by multiplication of each individual piezo layer show in the following equation:

$$\begin{bmatrix} F_k \\ v_k \\ U_k \\ \{I_k\} \end{bmatrix} = \prod_{n=1}^{k} T_{p,n} \cdot \begin{bmatrix} F_0 \\ v_0 \\ U_0 \\ \{I_0\} \end{bmatrix}.$$

(2.13)

Then, combined with 3 boundary conditions (two boundary conditions from two mechanical boundaries at two ends of stack-type d33-mode LPT and one boundary condition from the electrical boundary condition of stack-type d33-mode LPT), the behaviours of the whole multi-layer piezoelectric transducer can be modelled and computed for analysis of stack-type d33-mode LPT. Transfer matrix method can be also applied to facilitate calculation, when stack-type d33-mode LPT is joined with other mediums, just by formulating the transfer matrix of the related mediums.

For either exact equivalent circuit or transfer matrix method in literature, although they facilitate the analysis and calculation of d33-mode LPT in comparison with direct analytical method, they all based on the complex electro-mechanical coupled fundamentals of d33-mode piezo layer shown in Equation (2.11), involving solving a position-varying electric field ($E(z,t) = (\frac{e'}{\varepsilon'}(A_1 h \cos(hz) - A_2 h \sin(hz)) + B_1)e^{jwt}$).

If the electric potential $\varphi(z,t)$ can be approximated to be uniformly distributed along the thickness direction (i.e. $E(z,t)$ can be directly derived by $E(z,t) = \dfrac{U(t)}{t_p}$ for any position along z axis), it could greatly simplify and facilitate the analysis and calculation of d33-mode LPT, especially the stack-type, which will be shown in the work of this research. This approximation is widely made for static case in literature (as for static

case, $$w = 0 \rightarrow h = w \sqrt{\dfrac{\rho}{c'(1 + \dfrac{e'^2}{\varepsilon'c'})}} = 0 \rightarrow$$ ). However, whether

$$E(z,t) = (\dfrac{e'}{\varepsilon'}(A_1 h \cos(hz) - A_2 h \sin(hz)) + B_1)e^{jwt} = B_1 = \dfrac{U(t)}{t_p}$$

this approximation is applicable to dynamic case, what is the rationale behind the approximation for d33-mode LPT, what is the scope and limitations of the approximation, and how this approximation could simplify and facilitate the analysis and calculation of d33-mode LPT, have not been well explored.

### 2.4.1.3 d31-mode LPT

To the best of authors' knowledge, only a few models of D31-LPT are available in literature (Xu et al 2011；Uchino and Giniewicz 2003; Tolliver L 2013). Xu et al (2011) and Uchino and Giniewicz (2003) focused on the static behaviours. Tolliver et al (2013) applied a finite element model to compute the dynamic behaviours of D31-LPT. Although it can effectively model D31-LPT, the finite element model, which is based on 3D complex electro-mechanical coupled fundamentals of piezoelectricity, is computationally inefficient. Simple and effective dynamic modelling of D31-LPT, which can predict the behaviours in time/frequency domain, has not been well explored in literature.

This approximation is widely made for static case in literature. However, whether this approximation is applicable to dynamic case, what is the rationale behind the approximation for d31-mode LPT, what is the scope and limitations of the approximation, and how this approximation could simplify and facilitate the analysis and calculation of d31-mode LPT, have not been well explored.

### 2.4.2 Approximate Models based on a whole LPT system

To simply the modelling for some purposes such as describing the behaviours of piezo system or on-line control, approximate models based on a whole LPT system are proposed in literature.

To describing behaviours of a piezo system, the Van Dyke equivalent Circuit(Van 1925), which has been adopted by IEEE committee (Meitzler et al 1988), is widely used. With reference to Figure 2.15, the circuit consists of a lump capacitance C0 connected in parallel with an inductance L1, a resistance R1, and a capacitance C1. C0 represents the property of electrical side, while L1, R1, and C1 represents the feature of mechanical side. The configuration of the Van Dyke equivalent Circuit only allows one-resonant mode to be modelled. However, a piezo system is actually a continuous system, which often shows multiple resonant modes in practices. To allow more resonate modes to be modelled, the Van Dyke model was modified and extended with additional RCL branches in parallel shown in Figure 2.16 (Meitzler et al 1988). Other configurations of equivalent electrical circuit models were also explored in literature (Meitzler et al 1988;Guan and Liao 2004; Kim et al. 2008). The electrical parameters in those equivalent electrical circuits can be determined by various types of system identification methods based on measured information (Meitzler et al 1988;Guan and Liao 2004; Kim et al. 2008).
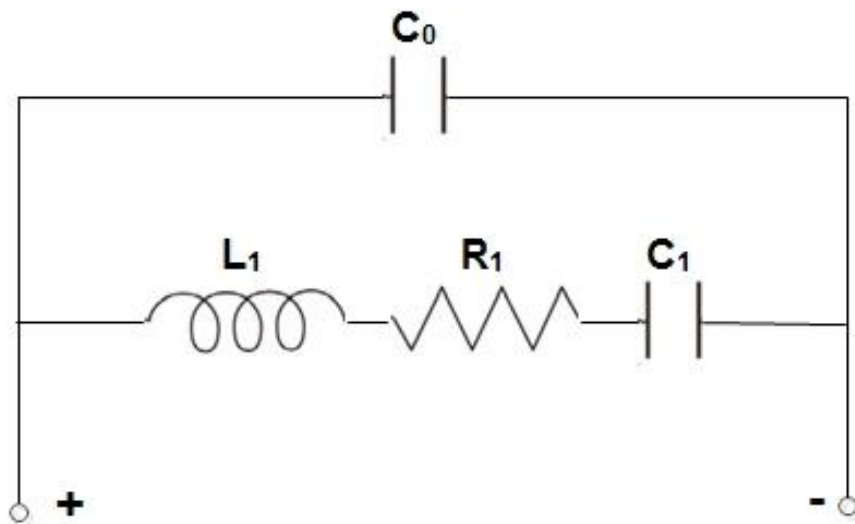


**Figure 2.15 The Van Dyke Equivalent Circuit**
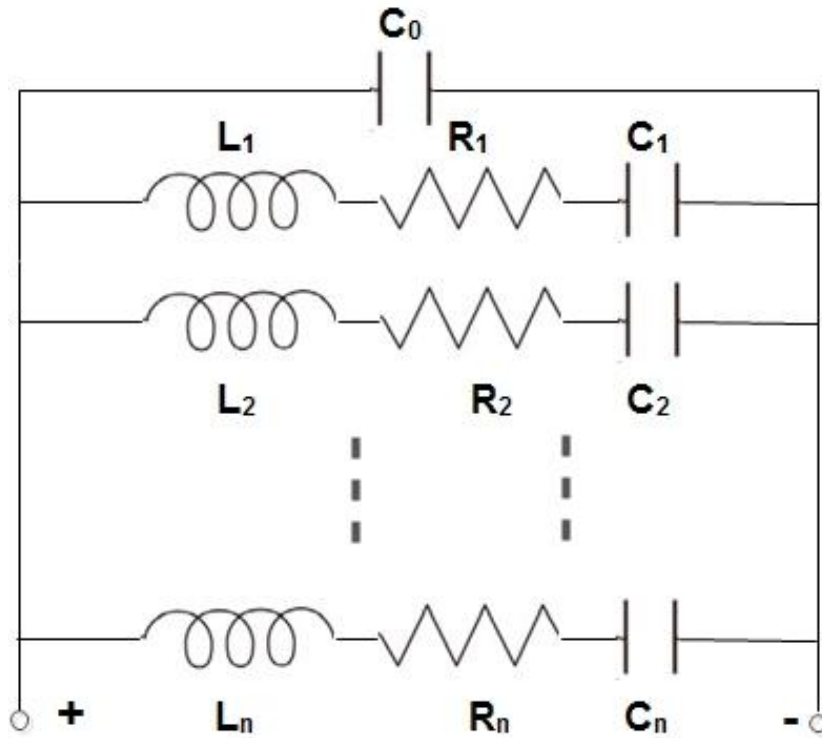
**Figure 2.16 The extended Van Dyke Model**

Although these equivalent circuits can be used to describe the behaviours of piezo-electrically excited system, the electromechanical interaction and physically mechanical quantities are obscure. To describe the electro-mechanical coupled interaction of MPS, a more physical approximate model, which is widely used in the control of piezoelectric systems, is proposed (Goldfarb and Celanovic, 1997).
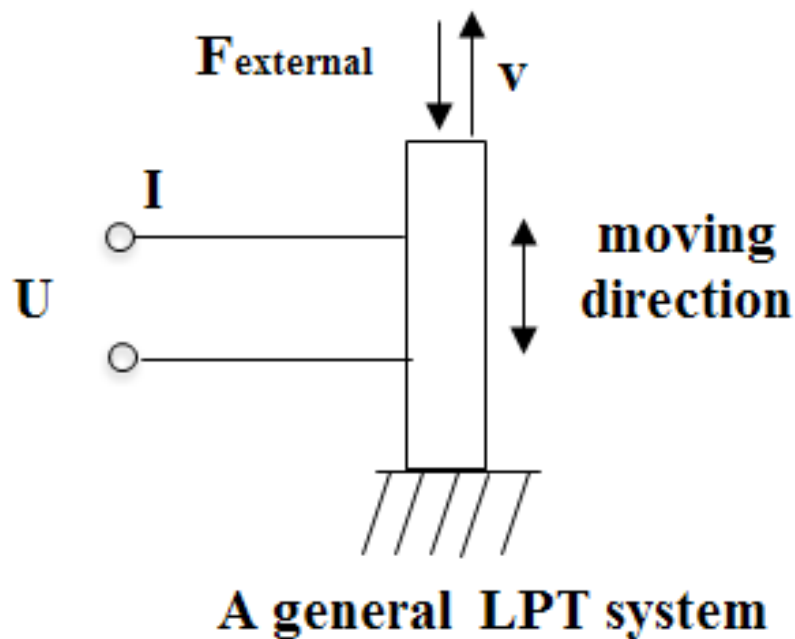
**Figure 2.17 A general LPT system**

For a general LPT system shown in Figure 2.17, the model describes the mechanical side as a lumped mass-spring-damper system with an electrical port, which can introduce a lumped piezo force from applied voltage in the electrical side, based on the inverse piezoelectric effect. The electrical side is modelled by a lumped capacitance with a mechanical port, which can introduce a counter charge from the induced piezo displacement in the mechanical side (similar to counter EMF).

The equations of motion can be shown below:

$$M\frac{\partial^2 u(t)}{\partial^2 t} + C\frac{\partial u(t)}{\partial t} + K \cdot u(t) = N \cdot U(t) - F_{external}(t), \tag{2.14.a}$$

$$q(t) = C \cdot U(t) + N \cdot u(t), \tag{2.14.b}$$

Where $u(t)$ is the displacement along the longitudinal direction, $M$, $C$, $K$ are respectively the equivalent mass, damping constant, and stiffness of the mechanical system, $N$ is the piezoelectric coefficient, $F_{external}$ is the external force applied on the LPT system, $C_0$ is the internal electric capacitance of LPT, $U(t)$ and $q(t)$ are respectively the voltage and the induced charge of the LPT system. The equation (2.14)

can be converted into the equivalent circuit form shown in Figure 2.18. In the circuit, $v(t)$ is the velocity ($v(t) = \dfrac{\partial u(t)}{\partial t}$) and $I(t)$ is the current ($I(t) = \dfrac{\partial q(t)}{\partial t}$).
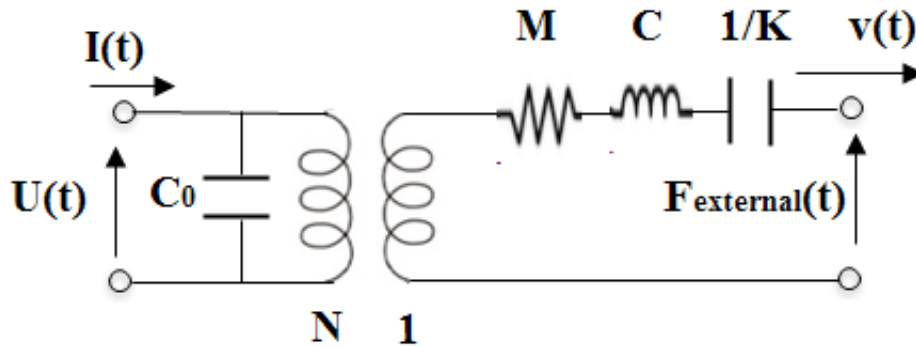


**Figure2.18 An equivalent circuit widely used in control area**

This equivalent circuit model is easily implemented and computationally efficient. Consequently, it is widely used with non-linear models for the positioning control purpose of a LPT system. However, as how LPT is coupled into the LPT system is implicit and the equivalent constants ($M$, $C$, $K$, $N$ and $C_0$) need to be determined from experiments rather than from the dimension and material properties of the LPT system, this model cannot be used to predict the behaviors for the design and optimization of a LPT system prior to experiments.

## 2.5 Review summary and research gaps

In summary, LPT can, in principle, be divided into d33-mode LPT and d31-mode LPT. Approximate models based on a whole LPT system is easily implemented and computationally efficient. They can be quite effective for describing the behaviours or online control of the LPT system. However, as how LPT is coupled into the LPT system is implicit in these models and model parameters need to be determined from experiments rather than from the dimension and material properties of the LPT system, this model cannot be used to predict behaviours of the design and optimization of LPT system prior to experiments.

Existing exact modellings of d33-mode LPT are based upon complex 1D electro-mechanical coupled fundamentals, involving a position-varying electric field. Although the exact equivalent circuit method and transfer matrix method are proposed in literature to facilitate the analysis and calculation, solving such complex fundamentals is still inefficient, especially for the stack-type d33-mode LPT. An opportunity exists to simply complex 1D electro-mechanical coupled fundamentals of d33-mode LPT by applying the uniform-electric-field approximation. This approximation is mathematically shown to be true for static cases in this chapter. However, whether this approximation is applicable to dynamic cases, what is the rationale behind the approximation for d33-mode LPT, what is the scope and limitations of the approximation, and how this approximation could simplify the fundamentals of d33-mode LPT and the related modelling methods to facilitate the analysis and calculation of d33-mode LPT, have not been well explored.

For d31-mode LPT, only a few static models are available in literature. Although the dynamic behaviours of D31-LPT can be predicted by using 3D finite element method, the finite element model, which is based on 3D complex electro-mechanical coupled fundamentals of piezoelectricity, is computationally inefficient. Again, whether the electric field for the operation of d31-mode LPT can be approximated to be uniform to simplify the fundamentals, what is the rationale behind the approximation, what is the scope and limitation, and the related modelling methods to facilitate the analysis and calculation of d31-mode LPT, have not been well explored.

These research gaps concerning the application of the uniform-electric-field approximation to simplify the complex fundamentals of d33-mode LPT and d31-mode LPT will be addressed in the following 6 chapters, with each based on an individual scientific paper.

## Reference

Adhikari, S., Friswell, M. I., & Inman, D. J. (2009). Piezoelectric energy harvesting from broadband random vibrations. *Smart Materials and Structures*, *18*(11), 115005.

Bloomfield, P. E. (2002). Multilayer transducer transfer matrix formalism.*Ultrasonics, Ferroelectrics, and Frequency Control, IEEE Transactions on*,*49*(9), 1300-1311.

Foster, F. S., Ryan, L. K., & Turnbull, D. H. (1991). Characterization of lead zirconate titanate ceramics for use in miniature high-frequency (20-80 MHz) transducers. *Ultrasonics, Ferroelectrics, and Frequency Control, IEEE Transactions on*, *38*(5), 446-453.

Guan, M. and W.-H. Liao (2004). Studies on the circuit models of piezoelectric ceramics. Proceedings. *IEEE International Conference on Information Acquisition*,2004.

Goldfarb, M., & Celanovic, N. (1997). Modeling piezoelectric stack actuators for control of micromanipulation. *Control Systems, IEEE*, *17*(3), 69-79.

Kim, J., B. L. Grisso, et al. (2008). Electrical modeling of piezoelectric ceramics for analysis and evaluation of sensory systems. *Sensors Applications Symposium*, 2008. SAS 2008. IEEE, IET.

Krimholtz, R., Leedom, D. A., & Matthaei, G. L. (1970). New equivalent circuits for elementary piezoelectric transducers. *Electronics Letters*, *6*(13), 398-399.

Ma, J., & Ang Jr, M. H. (2000, October). High-bandwidth macro/microactuation for hard-disk drive. In *Intelligent Systems and Smart Manufacturing* (pp. 94-102). International Society for Optics and Photonics.

Mason, W. P. (1948). *Electromechanical transducers and wave filters*. D. Van Nostrand Co..

Mason, W. P. (1956). Physical acoustics and the properties of solids. *The Journal of the Acoustical Society of America*, *28*(6), 1197-1206.

Meitzler, A. H., Tiersten, H. F., Warner, A. W., Berlincourt, D., Couqin, G. A., & Welsh III, F. S. (1988). IEEE standard on piezoelectricity.

Morita, T., Murakami, H., Yokose, T., & Hosaka, H. (2012). A miniaturized resonant-type smooth impact drive mechanism actuator. *Sensors and Actuators A:Physical*, *178*, 188-192.

Morita, T., Niino, T., Asama, H., & Tashiro, H. (2001). Fundamental study of a stacked lithium niobate transducer. *Japanese Journal of Applied Physics*,*40*(5S), 3801.

Nishimura, T., Hosaka, H., & Morita, T. (2012). Resonant-type smooth impact drive mechanism (SIDM) actuator using a bolt-clamped Langevin transducer. *Ultrasonics*, 52(1), 75-80.

Peng, Y., Ito, S., Sakurai, Y., Shimizu, Y., & Gao, W. (2013). Construction and verification of a linear-rotary microstage with a millimeter-scale range. *International Journal of Precision Engineering and Manufacturing*, 14(9), 1623-1628.

Tolliver L, Xu T B, Jiang X. Finite element analysis of the piezoelectric stacked-HYBATS transducer. Smart Materials and Structures, 2013, 22(3): 035015.

Uchino K and Giniewicz J 2003 *Micromechatronics* (Boca Raton, FL: Taylor & Francis) Page 383

Wood, R. J., Steltz, E., & Fearing, R. S. (2005, April). Nonlinear performance limits for high energy density piezoelectric bending actuators. In *Robotics and Automation, 2005. ICRA 2005. Proceedings of the 2005 IEEE International Conference on* (pp. 3633-3640). IEEE.

Xu, T. B., Jiang, X., & Su, J. (2011). A piezoelectric multilayer-stacked hybrid actuation/transduction system. *Applied Physics Letters*, *98*(24), 243503.

Xu, T. B., Siochi, E. J., Kang, J. H., Zuo, L., Zhou, W., Tang, X., & Jiang, X. (2013). Energy harvesting using a PZT ceramic multilayer stack. *Smart Materials and Structures*, *22*(6), 065015.

Zipparo, M. J., Shung, K. K., & Shrout, T. R. (1997). Piezoceramics for high-frequency (20 to 100 MHz) single-element imaging transducers. *Ultrasonics, Ferroelectrics, and Frequency Control, IEEE Transactions on*, *44*(5), 1038-1048.

# Chapter 3

# SIMPLIFIED FUNDAMENTALS of

# D33-MODE LPT

# CHAPTER 3

# SIMPLIFIED FUNDAMENTALS OF D33-MODE LPT

This chapter is based on the following paper:

*Full citation*: Zhang, Y., Lu, T. F., & Al-Sarawi, S. (2015). Formulation of a simple distributed-parameter model of multilayer piezoelectric actuators. *Journal of Intelligent Material Systems and Structures*, 1045389X15595294.

*Contributions of this chapter*: This chapter presents the rationale behind the uniform-electric-field-approximation for modelling d33-mode LPT together with its scope and limitation. Then, based on the approximation, simplified fundamentals of both simple-layer-type and stack-type d33-mode LPT are formulated. It is interestingly found that, by applying the uniform-electric-field-approximation, the multi-layer stack configuration of stack-type d33-mode LPT can be effectively modelled as a whole. It greatly simplifies and facilitates the modelling of the stack-type d33-mode LPT, which could provide very simple analytical solutions. The effectiveness of the proposed simplified fundamentals of d33-mode LPT has been validated by 3D finite element model in commercial software ANSYS.

# Statement of Authorship

| Title of Paper | Formulation of A Simple Distributed-Parameter Model of Multi-layer Piezoelectric Actuators |
|---|---|
| Publication Status | ☑ Published    ☐ Accepted for Publication<br>☐ Submitted for Publication    ☐ Unpublished and Unsubmitted work written in manuscript style |
| Publication Details | Zhang, Y., Lu, T. F., & Al-Sarawi, S. (2015). Formulation of a simple distributed-parameter model of multilayer piezoelectric actuators. *Journal of Intelligent Material Systems and Structures*, 1045389X15595294. |

## Principal Author

| Name of Principal Author (Candidate) | Mr. Yangkun Zhang |
|---|---|
| Contribution to the Paper | Developed theory, performed simulations, analyzed data and wrote the manuscript |
| Overall percentage (%) | 80% |
| Certification: | This paper reports on original research I conducted during the period of my Higher Degree by Research candidature and is not subject to any obligations or contractual agreements with a third party that would constrain its inclusion in this thesis. I am the primary author of this paper. |
| Signature | Date  16/02/2016 |

## Co-Author Contributions

By signing the Statement of Authorship, each author certifies that:

i.    the candidate's stated contribution to the publication is accurate (as detailed above);

ii.    permission is granted for the candidate in include the publication in the thesis; and

iii.    the sum of all co-author contributions is equal to 100% less the candidate's stated contribution.

| Name of Co-Author | Dr. Tien-Fu Lu |
|---|---|
| Contribution to the Paper | Supervised research, reviewed manucript |
| Signature | Date  16/02/16 |

| Name of Co-Author | Dr. SAID Al-SARAWI |
|---|---|
| Contribution to the Paper | Supervised research, reviewed manucript |
| Signature | Date |

Chapter 4

# A SIMPLE EQUIVALENT CIRCUIT

# OF D33-MODE LPT

# CHAPTER 4

# A SIMPLE EQUIVALENT CIRCUIT OF D33-MODE LPT

This chapter is based on the following paper:

*Full citation*: Zhang, Y., Lu, T-F., & Peng, Y. (2015). Three-port equivalent circuit of multi-layer piezoelectric stack. *Sensors and Actuators A: Physical*, 236, 92-97.

*Contributions of this chapter:* To facilitate the modelling of free and loaded vibration of stack-type d33-mode LPT in a straightforward way, the simplified fundamentals of stack-type d33-mode LPT proposed in Chapter 3 is wrapped into a simple three-port equivalent circuit, which is inspired by the idea of network theory. Note, although the circuit is aimed at stack-type, it can be also applied to single-type LPT simply by letting the number of piezo layer equal to 1. Compared with the existing equivalent circuits, the proposed circuit of d33-mode LPT has a simpler structure and can be extended to any electrical and mechanical condition. Besides, as the proposed circuit elements are explicitly and exactly derived in terms of material and dimension information rather than determined from measured information, the proposed circuit model allows one to predict behaviours with material properties and structural dimension. For both free and loaded vibrations, the effectiveness of the proposed circuit has been validated by 3D FEA models.

# Statement of Authorship

| Title of Paper | Three-Port Equivalent Circuit of Multi-layer Piezoelectric Stack |
|---|---|
| Publication Status | ☑ Published ☐ Accepted for Publication<br>☐ Submitted for Publication ☐ Unpublished and Unsubmitted work written in manuscript style |
| Publication Details | Zhang, Y., Lu, T. F., & Peng, Y. (2015). Three-port equivalent circuit of multi-layer piezoelectric stack. *Sensors and Actuators A: Physical, 236*, 92-97. |

## Principal Author

| Name of Principal Author (Candidate) | Mr. Yangkun Zhang |
|---|---|
| Contribution to the Paper | Developed theory, performed simulations, analyzed data and wrote the manuscript |
| Overall percentage (%) | 80% |
| Certification: | This paper reports on original research I conducted during the period of my Higher Degree by Research candidature and is not subject to any obligations or contractual agreements with a third party that would constrain its inclusion in this thesis. I am the primary author of this paper. |
| Signature | Date  16/02/2016 |

## Co-Author Contributions

By signing the Statement of Authorship, each author certifies that:

   i.   the candidate's stated contribution to the publication is accurate (as detailed above);

   ii.   permission is granted for the candidate in include the publication in the thesis; and

   iii.   the sum of all co-author contributions is equal to 100% less the candidate's stated contribution.

| Name of Co-Author | Dr. Tien-Fu Lu |
|---|---|
| Contribution to the Paper | Supervised research, reviewed manuscript |
| Signature | Date  16/02/16 |

| Name of Co-Author | Dr. Yuxin Peng |
|---|---|
| Contribution to the Paper | reviewed the manuscript |
| Signature | Date  19/02/16 |

Contents lists available at ScienceDirect

# Sensors and Actuators A: Physical

journal homepage: www.elsevier.com/locate/sna
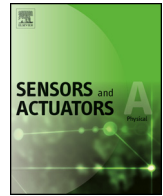
# Three-port equivalent circuit of multi-layer piezoelectric stack

Yangkun Zhang [a,*], Tien-Fu Lu [a], Yuxin Peng [b]

[a] *School of Mechanical Engineering, University of Adelaide, 5005, Australia*
[b] *Department of Biomedical Engineering, National University of Singapore, 117575, Singapore*

## ARTICLE INFO

## ABSTRACT

Multi-layer piezoelectric transducers (MPS) is a transducer stacked by numerous thin piezo layers, which can used as an actuator, sensor, or energy harvester. This paper points out the limitations of existing equivalent circuits for the effective modelling of MPS and proposes a 3-port equivalent circuit of MPS which is inspired by the idea of network theory and formulated exactly on the basis of the simplified fundamentals. The 3-port equivalent circuit, which separates the MPS into two acoustic ports and one electrical port through an electro-mechanical transformer, offers an exact and explicit representation of electro-mechanical coupled interaction of MPS. It is very straightforward to apply and effectively simplifies and facilitates the analysis, modelling, and calculation of free and loaded vibration of MPS in either transmitter mode (actuator) or receiver mode (sensor or energy harvester). Compared with existing circuit models in literature, the proposed circuit can be extended to any electrical and mechanical condition. Besides, as the proposed circuit elements are explicitly and exactly derived in terms of material and dimension information rather than determined from measured information, the proposed circuit model allows one to predict behaviors with material properties and structural dimension. For validation, a simple case study is carried out. For both free and loaded vibrations of MPS in the case study, the effectiveness of the proposed circuit has been validated by 3D FEA models.

© 2015 Elsevier B.V. All rights reserved.

## 1. Introduction

Multi-layer piezoelectric stack (MPS) is a transducer stacked by numerous thin piezo layers which can convert the electrical energy into mechanical energy (actuators) and can also convert the mechanical energy into electrical response (sensors and energy harvesters). In many MPS-based applications such as design of free and loaded resonators, determination of unknown material property and design of harvester scavenging energy from ambient vibrations, modelling vibration behaviours of MPS is a key step. To facilitate analysis, modelling, and calculation of free and loaded vibrations of MPS in either transmitter mode (actuator) or receiver mode (sensor or energy harvester), a three-port equivalent circuit of MPS is proposed in this paper.

Section 2 reviews the existing equivalent circuits in literature. Their limitations are pointed out and a novel equivalent circuit is proposed. Section 3 presents the fundamentals of MPS, which provide a basis for the construction of the proposed equivalent circuit presented in Section 4. To validate the formulated equivalent cir-

cuit, 3D FEA models of MPS are developed in commercial software 'ANSYS' in Section 5. Simulation results between the two models are compared and the limitations of the proposed model are discussed. Section 6 presents the summary.

## 2. Existing equivalent circuits

For the facility in describing behaviours of piezo-electrically excited vibration system, equivalent electrical circuits are often used. A widely used equivalent electrical circuit, which has been standardized in IEEE [1], is the Van Dyke circuit [2] shown in Fig. 1, which consists of a lump capacitance $C_0$ connected in parallel with an inductance $L_1$, a resistance $R_1$, and a capacitance $C_1$. The Van Dyke circuit can be used to represent a piezo-electrically excited mechanical vibration system with one dominant resonant mode captured. However, a piezo-electrically excited mechanical vibration system is actually a continuous system rather than discrete systems, which shows multiple resonant modes in practices. To capture more modes, the Van Dyke model was modified and extended with additional RCL branches in parallel shown in Fig. 2 [1]. Other similar equivalent electrical circuit models were also explored to model multiple resonant modes and improve the accuracy [3,4]. The electrical parameters in those equivalent electrical
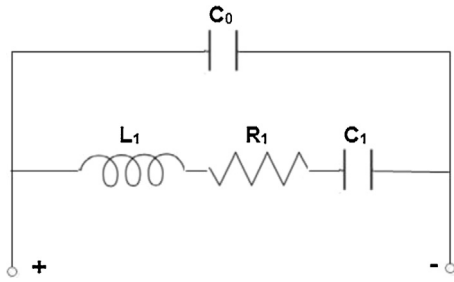
**Fig. 1.** The Van Dyke equivalent circuit.



**Fig. 2.** The extended Van Dyke model.



**Fig. 3.** Schematic of multi-layer piezoelectric stack.
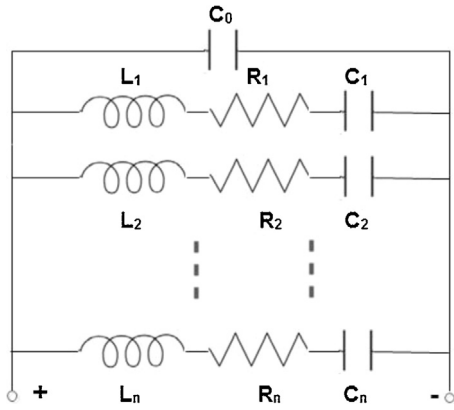
circuits can be determined by various types of system identification methods based on measured information [1–4]. Although these equivalent circuits can be used to describe the behaviours of piezo-electrically excited system, the electromechanical interaction and physically mechanical quantities are obscure. Therefore, they are incapable to predict the behaviours, when mechanical boundary conditions are changed.

To describe the electro-mechanical coupled interaction of MPS, a widely recognized lumped model is proposed by Goldfarb and Celanovic [5]. This model is composed of an electrical side, a mechanical side, and the ports which couples the electrical and mechanical models. The mechanical side is modelled as a lumped mass-spring-damper system with an electrical port, which can introduce a lumped piezo force from applied voltage in the electrical side, based on the inverse piezoelectric effect. The electrical side is modelled by a lumped capacitance with a mechanical port, which can introduce a counter charge from the induced piezo displacement in the mechanical side (similar to counter EMF).

The lumped model can be easily implemented with some non-linear models [6] for positioning control purpose. However, lumped-models are just approximated models, as a MPS is actually a distributed system. Adriaens et al. [6] and Chen et al. [7] further elaborated this lumped electromechanical model of MPS into distributed-parameter models. In their models, the MPS is proposed to be taken as an equivalent distributed normal solid with no piezoelectricity and the action of voltage is taken as equivalent force acting on the MPS. However, their proposition is not well proved. Besides, the related equivalent constants, which are required to be determined from experiments, make the models hard to predict behaviours, when the experiments are not available.

The 3-port equivalent circuit proposed herein offers an explicit representation of electro-mechanical coupled behaviours of MPS, which separates the MPS into two acoustic ports and one electrical port through an electromechanical transformer. Compared with existing circuit models in literature, the proposed circuit model can
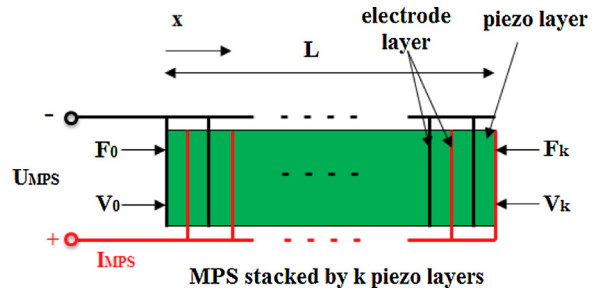
be extended to any electrical and mechanical condition. Besides, as the proposed circuit elements are explicitly and exactly derived in terms of material and dimension information rather than determined from measured information, the proposed circuit model allows one to predict behaviours with material properties and structural dimension. The configuration of the proposed circuit is inspired by the idea of network theory and each electrical element in the proposed equivalent circuit is derived exactly on the basis of simplified fundamental of MPS presented in the previous paper of the authors [8].

## 3. Fundamentals of MPS

The schematic of MPS is shown in Fig. 3, where each piezo layer is mechanically connected in series and electrically connected in parallel. By applying voltage/charge to MPS, it can produce force/displacement in the longitudinal direction of MPS ($x$ direction shown in Fig. 3) and vice versa. The former is called transmitter mode which can be used as an actuator and the latter is called receiver mode which can be used as a sensor or energy harvester. In transmitter mode, the stack configuration of MPS allows a large displacement output with a low voltage input in a compact size. In receiver mode (sensors and energy harvesters), the stack configuration enables a large charge output for equivalent force inputs.

The proposed equivalent circuit is based on the simplified fundamentals of MPS, which is presented and justified in the previous paper of the authors [8]. For the completeness of the formulation of the equivalent circuit, the simplified fundamentals of MPS are reproduced here.

To facilitate the model formulation, define MPS with overall length $L$ stacked by $k$ piezo layers and assign an $x$ axis along the length. Since, MPS is designed for its longitudinal vibration (the stack is more than three times longer than wide), the vibration is associated with a uniaxial stress state (i.e. the lateral stress is zero). For the operation of MPS, the electrical field is only applied to the direction of vibration (i.e. the electrical field in lateral directions is zero). Based on these two conditions, the constitutive equations of each piezo layer in MPS along the longitudinal direction can derived from the 3-D piezoelectric constitutive equations of IEEE standards [1], shown in Eq. (1).

$$T_3 = c'S_3 - e'E_3, \tag{1.a}$$

$$D_3 = e'S_3 + \epsilon'E_3, \tag{1.b}$$

where $T$, $S$, $E$, and $D$ are respectively stress, strain, electrical field, and electrical displacement. $c'$, $e'$, and $\epsilon'$ are piezoelectric coefficients ($c' = 1/s_{33}^E$, $e' = d_{33}/s_{33}^E$, and $\epsilon' = \epsilon_{33}^T - d_{33}^2/s_{33}^E$). $s_{33}^E$, $d_{33}$, and $\epsilon_{33}^T$ are the standardized piezoelectric coefficients [1]. The subscript '3' stands for the direction of polarization (i.e. $x$ direction in this case). For the convenience, this subscript '3' will be omitted in the later notations.
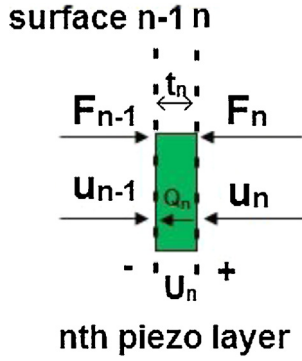
**Fig. 4.** Analysis of nth piezo layer in MPS.

$T$, $S$, $E$, and $D$ can be respectively expressed as follows:

$$T(x,t) = \frac{N(x,t)}{A}, \tag{2.a}$$

$$S(x,t) = \frac{\partial u(x,t)}{\partial x}, \tag{2.b}$$

$$E(x,t) = -\frac{\partial \phi(x,t)}{\partial x}, \tag{2.c}$$

$$D(x,t) = \frac{Q(x,t)}{A}, \tag{2.d}$$

where $N$ and $u$ are respectively the normal force and displacement, $\phi$ and $Q$ are electrical potential and electrical charge respectively, $A$ is the cross-section of the piezo layer. The arguments '$x$' and '$t$' are position and time variables respectively, which will be omitted in the later notations for briefness.

To derive a simple but effective distributed-parameter analytical model, the following simplifications for MPS are mathematically justified and applied.

With reference to Fig. 4, consider the $n$th piezo layer at certain position $x_n$ of MPS with thickness $t_n$ (where $n = 1, 2, 3...k$). The charge balance in the $x$ direction gives:

$$\frac{\partial Q_n}{\partial x} = 0. \tag{3}$$

Substituting Eq. (1.b) into Eq. (3) with Eqs. (2.b), (2.c), and (2.d) results in:

$$\frac{\partial^2 \phi}{\partial^2 x} = -\frac{e'}{\epsilon'}\frac{\partial^2 u}{\partial^2 x}, \tag{4}$$

Integrating Eq. (4) with regard to $x$ yields:

$$E_3 = -\frac{e'}{\epsilon'}S_3 + B_1, \tag{5}$$

where $B_1$ is an integration constant.

Considering that each piezo layer is often far less than the overall length of MPS in longitudinal direction (i.e. $t_n = \frac{L}{k}$ is far smaller than $L$), the distribution of the displacement across $t_n$ can be assumed to be uniform (i.e $S$ is a constant) for a certain number of the first vibration modes whose quarter wavelength is far larger than the thickness of piezo layer $t_n$. This fact limits the frequency range of the simplification to a certain number of the first vibration modes and errors might occur, when the simplification is applied to model high-order vibration modes. Note, as high-order vibration modes in practice are almost damped out due to the mechanical and electrical loss and are trivial in practical applications of MPS, this issue is of minor importance.

Then, based on Eq. (5), $E_3$ can be seen as a constant (i.e. the distribution of the electrical field across $t_n$ is uniform). Therefore, $E_3$ can be simplified as follows:

$$E_3 = -\frac{\partial \phi}{\partial x} \rightarrow -\frac{\phi(x_p + t_n) - \phi(x_p)}{t_n} = \frac{U_n}{t_n}. \tag{6}$$

For the electrical side, also considering that the distribution of the displacement across $t_n$ can be assumed to be uniform as reasoned before, the induced charge on the surfaces of $n$th piezo layer can be simplified in the following way:

$$Q_n = AD_n = A(e'S_3 + \epsilon'E_3)$$
$$\rightarrow A(e'\frac{u_n - u_{n-1}}{t_n} + \epsilon'\frac{U_n(t)}{t_n}). \tag{7}$$

The above justified simplifications allow MPS to be effectively modelled as a whole in a following simple way.

By substituting Eq. (6), Eqs. (2.a) and (2.b), Eq. (1.a) can be simplified as follows:

$$N = A_n(c'\frac{\partial u}{\partial x} - e'\frac{U_n}{t_n}). \tag{8}$$

Assuming negligible thickness of electrode layers and considering that each piezo layer in MPS has the same material properties ($c', e', \epsilon'$ and density), dimensions (thickness and cross-section area). and the same applied voltage ($U_n = U_{MPS}$) due to the electrically parallel connected structure, it is possible and effective to apply a single constitutive equation for the whole MPS, shown in the following form:

$$N = A(c'\frac{\partial u}{\partial x} - e'\frac{U_{MPS}}{t_p}). \tag{9}$$

Based on the Newton's Second law in the $x$ direction, the following equation of motion can be derived:

$$\frac{\partial N}{\partial x} = \rho A\frac{\partial^2 u}{\partial^2 t}, \tag{10}$$

where $\rho$ is the density of piezo layer.

Substituting Eq. (9) in Eq. (10) gives:

$$c'\frac{\partial^2 u(x,t)}{\partial^2 x} = \rho\frac{\partial^2 u(x,t)}{\partial^2 t}, \tag{11}$$

Using the principle of separation of variables, for excitation voltage $U_{MPS}(t) = U_0 e^{jwt}$, the general solution of displacement $u(x,t)$ to Eq. (11) can be written in the following form:

$$u = (A_1 \sin(ax) + A_2 \cos(ax))e^{jwt}, \tag{12}$$

where $a = \sqrt{\frac{\rho w^2}{c'}}$, $A_1$ and $A_2$ are constants, which can be calculated from the boundary conditions at two ends of MPS.

Substituting Eq. (12) into Eq. (9) gives the general solution of the normal force

$$N = A\begin{bmatrix} c'(A_1 a\cos(ax) \\ -A_2 a\sin(ax)) - \epsilon'\frac{U_0}{t_n} \end{bmatrix}e^{jwt}. \tag{13}$$

For the electrical side, as each piezo layer in MPS is electrically connected in parallel, the general solution of the total induced charge of MPS can be derived as follows by substituting Eq. (7):

$$Q_{MPS} = \sum_{n=1}^{k} Q_n = A(e'\frac{u_k - u_0}{t_p} + k\epsilon'\frac{U_{MPS}(t)}{t_p}), \tag{14}$$

where $k$ is the total number of piezo layers in MPS ($k = \frac{L}{t_p}$).
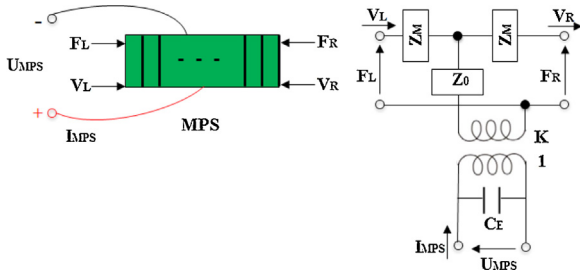
47

**Fig. 5.** Three-port equivalent circuit of MPS.

By differentiating displacement $u(x, t)$ and electrical charge $Q_{MPS}(t)$ with respect to time variable $t$, the general solution of the velocity $v(x, t)$ and induced current $I_{MPS}(t)$ can be derived:

$$v(x, t) = jw(A_1 \sin(ax) + A_2 \cos(ax))e^{jwt}, \tag{15.a}$$

$$I_{MPS}(t) = A(e' \frac{v_k - v_0}{t_p} + k\epsilon' \frac{U_{MPS}(t)}{t_p} jw). \tag{15.b}$$

Note, the mechanical damping and electrical damping, which respectively account for the mechanical loss and mechanical loss, can be easily considered by adding positive imaginary part to stiffness material constant ($c'$ in this case) and adding negative imaginary part to permittivity material constant ($\epsilon'$ in this case) [9].

## 4. Construction of equivalent circuit

Based on the fundamentals of MPS presented in Section 3, an exact equivalent circuit is constructed in this section, which is inspired by the idea of network theory.

Referring to Figs. 3 and 4 boundary conditions at both ends of MPS can be derived, shown as follows:

$$v_0 = v(0, t), \tag{16.a}$$

$$v_k = v(L, t). \tag{16.b}$$

$$F_0 = N(0, t), \tag{16.c}$$

$$F_k = N(L, t). \tag{16.d}$$

There are 8 unknowns $(A_1, A_2, , U_{MPS} U_{MPS}, v_0, v_k, \text{and})$ in 5 equations (Eqs. (15.b), (16.a), (16.b), (16.c) and (16.d)). Therefore, $F_0$, $F_k$ and $U_{MPS}$ $(A_1, A_2)$ can be expresses with regard to $v_0$, $v_k$ and $I_{MPS}$ in the following matrix form:

Based on Eq. (17), the following MPS circuit shown in Fig. 5 with exact equivalence can be found. In the equivalent circuit, $C_E = \frac{k\epsilon'A}{t_p}$, $K = A\frac{e'}{t_p}$, $Z_0 = \frac{c'aA}{jw \sin(aL)}$ and $Z_M = \frac{c'a(\cos(aL)-1)A}{jw \sin(aL)}$. The subscript '$L$' and '$R$' stands for the left and right side of MPS (corresponding with the '0' and '$k$' in this case). $C_E$ is electrical impedance of MPS, while $Z_0$ and $Z_M$ are the impedance from the mechanical side. $K$ is the value of the electro-mechanical transformer. Note, the mechanical damping and electrical damping, which respectively account for the mechanical loss and mechanical loss, can be easily considered by adding positive imaginary part to stiffness material constant ($c'$ in this case) and adding negative imaginary part to permittivity material constant ($\epsilon'$ in this case) [9].

The 3-port equivalent circuit, which separates the MPS into two acoustic ports and one electrical port through an electro-mechanical transformer, offers an explicit representation of electro-mechanical coupled behaviours of MPS. Compared with existing circuit models in literature, the proposed circuit model can be extended to any electrical and mechanical condition. Besides, as the proposed circuit elements are explicitly and exactly derived in terms of material and dimension information rather than determined from measured information, the proposed circuit model allows one to predict behaviours with material properties and structural dimension for design, fabrication, and optimization purpose. It is very straightforward to apply and effectively simplifies and facilitates the analysis, modelling, and calculation of free and loaded vibration of MPS in either transmitter mode (actuator) or receiver mode (sensor or energy harvester).

## 5. Validation and discussion

To further validate the formulated equivalent circuit model, a simple case study of free and loaded vibration of MPS shown in Fig. 6 is carried out. The MPS is stacked by 10 piezo layers with negligible thickness of electrode layers and with the left end fixed. The right end of MPS is set free for case 1 and loaded with a propagating medium for case 2. The dimension of the MPS is defined in Table 1 and the piezoelectric material properties are with reference to N10[8]. The propagating medium is chosen to have the same dimension with MPS and its material is chosen to be epoxy resin

**Table 1**
Simulation parameters.

| $L$ (m) | $A$ (m$^2$) | $k$ | Material property |
|---|---|---|---|
| 0.04 | $1.6 \times 10^{-5}$ | 10 | N10 [8] |

$$
\begin{bmatrix} F_0 \\ F_k \\ U_{MPS} \end{bmatrix} = \begin{bmatrix} \frac{A}{jw}\left(\frac{e'^2}{k\epsilon't_p} + \frac{c'a}{\tan(aL)}\right) & -\frac{A}{jw}\left(\frac{c'a}{\sin(aL)} + \frac{e'^2}{k\epsilon't_p}\right) & \frac{e'}{jwk\epsilon'} \\ \frac{A}{jw}\left(\frac{e'^2}{k\epsilon't_p} + \frac{c'a}{\sin(aL)}\right) & -\frac{A}{jw}\left(\frac{c'a}{\tan(aL)} + \frac{e'^2}{k\epsilon't_p}\right) & \frac{e'}{jwk\epsilon'} \\ \frac{e'}{jwk\epsilon'} & -\frac{e'}{jwk\epsilon'} & \frac{t_p}{jwk\epsilon'A} \end{bmatrix} \begin{bmatrix} v_0 \\ v_k \\ I_{MPS} \end{bmatrix} . \tag{17}
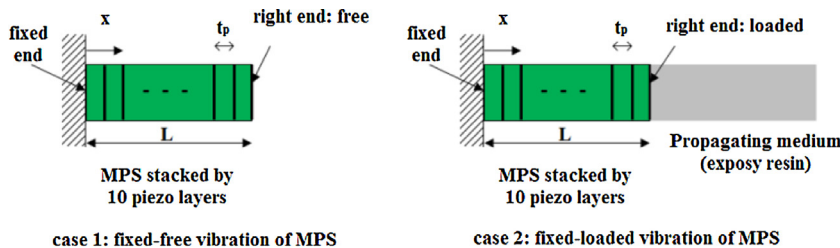$$



**Fig. 6.** Case study: free and loaded vibrations of MPS.
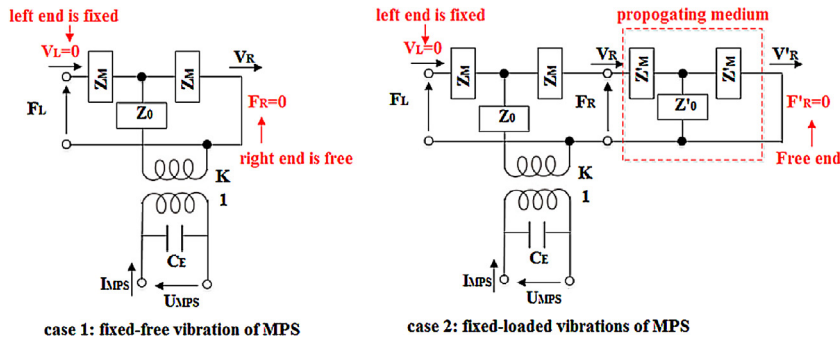
**Fig. 7.** Equvalent circuit of the study case.
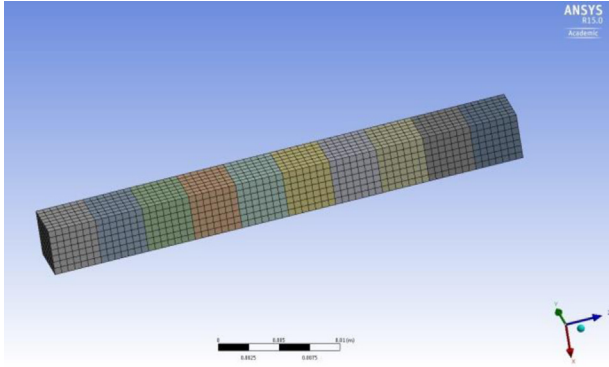


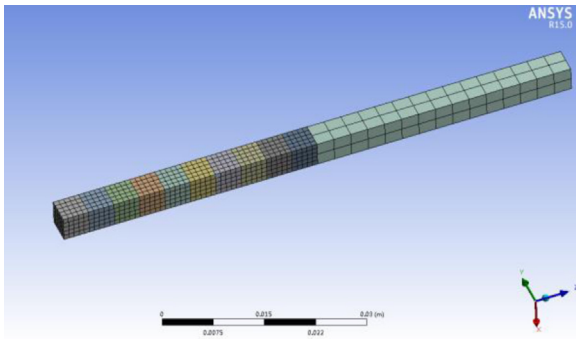**Fig. 8.** Meshed FEA model of fixed-free MPS.



**Fig. 9.** Meshed FEA model of fixed-loaded MPS.



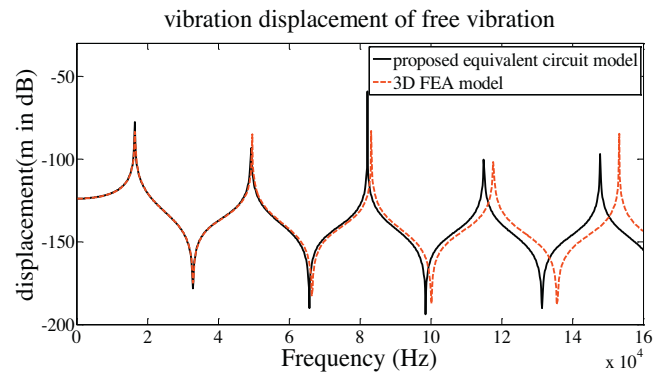**Fig. 10.** Vibration velocity of free vibration.



Fig. 11. vibration deformation of free vibration

**Fig. 11.** Vibration deformation of free vibration.

(density: 1170 kg/m$^3$; Young's modulus: 8.2163 × 10$^9$ Pa; Poisson ratio: 0.3). The validation is achieved by checking the results simulated by the proposed equivalent circuit against those simulated by a 3D FEA model developed in ANSYS. The frequency response of the vibration velocity $v_R$ and deformation $u_R$ (can be derived by integrating $v_R$) at the right end of MPS, are chosen to be simulated and compared for both case 1 and 2.

Based on the proposed equivalent circuit shown in Fig. 5, the equivalent circuits of case 1 and 2 can be constructed as shown in Fig. 7. A 3D FEA model of both case 1 and 2 is developed on the commercial software ANSYS. Case 1 and 2 are finely auto meshed respectively with 18,560 nodes and 3430 elements shown in Fig. 8 and with 8031 nodes and 1310 elements shown in Fig. 9, which is sufficient enough to ensure a high resolution. Other conditions are defined as specified in the study case. By applying a harmonic voltage of 100 V, the frequency response of the right-end velocity $v_R$ and deformation amplitude $u_R$ of MPS are simulated to be compared with equivalent results simulated by the proposed circuit model.

Figs. 10 and 11 respectively show vibration velocity and deformation of case 1 simulated by the proposed equivalent circuit model and 3D FEA model. For the convenience of comparison, both mechanical loss and electrical loss are not taken into account. As motioned before, for the proposed equivalent circuit, the mechanical loss and electrical loss can be easily taken into account respectively by adding positive imaginary part to stiffness material coefficient and adding negative imaginary part to permittivity material coefficient [9]. Compared with 3D FEA models, the proposed circuit model shows a good match for the first two resonant modes of both velocity and displacement and the errors begin to occur at the second anti-resonant modes. The errors are expected due to the compromised assumption of simplification which the proposed circuit model is based on. As the thickness of piezo layer ($t_n = \frac{L}{10}$) is approaching to the quarter wavelength (approximately $\frac{L}{4}$) of the second anti-resonant mode, it becomes less effective to assume that the displacement of each piezo layer is uniformly
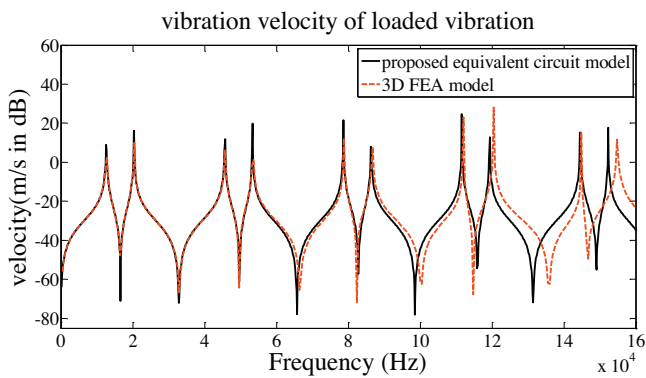
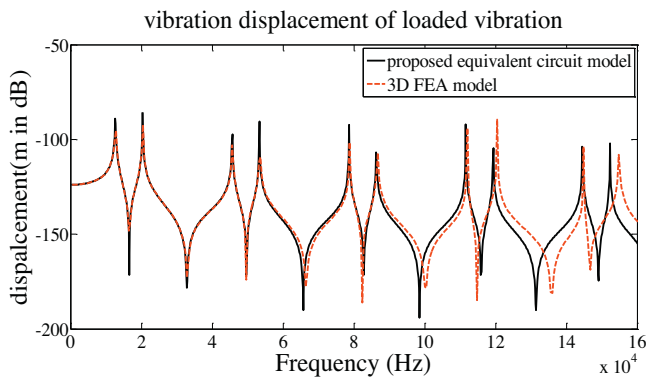**Fig. 12.** Vibration velocity of loaded vibration.



**Fig. 13.** Vibration deformation of loaded vibration.

distributed across each layer. Figs. 12 and 13 respectively show vibration velocity and deformation of loaded vibration in case 2. The results show that the proposed circuit model is also effective for loaded MPS vibration. Besides, the proposed circuit model can effectively capture more resonant modes (6 resonant modes) for loaded MPS vibration, compared with free MPS vibration (2 resonant modes). This is under expectation. As the vibration wavelength for the loaded MPS becomes larger, it is more effective to assume that the displacement of each piezo layer is uniformly distributed across each layer. It was worth noting from the assumption of the proposed circuit model that more vibration modes can be effectively captured by the proposed circuit model, when more piezo layers are stacked or when MPS is connected with other propagating mediums. The limitation for modelling high-order vibration modes is of minor importance, as high-order resonant modes in practice are almost damped out due to the mechanical and electrical loss and are trivial in practical applications of MPS.

## 6. Summary

In this paper, inspired by the idea of network theory, a 3-port equivalent circuit of multi-layer piezoelectric stack (MPS) is proposed and formulated exactly on the basis of simplified fundamentals of MPS. The 3-port equivalent circuit, which separates the MPS into two acoustic ports and one electrical port through an electro-mechanical transformer, offers an explicit representation of electro-mechanical coupled behaviours of MPS. It is very straightforward to apply and effectively simplifies and facilitates the analysis, modelling, and calculation of free and loaded MPS vibration in either transmitter mode (actuator) or receiver mode (sensor or energy harvester). Compared with existing circuit models in literature, the proposed circuit can be extended to any electrical and mechanical condition. Besides, as the proposed cir-

cuit elements are explicitly and exactly derived in terms of material and dimension information rather than determined from measured information, the proposed circuit model allows one to predict behaviours with material properties and structural dimension. A simple case study of free and loaded vibrations of MPS has been carried out for validation. For both free and loaded vibrations of MPS in the case study, the effectiveness of the proposed circuit has been validated by 3D FEA models.

## References

[1] A. Meitzler, H.F. Tiersten, A.W. Warner, D. Berlincourt, G.A. Couqin, F.S. Welsh III, IEEE Standard on Piezoelectricity, IEEE, Ultrasonics, Ultrason. Ferro-electr. Freq. Control Society, 1987.
[2] K.S. Van Dyke, The electric network equivalent of a piezoelectric resonator, Phys. Rev. 25 (6) (1925) 895.
[3] M. Guan, W.-H. Liao, Studies on the circuit models of piezoelectric ceramics Information Acquisition, IEEE Proceedings in International Conference on Information Acquisition (2004) 26–31.
[4] B.L. Grisso, J.K. Kim, D.S. Ha, D.J. Inman Guan, W.-H. Liao, Electrical modelling of piezoelectric ceramics for analysis and evaluation of sensory systems, IEEE Sensors Applications Symposium (2008) 122–127.
[5] M. Goldfarb, N. Celanovic, Modeling piezoelectric stack actuators for control of micromanipulation, IEEE Control Systems 17 (3) (1997) 69–79.
[6] H. Adriaens, W.D. Koning, R. Banning, IEEE/SME Transactions on Mechatronics, 5 2000 331–341.
[7] X.B. Chen, Q.S. Zhang, D. Kang, W.J. Zhang, On the dynamics of piezoactuated positioning systems, Rev. Sci. Instrum. 79 (11) (2008), 116101. 1–116101.3.
[8] Y.K. Zhang, T.-F. Lu, A. Sarawi, Formulation of a simple distributed-parameter model of multi-layer piezoelectric actuators, J. Intell. Mater. Syst. Struct. (2015), http://dx.doi.org/10.1177/1045389x15595294 (published online).
[9] R. Holland, Representation of dielectric, elastic, and piezoelectric losses by complex coefficients, IEEE Trans. Sonics Ultrasonics 14 (1) (1967) 18–20.

## Biographies
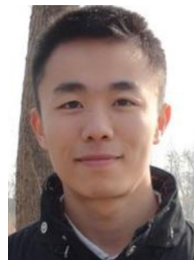
**Yangkun Zhang** received his Bachelor (1st class honours) degree from University of Adelaide, Australia in 2012. He is now a PhD student in School of Mechanical Engineering, University of Adelaide, Australia. His research focuses on modelling of multi-layer piezoelectric stacks and their applications.
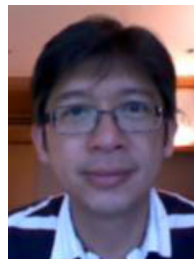
**Tien-Fu Lu** received his Bachelor and MS of Science in Mechanical Engineering from National Cheng Kung University, Taiwan, followed by PhD in Manufacturing and Mechanical Engineering from University of south Australia, Australia, in 1997. He is currently a senior lecturer at the School of Mechanical Engineering, University of Adelaide. His research interests include nano-manipulation and measurement technologies, flexure hinges, compliant mechanisms, chemical plume tracing using robots, operation modelling and optimisation, robotics in mining and agriculture.

**Yuxin Peng** received his Bachelor and Master degrees from Chongqing University, China, in 2007 and 2010. He received his PhD from Department of Nanomechanics, Tohoku University, Japan. He is currently a Research Fellow at the Department of Biomedical Engineering, National University of Singapore, Singapore. His research focuses on piezoelectric actuators and sensor calibration.

**Chapter 5**

**A SIMPLIFIED TRANSFER MATRIX**

**OF D33-MODE LPT**

# CHAPTER 5

# A SIMPLIFIED TRANSFER MATRIX OF D33-MODE LPT

This chapter is based on the following paper:

*Full citation*: Zhang, Y., Lu, T. F., Al-Sarawi, S., Tu, Z. (2016). A Simplified Transfer Matrix of Multi-layer Piezoelectric Stack. *Journal of Intelligent Material Systems and Structures*, 1045389X16651153.

*Contributions of this chapter*: In this chapter, the simplified fundamentals of stack-type d33-mode LPT proposed in Chapter 3 is formulated into a transfer matrix form. Combined with transfer matrix method, the proposed transfer matrix form can greatly facilitate the calculations when stack-type d33-mode LPT is joined by other mediums. For modelling stack-type d33-mode LPT, compared with using the transfer matrix proposed in literature, which is subjected to individual piezo layer in stack-type d33-mode LPT, the proposed simplified transfer matrix, which considers the whole stack-type d33-mode LPT to be an equivalent homogenous bulk, contributes to a much simpler form of analytical solution and greatly cut down the computational effort. Note, although the proposed transfer matrix is aimed at stack-type, it can be also applied to single-type LPT simply by letting the number of piezo layer equal 1. Even for modelling individual piezo layer, the proposed transfer matrix based on the simplified fundamentals is simpler and more computationally efficient than the transfer matrix formulated in literature on the basis of the complex fundamentals. The effectiveness of the proposed simple transfer matrix is validated by the transfer matrix proposed in literature.

# Statement of Authorship

| Title of Paper | A Simplified Transfer Matrix of Multi-layer Piezoelectric Stack |
|---|---|
| Publication Status | ☐ Published   ☑ Accepted for Publication<br>☐ Submitted for Publication   ☐ Unpublished and Unsubmitted work written in manuscript style |
| Publication Details | Zhang, Y., Tu, Z., Lu, T.F., Al-Sawari, S.(2016). A Simplified Transfer Matrix of Multi-layer Piezoelectric Stack, Journal of Intelligent Material Systems and Structures (Accepted on 22/04/2016). The editor's email concerning the acceptance of the manuscript has been attached as evidence. |

## Principal Author

| Name of Principal Author (Candidate) | Mr. Yangkun Zhang |
|---|---|
| Contribution to the Paper | Develop theory, performed simulations, analysed data and wrote the manuscript |
| Overall percentage (%) | 70% |
| Certification: | This paper reports on original research I conducted during the period of my Higher Degree by Research candidature and is not subject to any obligations or contractual agreements with a third party that would constrain its inclusion in this thesis. I am the primary author of this paper. |
| Signature | Date 27/04/2016 |

## Co-Author Contributions

By signing the Statement of Authorship, each author certifies that:

i.   the candidate's stated contribution to the publication is accurate (as detailed above);

ii.  permission is granted for the candidate in include the publication in the thesis; and

iii. the sum of all co-author contributions is equal to 100% less the candidate's stated contribution.

| Name of Co-Author | Dr. Tien-Fu Lu |
|---|---|
| Contribution to the Paper | Supervised the research, review and revised the manuscript |
| Signature | Date 2/05/16 |

| Name of Co-Author | Dr. SAID Al-SARAWI |
|---|---|
| Contribution to the Paper | Supervised the research, review and revised the manuscript |
| Signature | Date 27/4/2016 |

Please cut and paste additional co-author panels here as required.

| Name of Co-Author | Mr. Zhen Tu |
|---|---|
| Contribution to the Paper | Help edit the manuscript |
| Signature | |

| Date | 27/04/2016 |
|---|---|

54

Zhang, Y., Lu, T. F., Al-Sarawi, S., Tu, Z. (2016). A Simplified Transfer Matrix of Multi-layer Piezoelectric Stack.
*Journal of Intelligent Material Systems and Structures*, 28(5), 595-603.

# Chapter 6

# SIMPLIFIED EQUIVAELNT FINITE ELEMENT MODELS OF D33-MODE LPT

# CHAPTER 6

# SIMPLFIED EQUIVALENT FINITE ELEMENT MODELS OF D33-MODE LPT

This chapter is based on the following submitted paper:

Zhang, Y., & Lu, T-F. (2016). Simple Equivalent Finite Element Models of D33-Mode Multi-layer Piezoelectric Actuator, submitted to *Smart Materials and Structures*

*Contributions of this chapter*: In this chapter, based on the uniform-electric-field approximation, two simple equivalent finite element models of stack-type d33-mode LPT are proposed and developed for computation when stack-type d33-mode LPT are used in complex structures. The proposed finite element models consider multi-layer d33-mode LPT as equivalent homogenous bulk which could simply meshed with pure-solid and consider the inverse piezoelectric effect of the applied voltage with equivalent external forces. Compared with direct finite element modelling of stack-type d33-mode LPT by using an electro-mechanical coupled and multi-layer model, the proposed finite element models greatly facilitate the modelling processes and cut down the computational effort. Based on the IEEE standard 3D constitutive relations of piezoelectricity, the rationale behind the proposed equivalent models together with the scope and limitation are presented. Also, the related equivalent forces and other equivalent parameters are derived in terms of the standard 3D piezoelectric coefficients. The proposed models can be applied to both single-type and stack-type. The effectiveness of the proposed simple equivalent finite element models has been validated by direct finite element modelling of d33-mode LPT in commercial software ANSYS.

## Statement of Authorship

## Statement of Authorship

| Title of Paper | Simple Equivalent Finite Element Models of D33-Mode Multi-layer Piezoelectric Actuator |
|---|---|
| Publication Status | ☐ Published       ☐ Accepted for Publication <br> ☑ Submitted for Publication    ☐ Unpublished and Unsubmitted work written in manuscript style |
| Publication Details | Zhang, Y., & Lu, T. F. (2016). Simple Equivalent Finite Element Models of D33-Mode Multi-layer Piezoelectric Actuator, submitted to *Smart Materials and Structures* |

### Principal Author

| Name of Principal Author (Candidate) | Mr. Yangkun Zhang |
|---|---|
| Contribution to the Paper | Developed theory, performed simulations, analyzed data and wrote the manuscript |
| Overall percentage (%) | 80% |
| Certification: | This paper reports on original research I conducted during the period of my Higher Degree by Research candidature and is not subject to any obligations or contractual agreements with a third party that would constrain its inclusion in this thesis. I am the primary author of this paper. |
| Signature | Date   16 / 02 / 2016 |

### Co-Author Contributions

By signing the Statement of Authorship, each author certifies that:

i.   the candidate's stated contribution to the publication is accurate (as detailed above);

ii.  permission is granted for the candidate in include the publication in the thesis; and

iii. the sum of all co-author contributions is equal to 100% less the candidate's stated contribution.

| Name of Co-Author | Dr. Tien-Fu Lu |
|---|---|
| Contribution to the Paper | Supervised research, reviewed manuscript |
| Signature | Date   16 / 02 / 16 |

# Simple Equivalent Finite Element Models of D33-Mode Multi-layer Piezoelectric Actuator

YANGKUN ZHANG AND TIEN-FU LU

*School of Mechanical Engineering, University of Adelaide, 5005, Australia*
*Author to whom correspondence should be addressed. E-mail: yangkun.zhang@adelaide.edu.au

**ABSTRACT:** D33-mode multi-layer piezoelectric actuators (MPA) are widely used linear actuators. When d33-mode MPA are used in a complex structure, a finite element model is widely applied for computation and analysis. For direct finite element modelling of d33-mode MPA, the stacked configuration makes model defining process cumbersome and the electro-mechanical coupled behaviours of piezo material which need to be meshed with electro-mechanical coupled elements consumes large computational efforts, thus inducing a long model solving time. In this paper, two simple equivalent finite element models of d33-mode MPA are proposed. The proposed finite element models consider multi-layer d33-mode MPA as an equivalent homogenous bulk which could be simply meshed with pure-solid elements and consider the inverse piezoelectric effect of the applied voltage with equivalent external forces, which greatly facilitates the modelling processes and greatly cuts down the computational effort. Based on the IEEE standard 3D constitutive relations of piezoelectricity, the rationale behind the proposed equivalent models together with the scope and limitation are presented. Also, the related equivalent forces and other equivalent parameters are derived in terms of the standard 3D piezoelectric coefficients. Simulations are carried out in commercial software ANSYS, which validates the effectiveness and also shows the limitation of the proposed equivalent models.

**Keywords:** D33-mode, multi-layer, piezoelectric, actuator, 3D, equivalent, finite element model

**69**

## 1. Introduction

D33-mode multi-layer piezoelectric actuators (d33-mode MPA) are linear actuators characteristic of a nano-meter resolution in displacement and compact size. They are widely used as high-precision positioning units or vibrators for a wide range of applications, such as optical alignment in Lenz modules (Lee et al 2011) and cell manipulation in microbiology (Zhang et al 2002). In these applications, modelling electro-mechanical coupled behaviours of d33-mode MPA, which can be used to predict their performance, plays a vital role in their design, manufacture and optimization. When d33-mode MPA is used in a complex structure (for example, when combined with flexure mechanism for displacement amplification purpose) (Lu et al 2004;Li et al 2012; Yong and Mohemani 2013), a finite element model is widely applied for computation and analysis. For direct finite element modelling of d33-mode MPA, the stacked configuration makes model defining process cumbersome and the electro-mechanical coupled behaviours of piezo material which need to be meshed with electro-mechanical coupled elements consumes large computational efforts, thus inducing a long model solving time.

In this paper, two simple equivalent finite element models of d33-mode MPA are proposed. The proposed finite element models consider multi-layer d33-mode MPA as equivalent homogenous bulk which could simply meshed with pure-solid and consider the inverse piezoelectric effect of the applied voltage with equivalent external forces, which greatly facilitates the modelling processes and greatly cuts down the computation effort.

## 2. Physical Background
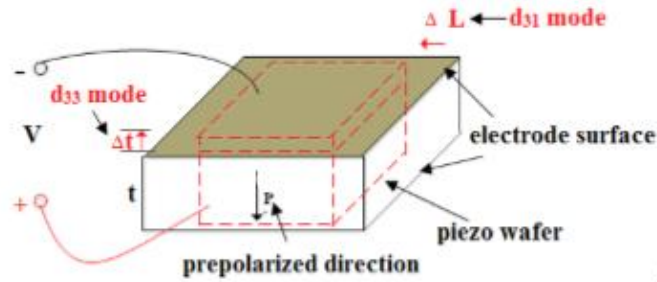


**Figure 1 D33-mode and d31-mode of piezoelectricity**
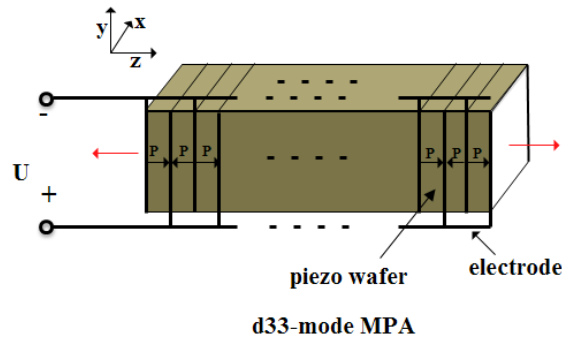


**Figure 2 Configuration of d33-mode MPA**

With reference to Figure 1, when a voltage is applied to the piezo wafer in the direction opposite to its pre-polarized direction, it will induce an expansion in the polarized direction $\Delta t$ (known as d33-mode of piezoelectricity) and a contraction in the direction orthogonal to the polarized direction $\Delta L$ (known as d31-mode of piezoelectricity). In principle, both d31-mode and d33-mode can be used as linear actuator. However, as the d33-mode often has a larger voltage-deformation conversion coefficient than the d31-mode (Arevalo and Foulds 2013), d33-mode is widely used. As the displacement for a single wafer is too small to be used, a multi-layer stack configuration with reference to Figure 2 is often used to enable a large deformation with a low voltage operation in a compact size (Adriaens et al 2000). For d33-mode MPA, each piezo layer is mechanically

connected in series and electrically connected in parallel. The following section will provide a rationale that such configurations of d33-mode MPA can be effectively considered as an equivalent homogenous pure-solid bulk actuated with equivalent external forces.

## 3. Rationale

Based on the IEEE standards on piezoelectricity (Meitzler, Tiersten et al 1988), the 3-D piezoelectric constitutive equations of piezoelectricity can be shown below:

$$
\begin{Bmatrix} T_1 \\ T_2 \\ T_3 \\ T_4 \\ T_5 \\ T_6 \end{Bmatrix} = \begin{bmatrix} c_{11}^E & c_{12}^E & c_{13}^E & 0 & 0 & 0 \\ c_{12}^E & c_{22}^E & c_{23}^E & 0 & 0 & 0 \\ c_{13}^E & c_{23}^E & c_{33}^E & 0 & 0 & 0 \\ 0 & 0 & 0 & c_{44}^E & 0 & 0 \\ 0 & 0 & 0 & 0 & c_{55}^E & 0 \\ 0 & 0 & 0 & 0 & 0 & c_{66}^E \end{bmatrix} \begin{Bmatrix} S_1 \\ S_2 \\ S_3 \\ S_4 \\ S_5 \\ S_6 \end{Bmatrix} + \begin{bmatrix} 0 & 0 & e_{31} \\ 0 & 0 & e_{32} \\ 0 & 0 & e_{33} \\ 0 & e_{24} & 0 \\ e_{15} & 0 & 0 \\ 0 & 0 & 0 \end{bmatrix} \begin{Bmatrix} E_1 \\ E_2 \\ E_3 \end{Bmatrix}, \tag{1.a}
$$

$$
\begin{Bmatrix} D_1 \\ D_2 \\ D_3 \end{Bmatrix} = \begin{bmatrix} 0 & 0 & 0 & 0 & e_{15} & 0 \\ 0 & 0 & 0 & e_{24} & 0 & 0 \\ e_{31} & e_{32} & e_{33} & 0 & 0 & 0 \end{bmatrix} \begin{Bmatrix} S_1 \\ S_2 \\ S_3 \\ S_4 \\ S_5 \\ S_6 \end{Bmatrix} + \begin{bmatrix} \varepsilon_{11}^s & 0 & 0 \\ 0 & \varepsilon_{22}^s & 0 \\ 0 & 0 & \varepsilon_{33}^s \end{bmatrix} \begin{Bmatrix} E_1 \\ E_2 \\ E_3 \end{Bmatrix}, \tag{1.b}
$$

where $S_q, T_p, E_k$, and $D_i$ ( $q, p = 1, 2, 3, 4, 5, 6$ and $k, i = 1, 2, 3$ ) are respectively the components of strain tensor $S$, stress tensor $T$, electric field tensor $E$ and electric displacement tensor $D$. $c_{pq}^E$, $e_{kp}$, $\varepsilon_{ik}^S$ are respectively the components of elastic stiffness matrix $c^E$ measured at constant electric fields, piezoelectric stress matrix $e$ measured at constant strains and dielectric coefficients $\varepsilon^S$ measured at constant strains. The subscript

notation follows the IEEE standards (Meitzler, Tiersten et al. 1988) and the measurements of these coefficients are also standardized there.



**Figure 3 Analysis of *n*th piezo layer of d33-mode MPA**

With reference to Figure 3, consider the $n$ th piezo layer at certain position $z_n$ of d33-mode MPA with thickness $t_n$ ( $n = 1, 2, 3...k$ where $k$ is the number of piezo layers in d33-mode MPA). The charge balance in the $z$ direction gives:

$$\frac{\partial D_3}{\partial z} = 0. \tag{2}$$

The third row of Equation (1.b) gives:

$$D_3 = e_{31}S_1 + e_{32}S_2 + e_{33}S_3. \tag{3}$$

Substituting Equation (3) into Equation (2) with $S_1 = \dfrac{\partial u(x,t)}{\partial x}$, $S_2 = \dfrac{\partial u(y,t)}{\partial y}$, $S_3 = \dfrac{\partial u(z,t)}{\partial z}$ and

$E_3 = -\dfrac{\partial \varphi(z,t)}{\partial z}$ gives:

$$e_{31}\frac{\partial^2 u(x,t)}{\partial x \partial z} + e_{32}\frac{\partial^2 u(y,t)}{\partial y \partial z} + e_{33}\frac{\partial^2 u(z,t)}{\partial^2 z} - \varepsilon_{33}^s \frac{\partial^2 \varphi(z,t)}{\partial^2 z} = 0. \tag{4}$$

As $\dfrac{\partial^2 u(x,t)}{\partial x \partial z} = 0$ and $\dfrac{\partial^2 u(y,t)}{\partial y \partial z} = 0$, Equation (4) can becomes:

$$\frac{\partial^2 \varphi(z,t)}{\partial^2 z} = \frac{e_{33}}{\varepsilon_{33}^s}\frac{\partial^2 u(z,t)}{\partial^2 z}, \tag{5}$$

Integrating Equation (5) with regard to $z$ yields:

$$E_3 = -\frac{e_{33}}{\varepsilon_{33}^s} S_3 + B_1, \tag{6}$$

where $B_1$ is an integration constant.

With reference to Figure 3, considering that each piezo layer $t_n$ is often far less than the propagation length in '3' direction (in this case, the propagation length is the overall length $L$ of d33-mode MPA ) (i.e. $t_n = \dfrac{L}{k}$ is far smaller than $L$), the distribution of the displacement across $t_n$ can be assumed to be uniform (i.e. $S_3$ is a constant) for a certain number of the first vibration modes whose quarter wavelength is far larger than the thickness of piezo layer $t_n$ as shown in Figure 3. Note, the mode shapes drawn in Figure 3 are just to illustrate the concept and might not be the exact mode shapes.

Then, based on Equation (6), $E_3$ can be seen as a constant (i.e. the distribution of the electric field across $t_n$ is uniform). Therefore,

$$E_3 = -\frac{\partial \varphi}{\partial z} \rightarrow -\frac{\varphi(x_p + t_n) - \varphi(x_p)}{t_n} = \frac{U_n}{t_n}. \tag{7}$$

The electrical configuration of d33-mode MPA gives $E_1 = E_2 = 0$.

By substituting $E_1$, $E_2$ and $E_3$ into Equation (1.a), the constitutive equation for the $n$ th piezo layer of d33-mode MPA can be derived shown in Equation (8).

$$\begin{Bmatrix} T_1 \\ T_2 \\ T_3 \\ T_4 \\ T_5 \\ T_6 \end{Bmatrix} = \begin{bmatrix} c_{11}^E & c_{12}^E & c_{13}^E & 0 & 0 & 0 \\ c_{12}^E & c_{22}^E & c_{23}^E & 0 & 0 & 0 \\ c_{13}^E & c_{23}^E & c_{33}^E & 0 & 0 & 0 \\ 0 & 0 & 0 & c_{44}^E & 0 & 0 \\ 0 & 0 & 0 & 0 & c_{55}^E & 0 \\ 0 & 0 & 0 & 0 & 0 & c_{66}^E \end{bmatrix} \begin{Bmatrix} S_1 \\ S_2 \\ S_3 \\ S_4 \\ S_5 \\ S_6 \end{Bmatrix} + \begin{bmatrix} e_{31}\dfrac{U_n}{t_n} \\ e_{32}\dfrac{U_n}{t_n} \\ e_{33}\dfrac{U_n}{t_n} \\ 0 \\ 0 \\ 0 \end{bmatrix}, \tag{8}$$

Assuming negligible thickness of electrode layers and considering that each piezo layer in MPA has the same material properties, thickness ($t_n = t_p$ where $t_p$ is the thickness of each piezo layer in MPA) and the same applied voltage ($U_n(t) = U(t)$) due to the electrically parallel connected structure, it is effective to consider Equation (8) as the constitutive equation for the whole d33-mode MPA, which can be written in the form:

$$
\begin{Bmatrix} T_1 \\ T_2 \\ T_3 \\ T_4 \\ T_5 \\ T_6 \end{Bmatrix} = \begin{bmatrix} c_{11}^E & c_{12}^E & c_{13}^E & 0 & 0 & 0 \\ c_{12}^E & c_{22}^E & c_{23}^E & 0 & 0 & 0 \\ c_{13}^E & c_{23}^E & c_{33}^E & 0 & 0 & 0 \\ 0 & 0 & 0 & c_{44}^E & 0 & 0 \\ 0 & 0 & 0 & 0 & c_{55}^E & 0 \\ 0 & 0 & 0 & 0 & 0 & c_{66}^E \end{bmatrix} \begin{Bmatrix} S_1 \\ S_2 \\ S_3 \\ S_4 \\ S_5 \\ S_6 \end{Bmatrix} + \begin{bmatrix} p_1 \\ p_2 \\ p_3 \\ 0 \\ 0 \\ 0 \end{bmatrix},
\tag{9}
$$

Where $p_1 = e_{31} \dfrac{U(t)}{t_p}$, $p_2 = e_{32} \dfrac{U(t)}{t_p}$ and $p_3 = e_{33} \dfrac{U(t)}{t_p}$.

Therefore, based on Equation (9), the electro-mechanical coupled and multi-layer finite element model of d33-mode MPA can be simply considered as an equivalent homogenous bulk meshed with pure-solid elements of elastic stiffness matrix $c^E$ and the effect of voltage can be equivalent to external forces which can induce the equivalent stress $p_1$, $p_2$ and $p_3$. An example of cuboid d33-mode MPA is shown in Figure 4 where the equivalent opposite forces can be calculated by $F_i = p_i \cdot A_i = e_{3i} \dfrac{U(t)}{t_p} A_i$ ($i = 1, 2, 3$ which denote x, y and z axis respectively). This is the proposed model 1.

The proposed model 1 can be further simplified into the proposed model 2 shown as follows.

Equation (9) can be transformed into the following form:

$$
\begin{Bmatrix} S_1 \\ S_2 \\ S_3 \\ S_4 \\ S_5 \\ S_6 \end{Bmatrix} = \begin{bmatrix} s_{11}^E & s_{12}^E & s_{13}^E & 0 & 0 & 0 \\ s_{12}^E & s_{22}^E & s_{23}^E & 0 & 0 & 0 \\ s_{13}^E & s_{23}^E & s_{33}^E & 0 & 0 & 0 \\ 0 & 0 & 0 & s_{44}^E & 0 & 0 \\ 0 & 0 & 0 & 0 & s_{55}^E & 0 \\ 0 & 0 & 0 & 0 & 0 & s_{66}^E \end{bmatrix} \begin{Bmatrix} T_1 + p_1 \\ T_2 + p_2 \\ T_3 + p_3 \\ T_4 \\ T_5 \\ T_6 \end{Bmatrix},
\tag{10}
$$

where the compliance matrix $s^E$ is the inverse matrix of matrix $c^E$ (i.e. $s^E = (c^E)^{-1}$ ) (Meitzler, Tiersten et al. 1988).

For applications of d33-mode MPA, the deformation along the $z(3)$ axis is of interest and the deformation along x and y axis is of little importance. Based on the equivalent deformation on z axis, $p_1$, $p_2$ and $p_3$ can be further equivalent to $p_3'(p_1'=p_2'=0)$ by using the third row of Equation (10):

$$s_{13}^E p_1 + s_{23}^E p_2 + s_{33}^E p_3 = s_{33}^E p_3' \tag{11}$$

Solving Equation (11) gives $p_3' = \dfrac{e_{31}s_{13}^E + e_{32}s_{23}^E + e_{33}s_{33}^E}{s_{33}^E t_p} \cdot U(t)$ .

So, the effect of voltage can be also equivalent to external forces which can simply induce the equivalent stress $p_3'(p_1'=p_2'=0)$. An example of cuboid d33-mode MPA is shown in Figure 5 where the equivalent opposite force $F_3'$ can be calculated by

$F_3' = p_3' \cdot A_3 = \dfrac{e_{31}s_{13}^E + e_{32}s_{23}^E + e_{33}s_{33}^E}{s_{33}^E t_p} A_3 \cdot U(t)$ . This is the proposed model 2.
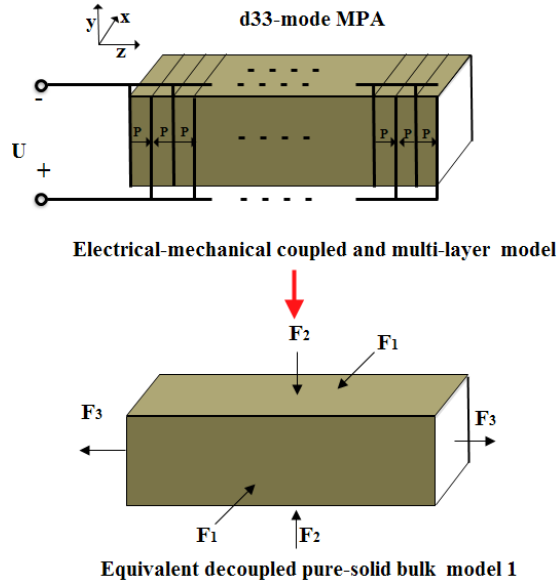
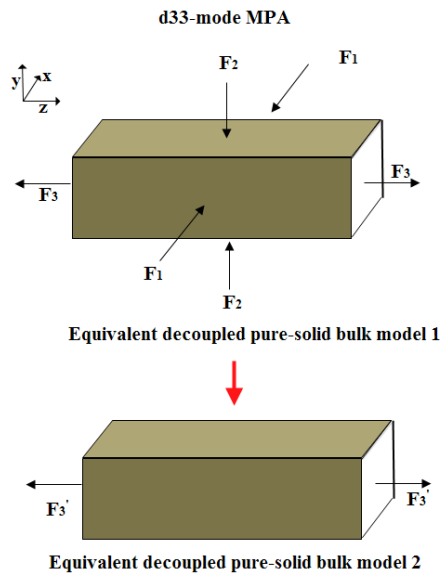**Figure 4 Equivalent decoupled pure-solid bulk model 1 of cuboid d33-mode MPA**



**Figure 5 Equivalent decoupled pure-solid bulk model 2 of cuboid d33-mode MPA**

Note, the proposed two simplified finite element models of d33-mode MPA are based on the condition that the distribution of the displacement across each piezo layer can be

assumed to be uniform. This condition limited the frequency range of the proposed simplified finite element models to a certain multiple of the first resonant frequencies whose corresponding quarter wavelengths are far larger than the thickness of piezo layer as shown in Figure 3. It is worth noting that the more piezo layers are stacked in d33-mode MPA or the more other layers are stacked with d33-mode MPA (i.e. the relative quarter wavelengths are increased, as the propagation length is increased), the more vibration modes will satisfy the condition that their quarter wavelengths are far larger than the thickness of piezo layer, thus resulting in the facts that the more vibration modes and a larger frequency range it can model. For a good performance of d33-mode MPA (i.e. a large output deformation with a low-voltage operation in a compact size), a large amount of piezo layers are often stacked in d33-mode MPA, thus enabling the proposed simplified finite element model of d33-mode MPA with a sufficient effective frequency range for applications. Therefore, the limitation is of minor importance in practice.

## 4. Validation and Discussion

To validate the effectiveness of the proposed two simple equivalent finite element models of d33-mode MPA, a case study is carried out in this section. Frequency responses of free-end displacement for a free-free vibration of d33-mode MPA are simulated for comparisons. The validation is carried out by checking the results simulated by the two proposed equivalent pure-solid bulk models actuated with equivalent external forces against those simulated by electro-mechanical coupled and multi-layer finite element model.

A d33-mode MPA of square cross-section stacked by 10 piezo layers ( $k = 10$, $L = 0.02m$, $A = 0.004 \times 0.004m^2$ and $t_p = \dfrac{L}{k} = 0.002m$ ), shown in Figure 3, is first investigated. The

materials properties of MPA are with reference to PZT-5H (Arevalo and Foulds 2013). The related finite element models are implemented on the commercial software ANSYS.

To obtain the frequency response, the 'Harmonic Response' module in ANSYS is performed. To implement the proposed two models, a bulk normal solid model is simply built and meshed with pure-solid elements shown in Figure 6 and then actuated with equivalent forces as shown in Figure 4 and Figure 5. To implement the electro-mechanical coupled and multi-layer finite element model, the extension package 'Piezo Extension_R150_v8'(ANSYS 2015) is used to allow analyzing electro-mechanical coupled behaviours. A multi-layer configuration of d33-mode MPA is build and meshed with electro-mechanical coupled elements as shown in Figure 7 and actuated with the voltage applied at two ends of each piezo layer.
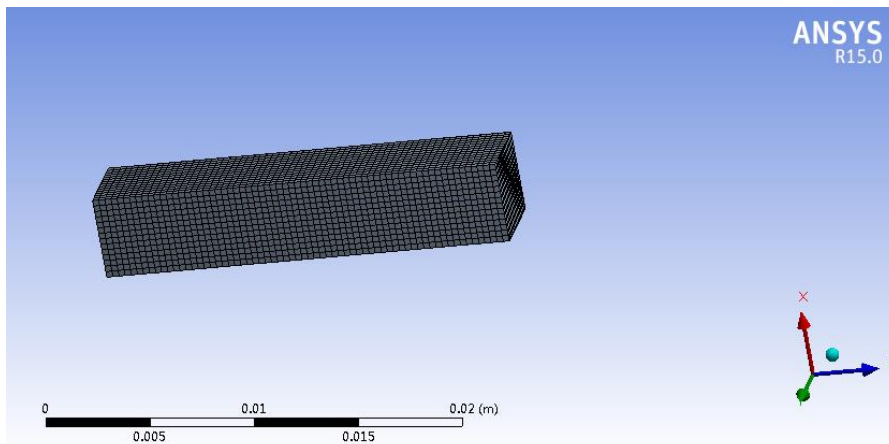


**Figure 6 Meshed pure-solid bulk equivalent model of cuboid d33-mode MPA**
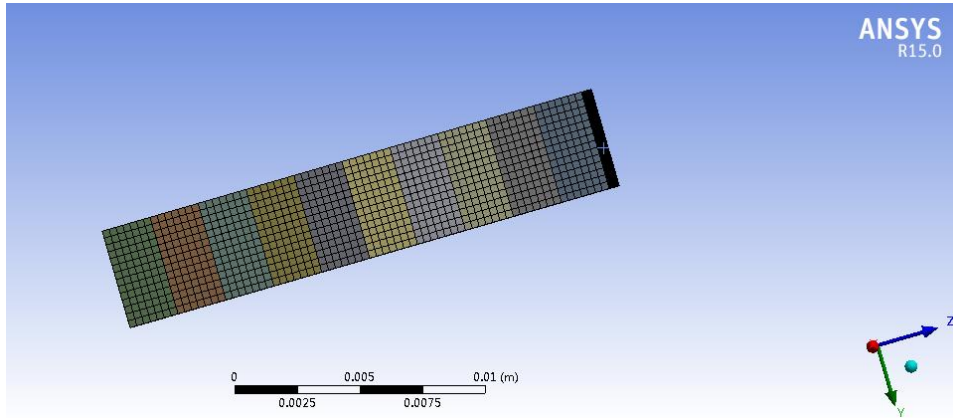
**Figure 7 Meshed electro-mechanical coupled model of cuboid d33-mode MPA**

The simulation results are shown in Figure 8. The simulation results show that the results simulated by the proposed model 2 almost overlap with those simulated by the proposed model 1, which validates their equivalence in modelling deformation along the $z(3)$ axis. Compared with electro-mechanical coupled and multi-layer finite element model, the proposed two models show good match until the frequency rises to the second resonant mode. This is expected. The proposed two simplified finite element models of d33-mode MPA are based on the condition that the distribution of the displacement across each piezo layer can be assumed to be uniform. This condition limits the frequency range of the proposed simplified finite element models to a certain multiple of the first resonant frequencies (in this case only the first resonant mode is accurate.) whose corresponding quarter wavelengths are far larger than the thickness of piezo layer. For the second resonant mode in this case, its quarter wavelength (around $\dfrac{L}{6}$) is not far larger than but approaching to thickness of piezo layer ($\dfrac{L}{10}$). Therefore, the errors are expected from the second resonant mode. For MPA stacked by more than 10 piezo layers (if the overall length $L$ of MPA is kept the same), due to the decrease of relative thickness of piezo layer, more vibrations modes will satisfy the condition that their quarter wavelengths are

far larger than the thickness of piezo layer, resulting in the fact that more vibration modes can be modelled by the proposed two simplified finite element models. The simulations of 20 piezo layer shown in Figure 9 demonstrate this fact. Likewise, for MPA stacked by less than 10 piezo layers (if the overall length $L$ of MPA is kept the same), due to the increase of relative thickness of piezo layer, less vibrations modes will satisfy the condition that their quarter wavelengths are far larger than the thickness of piezo layer, resulting in the fact that less vibration modes can be modelled by the proposed two simplified finite element models. The simulations of 1 piezo layer (the worst situation for the proposed two simplified finite element models) shown in Figure 10 demonstrate this fact. This is the limitation of the proposed two simplified finite element models. However, the limitation is of minor importance in practice. This is because, to achieve a large output deformation with a low voltage input in a compact size, a large amount of piezo layers are often stacked, thus enabling the proposed transfer matrix with a sufficient effective frequency range for applications.
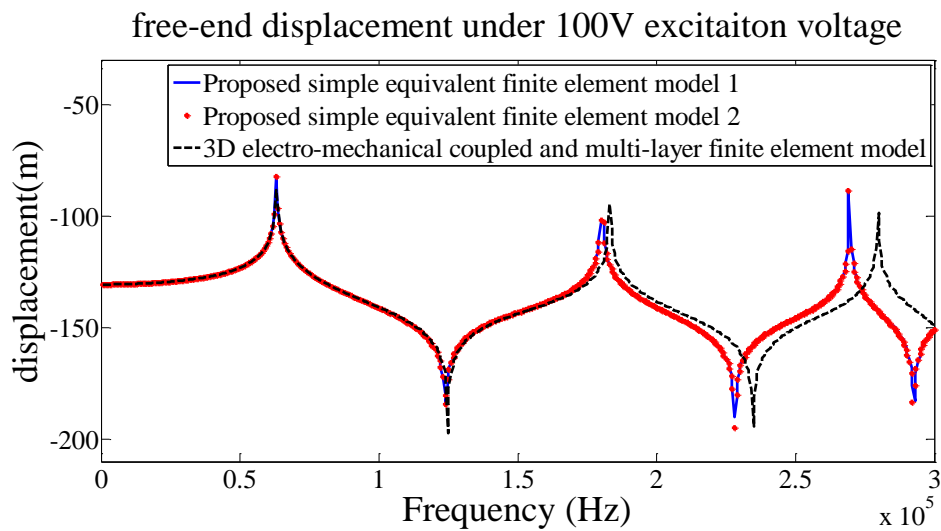


**Figure 8 Simulation results for d33-mode MPA of square cross-section with 10 piezo layers**

free-end displacement under 100V excitaiton voltage
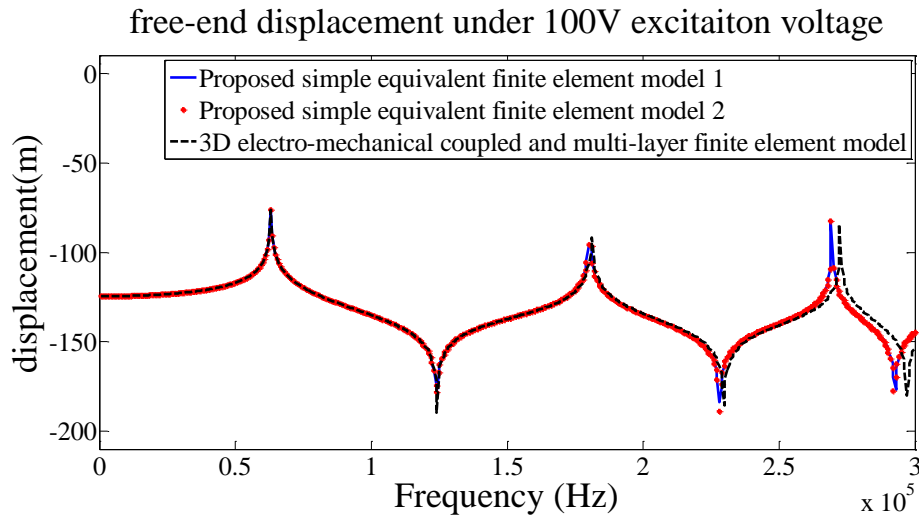


**Figure 9 Simulation results for d33-mode MPA of square cross-section with 20 piezo layers**

free-end displacement under 100V excitaiton voltage
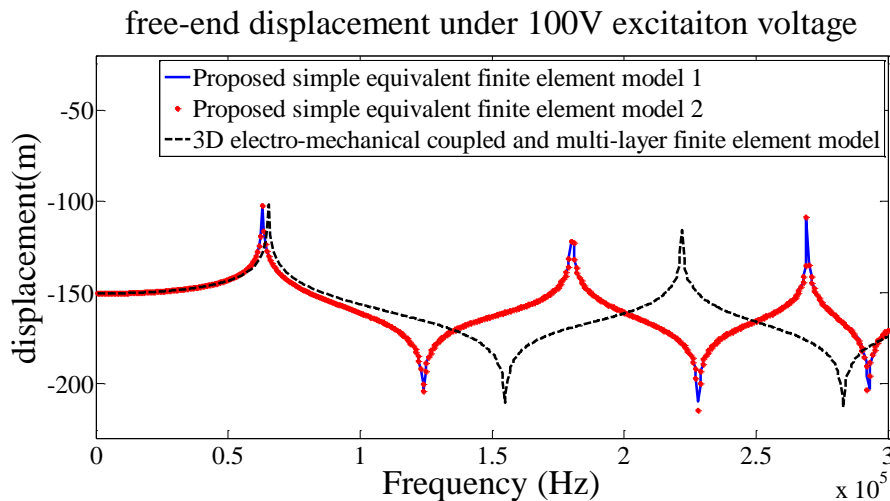


**Figure 10 Simulation results for d33-mode MPA of square cross-section with 1 piezo layer**

Simulations for d33-mode MPA of rectangle, circle and hollow circle cross-sections shown in Figure 11 are also investigated to validate the effectiveness of the proposed two simplified equivalent models. Other simulation parameters are kept the same ( $k = 10$,

$L = 0.02m$ and $t_p = \dfrac{L}{k} = 0.002m$ ). The simulation results for square, circle and hollow

circle are respectively shown in Figures 12, 13 and 14. Similarly to square cross section, for rectangle, circle and hollow circle cross-sections, the results simulated by proposed model 2 almost overlap with those simulated by proposed model 1, which validates their equivalence in modelling deformation along the $z(3)$ axis for different cross sections. Also, similarly to square cross section, for rectangle, circle and hollow circle cross-sections, the proposed two models show good match with electro-mechanical coupled and multi-layer finite element model until the frequency rises to the second resonant mode. The modelling errors starting from the second resonant mode are attributable to the limitation of the proposed two models which is justified before.
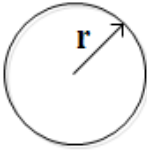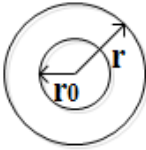


**Figure 11 d33-mode MPA with other shapes of cross section**

free-end displacement under 100V excitaiton voltage
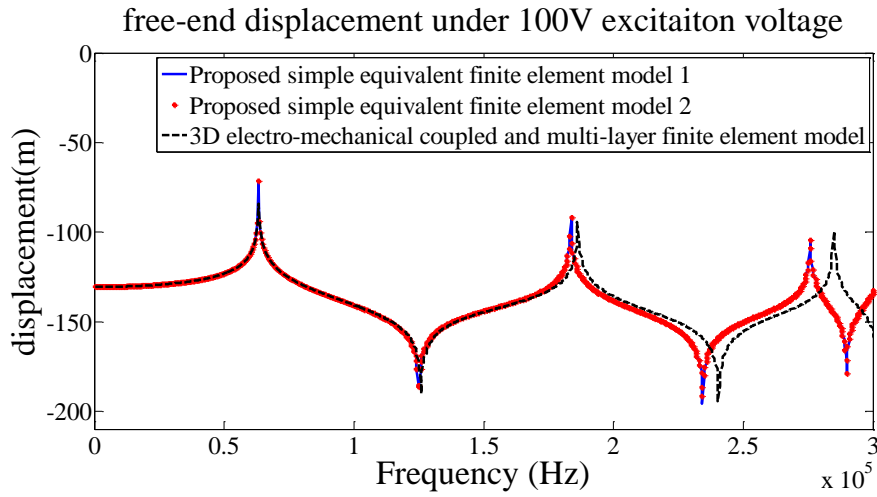


**Figure 12 Simulation results for d33-mode MPA of rectangle cross-section with 10 piezo layer**

free-end displacement under 100V excitaiton voltage
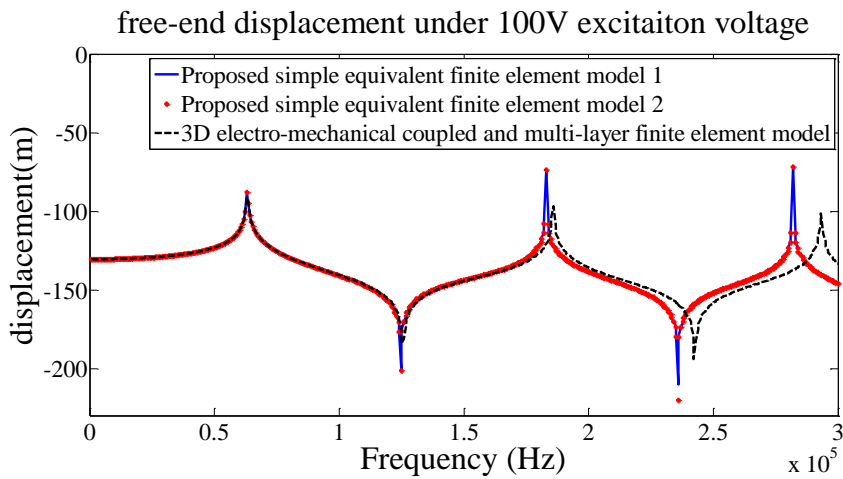


**Figure 13 Simulation results for d33-mode MPA of circle cross-section with 10 piezo layer**

free-end displacement under 100V excitaiton voltage
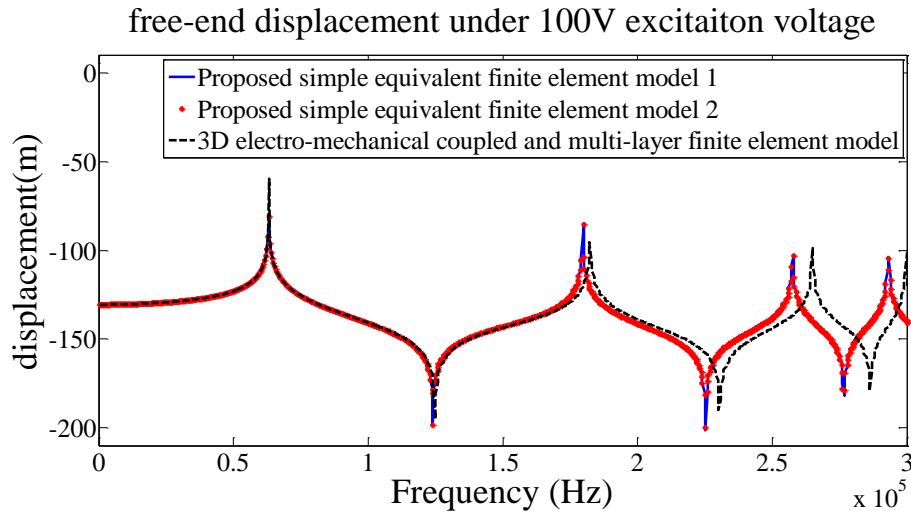


**Figure 14 Simulation results for d33-mode MPA of hollow circle cross-section with 10 piezo layer**

## 5. Conclusion

In this Chapter, two simple equivalent finite element models of d33-mode MPA are proposed. The proposed finite element models consider multi-layer d33-mode MPA as an equivalent homogenous bulk which could simply meshed with pure-solid and consider the inverse piezoelectric effect of the applied voltage with equivalent external forces. Compared with direct finite element modelling of d33-mode MPA, the proposed equivalent modelling method greatly facilitates the modelling processes and greatly cuts down the computation effort. The proposed models are developed on the basis of the condition that the distribution of the displacement across each piezo layer can be assumed to be uniform. This condition limits the frequency range of the proposed models to a certain multiple of the first resonant frequencies whose corresponding quarter wavelengths are far larger than the thickness of piezo layer. Simulations are carried out in commercial software ANSYS, which validates the effectiveness and shows the limitation of the proposed models. It is worth noting that the more piezo layers are stacked in d33-mode MPA or the more other layers are stacked with d33-mode MPA (i.e. the

relative quarter wavelengths are increased due to the increased wave propagation length), the more vibration modes will satisfy the condition that their quarter wavelengths are far larger than the thickness of piezo layer, thus resulting in the facts that the more vibration modes and a larger frequency range it can model. For a good performance of d33-mode MPA (i.e. a large output deformation with a low-voltage operation in a compact size), a large amount of piezo layers are often stacked in d33-mode MPA, thus enabling the proposed simplified finite element model of d33-mode MPA with a sufficient effective frequency range for applications. Therefore, the limitation of the proposed equivalent models is of minor importance in practice.

## References

Adriaens H J M T A, Koning W L D and Banning R 2000 Modelling piezoelectric actuators *IEEE/ASME Trans. Mechantron.* **5** 331–41

ANSYS 2014 "Piezo Extension_R150_v8" from https://support.ansys.com/portal/site/AnsysCustomerPortal.

Arevalo A and Foulds I G 2013. Parametric Study of Polyimide-Lead Zirconate Titanate Thin Film Cantilevers for Transducer Applications *In 2013 COMSOL Conference, Rotterdam, Holland*

Lee J, Kwon W S, et al. 2011 A novel smooth impact drive mechanism actuation method with dual-slider for a compact zoom lens system *Review of Scientific Instruments* **82** 085105

Li Y, Huang J and Tang H 2012 A compliant parallel XY micromotion stage with complete kinematic decoupling *Automation Science and Engineering, IEEE Transactions on* **9** 538-553

Lu T F, Handley D C, Yong Y K and Eales C 2004 A three-DOF compliant micromotion stage with flexure hinges *Industrial Robot: An International Journal* **31** 355-361.

Meitzler A, Tiersten H F, Warner A W, Berlincourt D, Couqin G A and Welsh III F S 1987 IEEE standard on piezoelectricity *IEEE Ultrasonics, Ultrason. Ferro-electr. Freq. Control Society* **43** 717-772

Yong Y K and Mohemani S R 2013 Design of an inertially counterbalanced Z-nanopositioner for high-speed atomic force microscopy *Nanotechnology, IEEE Transactions on*, **12** 137-145

Zhang W J, Zou J, Watson L J and Zhao W 2002 The constant Jacobian method for kinematics of 3 DOF planar micro-motion stage *Journal of Robotic Systems*, **19** 63-72

# Chapter 7

# UNIFORM-ELECTRIC-FIELD-APPROXIMAITON BASED SIMPLIFIED FUNDAMENTALS, EQUIVALENT CIRCUIT AND TRANSFER MATRIX OF D31-MODE LPT

# CHAPTER 7

# UNIFORM-ELECTRIC-FIELD-APPROXIMAITON BASED SIMPLIFIED FUNDAEMTNALS, EQUIVALENT CIRCTUI AND TRANSFER MATRIX OF D31-MODE LPT

This chapter is based on the following submitted paper:

Zhang, Y., Lu, T. F., & Gao, W. (2016). Model D31-mode Longitudinal Piezoelectric Transducers. Submitted to *Sensors and Actuators A: Physical*

*Contributions of this chapter*: This chapter presents the rationale behind the uniform-electric-field-approximation for modelling d31-mode LPT. Based on the approximation, simplified fundamentals of d31-mode LPT is derived. Besides, a simple equivalent mixing method, which can flexibly consider the electrode layers and adhesive layers, is proposed. Then, a simple 1D equivalent homogenous analytical model of D31-LPT is formulated. Also, inspired by d33-mode, the related the related equivalent circuit and transfer matrix of d31-mode LPT are formulated. The proposed models can flexibly consider the number of piezo layers and passive layers such as electrode layers and adhesive layers in d31-mode LPT.

## Statement of Authorship

## Statement of Authorship

| Title of Paper | Model D31-mode Longitudinal Piezoelectric Transducers |
|---|---|
| Publication Status | ☐ Published ☐ Accepted for Publication<br>☑ Submitted for Publication ☐ Unpublished and Unsubmitted work written in manuscript style |
| Publication Details | Zhang, Y., Lu, T. F., & Gao, W. (2016). Model D31-mode Longitudinal Piezoelectric Transducers. Submitted to Sensors and Actuators A: Physical |

### Principal Author

| Name of Principal Author (Candidate) | Mr. Yangkun Zhang |
|---|---|
| Contribution to the Paper | Developed theory, performed simulations, analyzed data and wrote the manuscript |
| Overall percentage (%) | 80% |
| Certification | This paper reports on original research I conducted during the period of my Higher Degree by Research candidature and is not subject to any obligations or contractual agreements with a third party that would constrain its inclusion in this thesis. I am the primary author of this paper. |
| Signature | Date | 16 / 02 / 2016 |

### Co-Author Contributions

By signing the Statement of Authorship, each author certifies that:

i.    the candidate's stated contribution to the publication is accurate (as detailed above);

ii.   permission is granted for the candidate in include the publication in the thesis; and

iii.  the sum of all co-author contributions is equal to 100% less the candidate's stated contribution.

| Name of Co-Author | Dr. Tien-Fu Lu |
|---|---|
| Contribution to the Paper | Supervised research, reviewed manuscript |
| Signature | Date | 16/02/16 |

| Name of Co-Author | Prof. Wei Gao |
|---|---|
| Contribution to the Paper | Reviewed the manuscript |
| Signature | Date | 23/02/16 |

# Model D31-mode Longitudinal Piezoelectric Transducers

YANGKUN ZHANG[1*], TIEN-FU LU[1] AND WEI GAO[2]

*School of Mechanical Engineering, University of Adelaide, 5005, Australia*

*Nano-Metrology and Control Lab, Department of Nanomechanics, School of Engineering, Tohoku University, 980-8579, Sendai, Japan*

∗*Author to whom correspondence should be addressed. E-mail: yangkun.zhang@adelaide.edu.au*

**ABSTRACT:** D31-mode longitudinal piezoelectric transducers (D31-LPT) are linear piezoelectric transducers which can be used as actuators or energy harvesters. Simple and effective dynamic modelling of D31-LPT, which can predict the behaviours in time/frequency domain, has not been well explored in literature. This paper proposes simplified fundamentals of D31-LPT based on uniform electric field approximation and a simple equivalent mixing method which can flexibly consider the electrode layers and adhesive layers. Then, a simple 1D equivalent homogenous analytical model of D31-LPT is formulated. Also, based on the proposed analytical model and borrowing the network theory, an exact equivalent circuit is formulated. The more straightforward form of the equivalent circuit facilitates the analysis and modelling of D31-LPT. Besides, the proposed analytical model is wrapped into a transfer matrix form. The formulated transfer matrix of D31-LPT can be used with transfer matrix method to facilitate the calculations, when D31-LPT are stacked with other layers. The proposed models are validated by a 3D finite element model of D31-LPT.

## 1. Introduction

D31-mode longitudinal piezoelectric transducers (D31-LPT) are one kind of linear-motion transducers which can be applied as either actuator [1-5] or energy harvester [6]. With reference to Figure 1, when a voltage is applied to a piezo layer in the direction opposite to its pre-polarized direction, it will induce a contraction $\Delta L$ in the lateral direction which is perpendicular to the polarization direction. On the other hand, when a force is applied in lateral direction, a charge can be generated on the electrode surfaces. These two effects are the operational principles of D31-LPT (the former known as transmitter mode can be employed for actuators and the latter known as receiver mode can be employed as sensors or energy harvesters).As the effects for single layer is too small to be used, D31-LPT is often used in a stack configuration [1-3] shown in Figure 2. Compared with D33-LPT shown in Figure 3, D31-LPT are less popular due to the fact that the d33 coefficient is around two times larger than the d31 coefficient. However, with reference to Figure 3, the configuration of multi-layer D31-LPT has more robust resistance to tension. Thus, D31-LPT are popular in the applications where transducers are subjected to a huge tension [1-7].
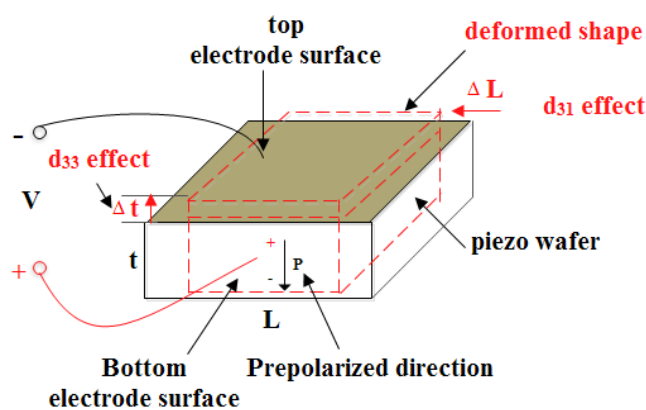


**Figure 1 Schematic of d31-mode of piezoelectricity**
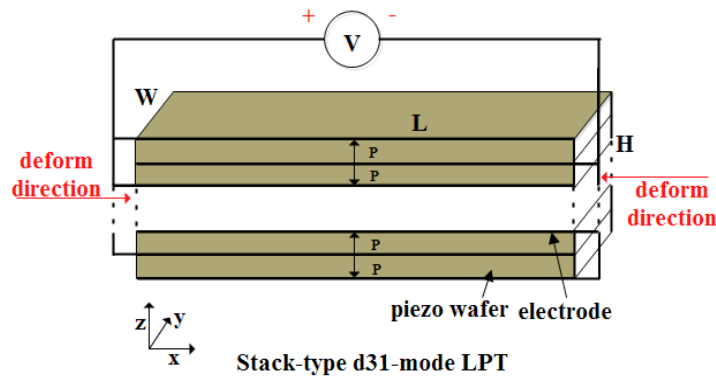
**Figure 2 Configurations of multi-layer D31-LPT**
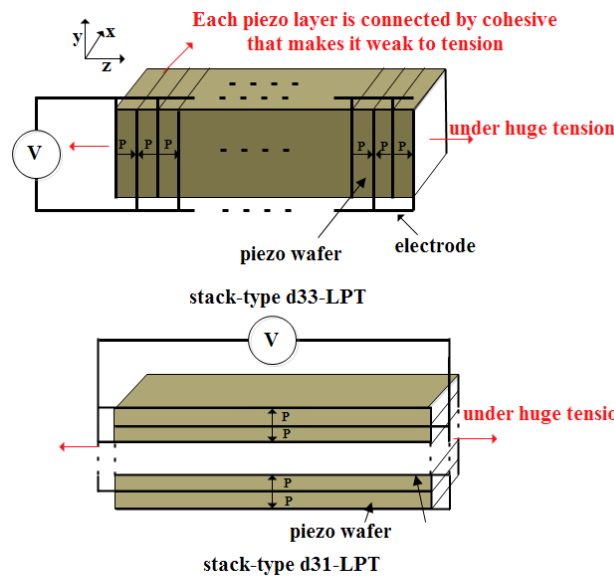


**Figure 3 Configurations of multi-layer D33-LPT**

Modelling D31-LPT plays an important role in the design, fabrication, and optimization of D31-LPT-based applications. To the best of authors' knowledge, only a few models of D31-LPT are available in literature [1-4]. Most [1, 2, 4] focused on the static behaviours. Tolliver et al [3] applied a finite element model to compute the dynamic behaviours of D31-LPT. Although it can effectively model D31-LPT, the finite element model, which is based on 3D complex electro-mechanical coupled fundamentals of piezoelectricity, is computationally inefficient. Simple and effective dynamic modelling of D31-LPT, which can predict the behaviours in time/frequency domain, has not been well explored in literature. In this paper, based on uniform-electric-field

approximation and then a simple equivalent mixing method, simple and effective 1D equivalent homogenous analytical model, equivalent circuit, and transfer matrix of D31-LPT, which can flexibly consider the electrode layers and adhesive layers, are proposed and formulated.

Section 2 proposes simplified fundamentals of D31-LPT based on uniform electric field approximation and a simple equivalent mixing method to formulate a simple equivalent homogenous analytical model of D31-LPT which can flexibly consider the electrode layers and adhesive layers. Based on the proposed analytical model, an exact equivalent circuit and a transfer matrix of D31-LPT are respectively formulated in Section 3 and Section 4. In Section 5, a 3D FEA model of D31-LPT is established in commercial software ANSYS for validations. Section 6 presents the summary.

## 2. Model Formulation

For model formulation, consider the D31-LPT shown in Figure 2 with a length $L$ in $x$ direction (i.e. longitudinal direction) and an overall thickness $H$ in $z$ direction stacked by piezo wafers polarized in $z$ direction and a width $W$ in $y$ direction. A more detailed view concerning how each piezo layer is connected can be seen in Figure 4. Each piezo layer is electrically connected in parallel and also mechanically connected in parallel for the operation direction (longitudinal direction). Note, electrode layers and adhesive layers are arranged in such a configuration shown in Figure 4 that there is no voltage drop across each adhesive layer when each electrode layer is pasted to the corresponding piezo layer.
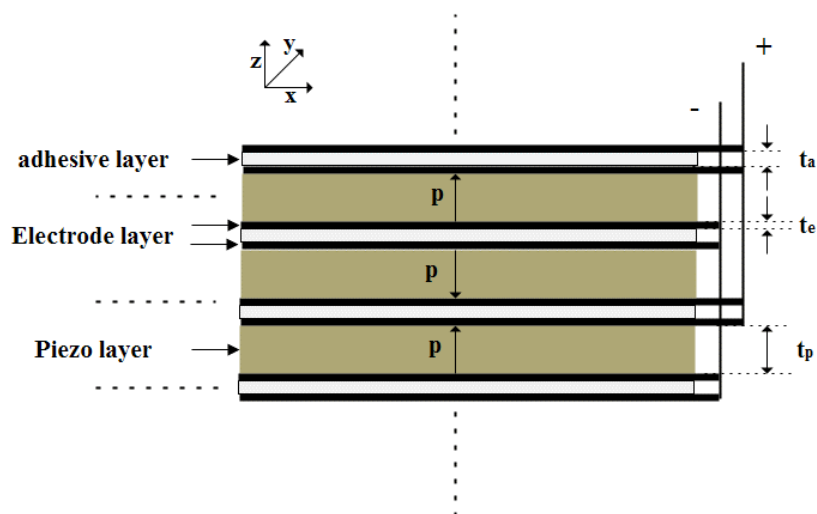
**Figure 4 a more detailed view of D31-LPT**

As D31-LPT is designed for longitudinal vibrations, it can be assumed to be at a uni-axial stress state:

$$T_1 \neq 0,$$
$$T_2 = 0, \qquad (1)$$
$$T_3 = 0.$$

The subscript '1','2', and '3' denote $x$ direction, $y$ direction, and $z$ direction respectively.

This assumption is true, if the frequency band of interest for the longitudinal direction is well below (more than 3 times smaller than) the lowest resonant lateral frequency.

As the electric field is only applied to the polarization direction, the following relations exist:

$$E_1 = 0,$$
$$E_2 = 0, \qquad (2)$$
$$E_3 \neq 0.$$

Based on the IEEE standards on piezoelectricity [7], the 3D piezoelectric constitutive equations can be written as shown below:

$$
\begin{Bmatrix} S_1 \\ S_2 \\ S_3 \\ S_4 \\ S_5 \\ S_6 \\ D_1 \\ D_2 \\ D_3 \end{Bmatrix} = \begin{bmatrix} s_{11}^E & s_{12}^E & s_{13}^E & 0 & 0 & 0 & 0 & 0 & d_{31} \\ s_{12}^E & s_{22}^E & s_{23}^E & 0 & 0 & 0 & 0 & 0 & d_{32} \\ s_{13}^E & s_{23}^E & s_{33}^E & 0 & 0 & 0 & 0 & 0 & d_{33} \\ 0 & 0 & 0 & s_{44}^E & 0 & 0 & 0 & d_{24} & 0 \\ 0 & 0 & 0 & 0 & s_{55}^E & 0 & d_{15} & 0 & 0 \\ 0 & 0 & 0 & 0 & 0 & s_{66}^E & 0 & 0 & 0 \\ 0 & 0 & 0 & 0 & d_{15} & 0 & \varepsilon_{11}^T & 0 & 0 \\ 0 & 0 & 0 & d_{24} & 0 & 0 & 0 & \varepsilon_{22}^T & 0 \\ d_{31} & d_{32} & d_{33} & 0 & 0 & 0 & 0 & 0 & \varepsilon_{33}^T \end{bmatrix} \begin{Bmatrix} T_1 \\ T_2 \\ T_3 \\ T_4 \\ T_5 \\ T_6 \\ E_1 \\ E_2 \\ E_3 \end{Bmatrix},
\tag{3}
$$

where $S_i, T_i, E_i$, and $D_i$ are respectively the components of strain, stress, electric field and electric displacement vectors. $s_{ij}^E$ are the components of compliance matrices measured at constant electric fields. $d_{ij}$ are the piezoelectric strain coefficients. $\varepsilon_{ii}^T$ are dielectric coefficients measured at constant stresses. Those piezoelectric material constants can be obtained by measuring and analysing electrical impedance [8, 9].

Substituting Equation (1) and (2) into the first row and the ninth row of Equation (3), the constitutive equations in the directions of interest can derived as follows:

$$
T_1 = c'S_1 - e'E_3,
\tag{4.a}
$$

$$
D_3 = e'S_1 + \varepsilon'E_3,
\tag{4.b}
$$

where $c' = \dfrac{1}{s_{11}^E}$, $e' = \dfrac{d_{31}}{s_{11}^E}$, and $\varepsilon' = \varepsilon_{33}^T - \dfrac{d_{31}^2}{s_{11}^E}$.

Consider a piezo layer at certain position $z_n$ of D31-LPT shown in Figure 4 with thickness $t_p$, length $L$, and width $W$ and it is excited by a voltage $U_p$.

The strain and electric field can be respectively expressed as follows:

$$
S_1 = S(x,t) = \frac{\partial u(x,t)}{\partial x},
\tag{5.a}
$$

$$
E_3 = E(z,t) = -\frac{\partial \varphi(z,t)}{\partial z},
\tag{5.b}
$$

where the arguments '$x$' and '$z$' are position variables, '$t$' is time variable, $u$ and $\varphi$ are respectively displacement and electric potential.

As illustrated in Figure 2, the charge balance in the $z$ direction gives:

$$\frac{\partial D_3}{\partial z} = 0. \tag{6}$$

Substituting Equation (4.b) into Equation (6) results in:

$$\frac{\partial^2 \varphi(z,t)}{\partial^2 z} = \frac{e'}{\varepsilon'} \frac{\partial^2 u(x,t)}{\partial z \partial x}, \tag{7}$$

As $\dfrac{\partial^2 u(x,t)}{\partial z \partial x} = 0$, $\dfrac{\partial^2 \varphi(z,t)}{\partial^2 z} = 0$. Therefore, $E_3 = -\dfrac{\partial \varphi(z,t)}{\partial z}$ can be seen as a constant, which gives:

$$E_3 = -\frac{\partial \varphi(z)}{\partial z} = -\frac{\varphi(z_p + t_p) - \varphi(z_p)}{t_p} = \frac{U_p(t)}{t_p} \tag{8}$$

Therefore, constitutive relations shown in Equation (4) can be simplified as follows:

$$T_1 = c'S_1 - e'\frac{U_p(t)}{t_p}, \tag{9.a}$$

$$D_3 = e'S_1 + \varepsilon'\frac{U_p(t)}{t_p}. \tag{9.b}$$

For D31-LPT, each piezo layer is electrically connected in parallel, which gives:

$$U_p(t) = U(t), \tag{10}$$

where $U(t)$ is the excitation voltage applied to D31-LPT.

Besides, considering each piezo layer in D31-LPT is stacked in $z$ direction and has the same material properties ($c'$, $e'$, and $\varepsilon'$) and dimensions ($t_p$, $L$, and $W$) and if electrode layers and adhesive layers shown in Figure 4 are neglected, $T_1$, $S_1$ and $E_3$ of the whole D31-LPT in $x$ direction can be considered to be homogenous as written in the following form:

$$T_1 = c'S_1 - e'\frac{U(t)}{t_p},$$ (11)

where $t_p$ is the thickness of each piezo layer ($t_p = t_n$).

However, for more accurate modelling of D31-LPT, passive layers such as electrode layers and adhesive layers in D31-LPT are needed to be considered. Therefore, an equivalent homogenous model shown in Equation (12) is proposed here to consider the passive layers in D31-LPT for accurate modelling.

$$\overline{T_1} = \overline{c}\,\overline{S_1} - \overline{e}\,\overline{E_3},$$ (12)

where the symbol '$-$' represents the homogenous property and $\overline{E_3} = \dfrac{U(t)}{t_p}$.

As both active layers and passive layers are connected in parallel and have the same strain ($S_1$) in the operation direction ($x$ axis), the following relations exist:

$$\overline{T_1} = \sigma_p \cdot T_{1\_p} + \sigma_a \cdot T_{1\_a} + \sigma_e \cdot T_{1\_e},$$ (13.a)

$$\overline{S_1} = S_{1\_p} = S_{1\_a} = S_{1\_e}.$$ (13.b)

The subscript 'p', 'a', 'e' respectively refer to the piezo, adhesive, and electrode ($T_{1\_p} = c'S_{1\_p} - e'\dfrac{U(t)}{t_p}$, $T_{1\_a} = c_a S_{1\_a} - 0\dfrac{U(t)}{t_p}$ and $T_{1\_e} = c_e S_{1\_e} - 0\dfrac{U(t)}{t_p}$). $\sigma$ denote

volume fraction ($\sigma_p = \dfrac{n_p \cdot t_p}{n_p \cdot t_p + n_a \cdot t_a + n_e \cdot t_e}$ , $\sigma_a = \dfrac{n_a \cdot t_a}{n_p \cdot t_p + n_a \cdot t_a + n_e \cdot t_e}$ and

$\sigma_e = \dfrac{n_e \cdot t_e}{n_p \cdot t_p + n_a \cdot t_a + n_e \cdot t_e}$ where $n$ denote the number of layers).

Substituting them into Equation (13) with Equation (12), the homogenous coefficients in Equation (12) can be calculated as follows:

$$\overline{c} = \sigma_p \cdot c' + \sigma_a \cdot c_a + \sigma_e \cdot c_e$$ (14.a)

$$\overline{e} = \sigma_p \cdot e'$$ (14.b)

The homogenous normal force of D31-LPT in $x$ direction can be expressed as follows:

$$\overline{N}(x,t) = H \cdot W \cdot \overline{T_1}, \text{where } H = n_p \cdot t_p + n_a \cdot t_a + n_e \cdot t_e. \tag{15}$$

Based on the Newton's Second law in $x$ direction, the following equation of motion can be derived:

$$\frac{\partial \overline{T_1}}{\partial x} = \overline{\rho} \frac{\partial^2 u(x,t)}{\partial^2 t}, \tag{16}$$

where $\overline{\rho}$ is the homogenous density ($\overline{\rho} = \sigma_p \cdot \rho_p + \sigma_a \cdot \rho_a + \sigma_e \cdot \rho_e$).

Substituting Equation (12) in Equation (16) with $\overline{S_1} = \dfrac{\partial \overline{u}(x,t)}{\partial x}$ gives:

$$\overline{c} \frac{\partial^2 \overline{u}(x,t)}{\partial^2 x} = \overline{\rho} \frac{\partial^2 \overline{u}(x,t)}{\partial^2 t}, \tag{17}$$

Using the principle of separation of variables, for excitation voltage $U(t) = U_0 e^{jwt}$ where $w$ is the operation frequency, the general solution of displacement $u(x,t)$ to Equation (17) can be written in the following form:

$$\overline{u}(x,t) = (A_1 \sin(mx) + A_2 \cos(mx)) e^{jwt}, \tag{18}$$

where $m = \sqrt{\dfrac{\overline{\rho} w^2}{\overline{c}}}$ , $A_1$ and $A_2$ are constants, which can be calculated from two boundary conditions at two ends of D31-LPT.

Substituting Equation (18) into Equation (12) gives the general solution of the homogenous normal force

$$\overline{N}(x,t) = H \cdot W \left[ \overline{c}(A_1 m \cos(mx) - A_2 m \sin(mx)) - \overline{e} \frac{U_0}{t_p} \right] e^{jwt}. \tag{19}$$

For the electrical side, the induced charge of the nth piezo layer can be expressed as follows:

$$Q_n = W \cdot \int_0^L D_3 dx = W \cdot \int_0^L (e'\overline{S_1} + \varepsilon'\frac{U(t)}{t_p})dx. \tag{20}$$

As each piezo layer is electrically connected in parallel, the total induced charge of the D31-LPT can be expressed as follows:

$$Q_{total} = \sum_{n=1}^{n_p} Q_n$$

$$= n_p \cdot W \cdot \int_0^L (e'\overline{S_1} + \varepsilon'\frac{U(t)}{t_p})dx. \tag{21}$$

Substituting Equation (18) into Equation (21) with $\overline{S_1} = \dfrac{\partial \overline{u}(x,t)}{\partial x}$ gives the general solution of the total induced charge:

$$Q_{total}$$
$$= n_p \cdot W \cdot \int_0^L (e'\overline{S_1} + \varepsilon'\frac{U(t)}{t_p})dx \tag{22}$$
$$= n_p \cdot W \cdot (e'(\overline{u}(L) - \overline{u}(0)) + L \cdot \varepsilon'\frac{U_0(t)}{t_p})e^{jwt}$$
$$= n_p \cdot W \cdot (e'(A_1 \sin(mL) + A_2 \cos(mL) - A_2) + L \cdot \varepsilon'\frac{U_0(t)}{t_p})e^{jwt}$$

By differentiating displacement $\overline{u}(x,t)$ and electric charge $Q_{total}(t)$ with respect to time variable $t$, the general solution of the velocity $\overline{v}(x,t)$ and induced current $I_{total}(t)$ can be derived:

$$\overline{v}(x,t) = jw(A_1 \sin(mx) + A_2 \cos(mx))e^{jwt}, \tag{23.a}$$

$$I_{total}(t)$$
$$= n_p \cdot W \cdot (e'(\overline{v}(L) - \overline{v}(0)) + L \cdot \varepsilon'\frac{U_0(t)}{t_p} jw)e^{jwt} \tag{23.b}$$
$$= n_p \cdot W \cdot jw(e'(A_1 \sin(mL) + A_2 \cos(mL) - A_2) + L \cdot \varepsilon'\frac{U_0(t)}{t_p})e^{jwt}.$$

Therefore, a simple 1D equivalent homogenous analytical model of D31-LPT, which can consider the electrode layers and adhesive layers based on an equivalent mixing

method, has been derived. Note, the mechanical damping and electrical damping, which respectively account for the mechanical loss and mechanical loss, can be easily considered by adding positive imaginary part to stiffness material constant and adding negative imaginary part to permittivity material constant [8-10]. The specific analytical solution can be derived simply by applying the two boundary conditions at two ends of the D31-LPT.

## 3. Equivalent Circuit

Equivalent circuits are widely used in modelling piezoelectric systems, as they are very straightforward to apply. Based on the fundamental of D31-LPT presented in Section 2 and by borrowing the idea of network theory [11], an exact equivalent circuit of D31-LPT is constructed herein.

Referring to Figure 5, four boundary conditions at both ends of D31-LPT can be derived, shown as follows:

$$\bar{v}(0,t) = v_L, \tag{24.a}$$

$$\bar{v}(L,t) = v_R. \tag{24.b}$$

$$\bar{N}(0,t) = -F_L, \tag{24.c}$$

$$\bar{N}(L,t) = -F_R, \tag{24.d}$$

where the subscript '$L$' and '$R$' stands for the left and right side of D31-LPT.

There are 8 unknowns($A_1$, $A_2$, $I_{total}$, $U$, $v_L$, $v_R$, $F_L$ and $F_R$) in 5 equations (Equation (23.b), (24.a), (24.b), (24.c) and(24.d)). Therefore, $F_L$, $F_R$ and $U$ ($A_1$, $A_2$) can be expressed with regard to $v_L$, $v_R$ and $I_{total}$ in the following matrix form:

$$\begin{bmatrix} F_L \\ F_R \\ U \end{bmatrix} = \begin{bmatrix} \dfrac{n_p t_p}{jw}\left( W\dfrac{e'\bar{e}}{\varepsilon'L} + \dfrac{W\cdot\bar{c}\cdot m}{\tan(mL)} \right) & -\dfrac{n_p t_p}{jw}\left( \dfrac{W\cdot\bar{c}\cdot m}{\sin(mL)} + W\dfrac{e'\bar{e}}{\varepsilon'L} \right) & \dfrac{t_p\bar{e}}{jwL\varepsilon'} \\[4mm] \dfrac{n_p t_p}{jw}\left( \dfrac{W\cdot\bar{c}\cdot m}{\sin(mL)} + \dfrac{We'\bar{e}}{\varepsilon'L} \right) & -\dfrac{n_p t_p}{jw}\left( \dfrac{We'\bar{e}}{\varepsilon'L} + \dfrac{W\cdot\bar{c}\cdot m}{\tan(mL)} \right) & \dfrac{t_p\bar{e}}{jwL\varepsilon'} \\[4mm] \dfrac{t_p e'}{jwL\varepsilon'} & -\dfrac{t_p e'}{jwL\varepsilon'} & \dfrac{t_p}{jwn_p\varepsilon'WL} \end{bmatrix} \begin{bmatrix} v_L \\ v_R \\ I_{total} \end{bmatrix}. \tag{25}$$

Based on Equation (25) and borrowing the network structure [11], the following circuit model of D31-LPT shown in Figure 5 with exact equivalence can be found.
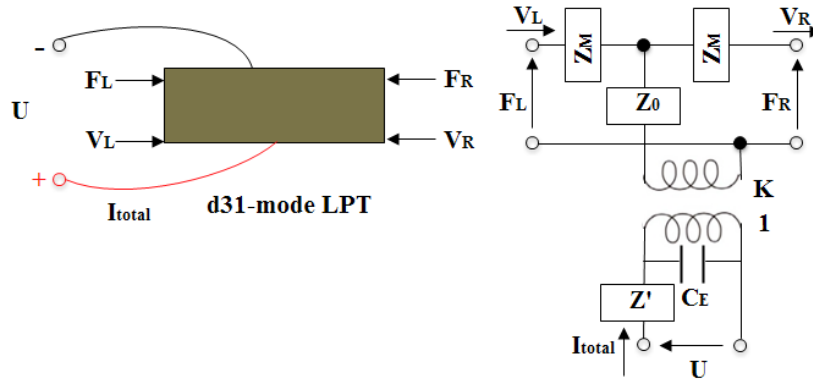


4. **Figure 5. Three-port equivalent circuit of D31-LPT**

In the equivalent circuit, the electrical elements can be expressed below:

$$C_E = \frac{n_p WL}{t_p}\varepsilon'\frac{\bar{e}}{e'} \tag{26.a}$$

$$Z' = \frac{t_p}{jwn_p WL\varepsilon'}(1-\frac{e'}{\bar{e}}) \tag{26.b}$$

$$K = n_p W\cdot\bar{e} \tag{26.c}$$

$$Z_0 = \frac{n_p t_p W\cdot\bar{c}\cdot m}{jw\sin(mL)} \tag{26.d}$$

$$Z_M = n_p t_p W\cdot\bar{c}\cdot m\frac{\cos(mL)-1}{jw\sin(mL)} \tag{26.e}$$

The formulated equivalent circuit of D31-LPT wraps the model into a more straightforward form, which further facilitates the analysis and modelling of D31-LPT.

## 4. Transfer Matrix Formalism

For real applications, D31-LPT is most often connected with other layers, such as backing layers and propagating mediums, in the direction of interest (longitudinal direction). For modelling those multi-layer structures, transfer matrix method greatly facilitates the calculations of directly deriving analytical solutions [10]. The transfer matrix method is based on the fact that some physical quantities, such as force and velocity, follow simple continuity conditions across the boundaries from one layer to the next. Therefore, if physical quantities on one side of certain layer can be correlated to the other side of the layer in a matrix form (known as transfer matrix), the dynamics of a stack of layers then can be simply derived by multiplication of individual layer matrix in the stack. The transfer matrix of D31-LPT in the form shown in Equation (24) is derived herein to facilitate the calculations, when D31-LPT is stacked with other layers.

$$
\begin{bmatrix} F_R \\ v_R \\ U \\ I_{out} \end{bmatrix} = T_{D31-LPT} \begin{bmatrix} F_L \\ v_L \\ U \\ I_{in} \end{bmatrix},
\tag{27}
$$

where the electrical current flowing into D31-LPT $I_{total} = I_{out} - I_{in}$. There are 8 unknowns ($A_1$, $A_2$, $I_{total}$, $U$, $v_L$, $v_R$, $F_L$ and $F_R$) in 5 equations (Equation (23.b), (24.a), (24.b), (24.c) and (24.d)). Therefore, $F_R$, $v_R$ and $I_{out}$ ($A_1$, $A_2$) can be expresses with regard to $F_L$, $v_L$, $I_{in}$ and $U$ and then the transfer matrix of D31-LPT shown in Equation (23) can be derived, shown below:

$$
T_{D31-LPT} = \begin{bmatrix}
\cos(mL) & \dfrac{-n_p t_p W \cdot \bar{c} \cdot m \sin(mL)}{jw} & n_p W \cdot \bar{e} \cdot (\cos(mL)-1) & 0 \\[2ex]
\dfrac{\sin(mL)\,jw}{n_p t_p W \cdot \bar{c} \cdot m} & \cos(mL) & \dfrac{\bar{e} \cdot jw \sin(mL)}{t_p \cdot \bar{c} \cdot m} & 0 \\[2ex]
0 & 0 & 1 & 0 \\[2ex]
\dfrac{e'\,jw\sin(mL)}{\bar{c} \cdot mt_p} & n_p We'(\cos(mL)-1) & jwn_p W(L\dfrac{\varepsilon'}{t_p} + \dfrac{e' \cdot \bar{e} \cdot \sin(mL)}{t_p \bar{c} \cdot m}) & 1
\end{bmatrix}
\tag{28}
$$

The formulated transfer matrix of D31-LPT can be used with transfer matrix method to facilitate the calculations, when D31-LPT is stacked with other layers.

## 5. Validations and Discussions

To validate the effectiveness of the proposed models of D31-LPT, a case study is carried out in this section. The validation is achieved by checking the results simulated by the proposed models against FEA results.

With reference to Figure 6, a multi-layer d31-LPT with electrode layers and adhesive layers considered is chosen as a study case. The D31-LPT is fixed at left end and set free at the right end. The frequency response of the free-end displacement is simulated and compared with a 3D FEA model for validations. The simulation parameters are listed in Table 1. PZT-5H [12], brass (density: $8500\,\text{kg/m}^3$; Young's modulus: $1.6*10^{10}$ Pa; Poisson ratio: 0.3), and epoxy resin (density: $1170\,\text{kg/m}^3$; Young's modulus: $8.2163*10^9$ Pa; Poisson ratio: 0.3) are respectively chosen as the materials of piezo, electrode, and adhesive.
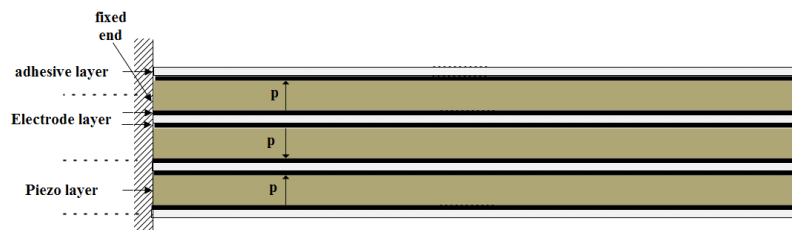


**Figure 6. Study Case**

**Table 1. Simulation parameters**

| | $L$ (mm) | $W$ (mm) | Layer thickness $t$ (mm) | Layer number $n$ | Material |
|---|---|---|---|---|---|
| Piezo | 20 | 2 | 0.4 | 3 | PZT-5H |
| Electrode | 20 | 2 | 0.08 | 6 | Brass |
| adhesive | 20 | 2* | 0.08 | 4 | Epoxy resin |

To apply the analytical model formulated in Section 2 for calculations, by substituting the boundary conditions ( $v_L = 0$ and $F_R = 0$ ), the specific solution to the free-end displacement $u_R$ and velocity $v_R$ of D31-LPT can be easily solved, shown below:

$$u_R(t) = \frac{k \cdot \overline{e} \cdot \sin(mL)}{c \cdot Lm \cos(mL)} U_0 e^{jwt}. \tag{29}$$

Turning to applying the equivalent circuit formulated in Section 3 for calculations, by substituting the boundary conditions ( $v_L = 0$ and $F_R = 0$ ) into the equivalent circuit shown in Figure 5, a simple circuit shown in Figure 7 can be derived. Then, it is very straightforward to solve the circuit to get $v_R$ . By integrating $v_R$ ( $u_R = \int v_R dt = \frac{v_R}{jw}$ ), $u_R$ can be also derived.
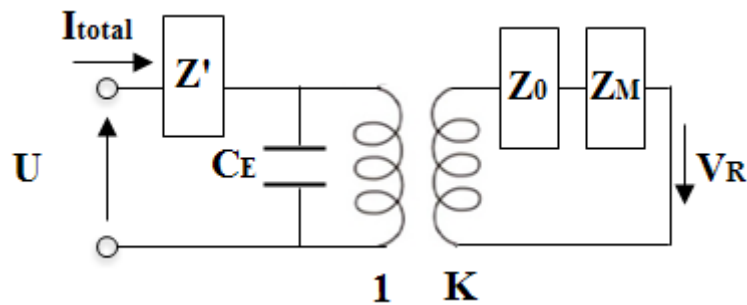


**Figure 7. Equivalent circuit of Study Case**

In terms of applying the transfer matrix of D31-LPT formulated in Section 4, the calculation process goes as follows. Two equations can be derived from the first and second rows of the matrix in Equation (28) and another two equations can be derived from two mechanical boundary conditions ( $v_L = 0$ and $F_R = 0$ in this case). With four equations available, $v_R$ (and other three unknowns $F_L, v_L$ and $F_R$ ) can be solved with regard to input voltage $U$ . The displacement $u_R$ can be also derived by integrating $v_R$ . Note, in this case, the advantages of applying the transfer matrix method is not very obvious. But, when D31-LPT is stacked with other layers, the transfer matrix method will become very convenient.

For validation, a 3D FEA model is developed on the commercial software ANSYS. To model the electromechanical coupled behaviours of piezoelectricity, the extension package 'Piezo Extension_R150_v8' [13] was used. With reference to the meshed models shown in Figure 8, it is auto-meshed with 54623 nodes and 7616 elements, which is sufficient enough to ensure a high resolution. The boundary conditions are set up as specified (one-end fixed and one-end free). By applying a harmonic voltage input of 100V from 0 Hz to 400 kHz, the frequency response of the D31-LPT free-end displacement is obtained and the data are transferred to matlab to be plotted against the results obtained by the aforementioned 3 methods.
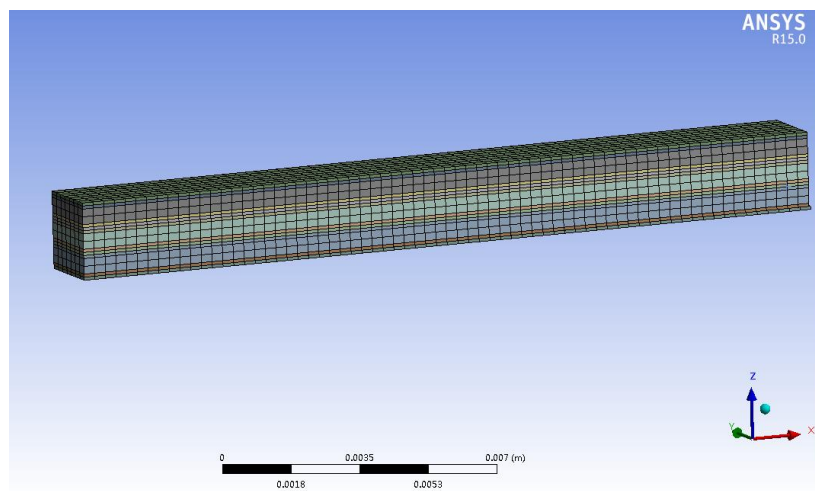


**Figure 8. Meshed FEA model**

Figure 9 shows the simulation results between 3 proposed models and 3D FEA model. Note, for convenience of comparison, both mechanical loss and electrical loss are not taken into account. As motioned before, for the proposed model, the mechanical loss and electrical loss can be easily taken into account respectively by adding positive imaginary part to stiffness material constant and adding negative imaginary part to permittivity material constant [8-10]. It can be seen that results simulated by using analytical models, equivalent circuit models and transfer matrix are completely overlapped. This is expected, as the proposed three modelling methods are based on the same fundamental of D31-LPT but with different forms. The proposed 3 models show a good match to the 3D FEA model from DC to the third resonant frequency, which validates their effectiveness in modeling D31-LPT. The deviations between the proposed models and 3D FEA models start to occur from the third resonant frequency.

This is because, for high-frequency excitation, the lateral effect cannot be neglected, which compromises the effectiveness of the proposed 1D models.
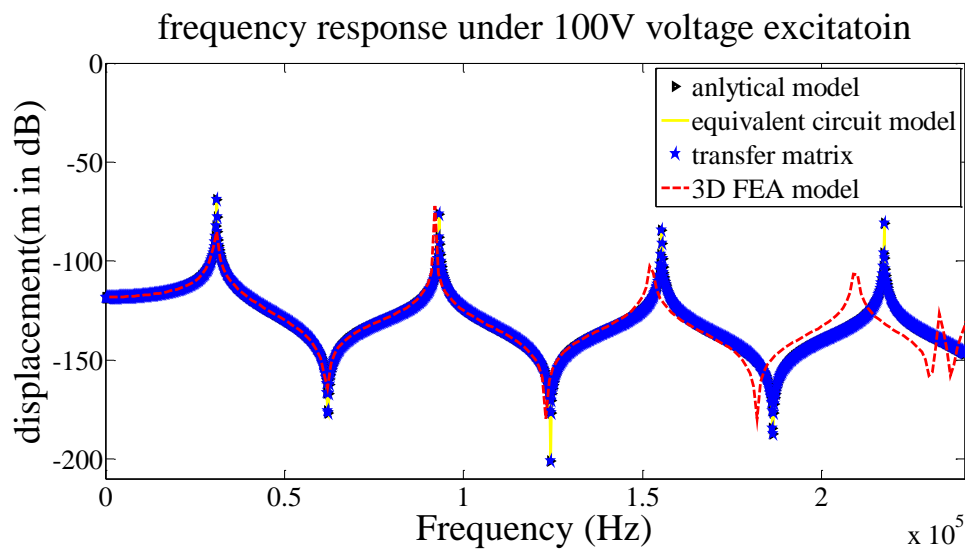


**Figure 9.Frequency response of free-end displacement**

## 6. Summary

In conclusion, modelling D31-LPT from the fundamental of piezoelectricity is presented in this paper. Simplified constitutive equations for modelling D31-LPT are derived from the IEEE standard 3D constitutive equations. Then, the electric field mathematically proves to be effectively seen as uniform for the operation of D31-LPT, which greatly simplifies the electro-mechanical coupled fundamental of D31-LPT. Based on the simplified fundamentals, an equivalent mixing method is proposed to formulate a simple 1D equivalent homogenous analytical model of D31-LPT, which can consider the electrode layers and adhesive layers.

Besides, based on the analytical model and borrowing the idea of network theory, an exact equivalent circuit of D31-LPT is formulated. The more straightforward form of the circuit facilitates the analysis and modelling of D31-LPT.

Also, the proposed analyticla model is wrapped into a transfer matrix form. The formulated transfer matrix of D31-LPT can be used with transfer matrix method to facilitate the calculations, when D31-LPT is stacked with other layers.

A 3D FEA model of D31-LPT is established in commercial software ANSYS. Simulations are carried out and the results validate the effectiveness of the proposed 3 models of D31-LPT.

## References

[1] Xu T-B, Jiang X and Su J 2011 A piezoelectric multilayer-stacked hybrid actuation/transduction system Appl. Phys. Lett. 98 243503

[2] Uchino K and Giniewicz J 2003 Micromechatronics (Boca Raton, FL: Taylor & Francis) Page 383

[3] Tolliver L, Xu T-B and Jiang X 2013. Finite element analysis of the piezoelectric stacked-HYBATS transducer Smart Materials and Structures,22(3), 035015.

[4] PI 2015 PIEZO Technology, http://www.piceramic.com/piezo-technology/properties-piezo-actuators/displacement-modes.html

[5] Ouyang P R, Zhang W J, and Gupta M M 2005 Design of a new compliant mechanical amplifier In ASME 2005 International Design Engineering Technical Conferences and Computers and Information in Engineering Conference, pp. 15-24

[6] Cali ò R, Rongala U B, Camboni D, Milazzo M, Stefanini C, de Petris G, and Oddo C M 2014 Review: Piezoelectric energy harvesting solutions Sensors,14(3), 4755-4790.

[7] Meitzler A, Tiersten H F, Warner A W, Berlincourt D, Couqin G A, and Welsh III F S 1987 IEEE standard on piezoelectricity, IEEE Ultrasonics, Ultrason. Ferro-electr. Freq. Control Society 43(5), 717-772.

[8] Holland R 1967 Representation of dielectric, elastic, and piezoelectric losses by complex coefficients, IEEE Transaction on Sonics and Ultrasonics 14 (1) 18-20.

[9] Bloomfield PE, Lo W-J and Lewin PA 2000 Determination of thickness acoustical properties of polymers utilized in the construction of PVDF ultrasonic transducers—Sonic and electric impedance measurements of thickness acoustical properties of PVDF and PVDF/TrFE IEEE Trans. Ultrason., Ferroelect.,Freq. Contr. 47: 1397–1405.

[10] Bloomfield P E 2002 Multilayer transducer transfer matrix formalism IEEE Ultrasonics, Ultrason. Ferro-electr. Freq. Control Society 49(9): 1300-1311.

[11] Zhang YK, Lu T-F, and Peng YX 2015 Three-Port Equivalent Circuit of Multi-layer Piezoelectric Stack Sensors & Actuators: A. Physical DOI: 10.1016/j.sna.2015.10.033

[12] Arevalo A and Foulds I G 2013 Parametric Study of Polyimide-Lead Zirconate Titanate Thin Film Cantilevers for Transducer Applications In 2013 COMSOL Conference, Rotterdam, Holland.

[13] ANSYS 2014 Piezo Extension_R150_v8 from https://support.ansys.com/portal/site/AnsysCustomerPortal.

# Chapter 8

# SIMPLIFIED EQUIVAELNT FINITE

# ELEMENT MODELS OF D31-MODE

# LPT

# CHAPTER 8

# SIMPLFIED EQUIVALENT FINITE ELEMENT MODELS OF D31-MODE LPT

This chapter is based on the following submitted paper:

Zhang, Y., Lu, T. F., & Al-Sarawi, S. (2016). Simple Equivalent Finite Element Models of D31-Mode Multi-Layer Piezoelectric Actuator. Submitted to *Journal of Intelligent Material Systems and Structures*

*Contributions of this chapter*: Inspired by simple equivalent finite element models of stack-type d33-mode LPT proposed in Chapter 6, two simple equivalent finite element models of d31-mode LPT are proposed. The proposed finite element models consider multi-layer d31-mode LPT as equivalent homogenous bulk which could simply meshed with pure-solid and consider the inverse piezoelectric effect of the applied voltage with equivalent external forces. Based on the IEEE standard 3D constitutive relations of piezoelectricity, the rationale behind the proposed equivalent models of d31-mode LPT together with the limitation and scope, which are different in nature to d33-mode LPT, are presented. Also, the related equivalent forces and other equivalent parameters are derived in terms of the standard 3D piezoelectric coefficients. Compared with direct finite element modelling of stack-type d31-mode LPT by using an electro-mechanical coupled and multi-layer model, the proposed equivalent modelling method could greatly facilitate the modelling processes and reduce the computational effort with little compromise of effectiveness. The proposed models can be applied to both single-type and stack-type. The effectiveness of the proposed simple equivalent finite element models has been validated by direct finite element modelling of d31-mode LPT in commercial software ANSYS.

# Statement of Authorship

| Title of Paper | Simple Equivalent Finite Element Models of D31-Mode Multi-Layer Piezoelectric Actuator |
|---|---|
| Publication Status | ☐ Published ☐ Accepted for Publication<br>☑ Submitted for Publication ☐ Unpublished and Unsubmitted work written in manuscript style |
| Publication Details | Zhang, Y., Lu, T. F., & Al-Sarawi, S. (2016). Simple Equivalent Finite Element Models of D31-Mode Multi-Layer Piezoelectric Actuator. Submitted to *Journal of Intelligent Material Systems and Structures* |

## Principal Author

| Name of Principal Author (Candidate) | Mr. Yangkun Zhang |
|---|---|
| Contribution to the Paper | Developed theory, performed simulations, analyzed data and wrote the manuscript |
| Overall percentage (%) | 80% |
| Certification: | This paper reports on original research I conducted during the period of my Higher Degree by Research candidature and is not subject to any obligations or contractual agreements with a third party that would constrain its inclusion in this thesis. I am the primary author of this paper. |
| Signature | Date  16 / 02 / 2016 |

## Co-Author Contributions

By signing the Statement of Authorship, each author certifies that:

i.   the candidate's stated contribution to the publication is accurate (as detailed above);

ii.  permission is granted for the candidate in include the publication in the thesis; and

iii. the sum of all co-author contributions is equal to 100% less the candidate's stated contribution.

| Name of Co-Author | Dr. Tien-Fu Lu |
|---|---|
| Contribution to the Paper | Supervised research, reviewed manucript |
| Signature | Date  16/02/16 |

| Name of Co-Author | Dr. SAID Al-SARAWI |
|---|---|
| Contribution to the Paper | Supervised research, reviewed manucript |

| Signature | | Date | |
|-----------|--|------|--|

114

# Simple Equivalent Finite Element Models of D31-Mode Multi-Layer Piezoelectric Actuator

YANGKUN ZHANG [1*], TIEN-FU LU [1] AND SAID Al-SARAWI [2]

[1]*School of Mechanical Engineering, University of Adelaide, 5005, Australia*
[2]*School of Electronic and Electrical Engineering, University of Adelaide, 5005, Australia*

_____
*Author to whom correspondence should be addressed. E-mail: yangkun.zhang@adelaide.edu.au

**ABSTRACT:** D31-mode multi-layer piezoelectric actuators (MPA) are often used as contracting actuators. Inspired by simple equivalent finite element models of d33-mode MPA, two simple equivalent finite element models of d31-mode MPA, are proposed and developed in this paper. The proposed finite element models consider multi-layer d31-mode MPA as an equivalent homogenous bulk which could simply meshed with pure-solid and consider the inverse piezoelectric effect of the applied voltage with equivalent external forces. Based on the IEEE standard 3D constitutive relations of piezoelectricity, the rationale behind the proposed equivalent models of d31-mode MPA together with the limitation and scope, which are different in nature to d33-mode MPA, are presented. Also, the related equivalent forces and other equivalent parameters are derived in terms of the standard 3D piezoelectric coefficients. Compared with direct finite element modelling of d31-mode by using an electro-mechanical coupled and multi-layer model, the proposed equivalent modelling method could greatly facilitate the modelling processes and reduce the computational effort with little compromise of effectiveness for modelling d31-mode MPA. For validation, a case study is carried out to compare the proposed equivalent modelling method with direct finite element modelling by using an electro-mechanical coupled and multi-layer model of d31-mode MPA. Simulations are implemented in ANSYS and simulation results validate the effectiveness and also show the limitation of the proposed equivalent models.

**Keywords:** D31-mode, longitudinal, piezoelectric, actuator, 3D, equivalent, finite element model

## 1. Introduction

D31-mode multi-layer piezoelectric actuators (d31-mode MPA) are often used as contracting actuators characteristic of a high-resolution in displacement and a compact size. With reference to the left part of Figure 1, when a voltage is applied to a piezo cuboid in the direction opposite to its pre-polarized direction, it will induce a contraction in the direction orthogonal to the polarized direction (known as d31-mode). As the deformation for a single block is too small to be used,

A multi-layer stack configuration shown in the right part of Figure 1 (i.e. d31-mode MPA) is often used to enable a large deformation with a low voltage operation in a compact size. Compared with d33-mode MPA, although d31-mode MPA produces a smaller deformation output for an equivalent size and voltage input as the d33 coefficient is around two times larger than the d31 coefficient (Arevalo and Foulds 2013), the configuration of d31-mode MPA is more robust to tension, especially when involving negative strain, thus making it widely used as a contracting actuator (Uchino and Giniewicz 2003; Xu et al 2011; Tolliver et al 2013).
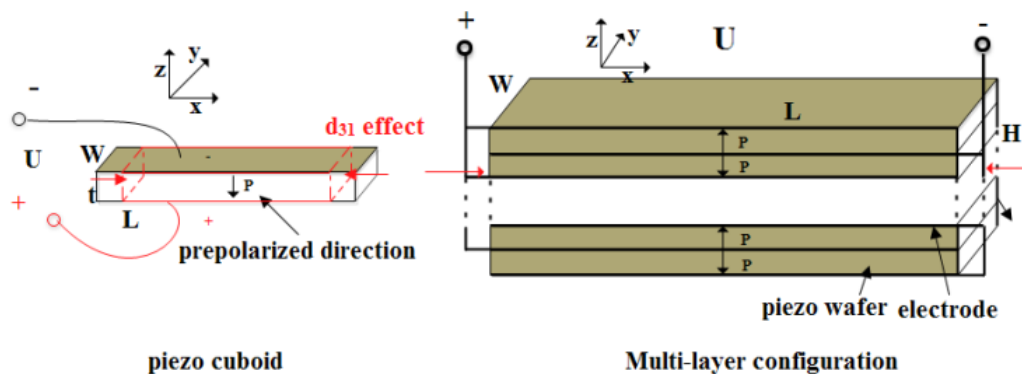


**Figure 1 Schematic of d31-mode MPA**

For the d31-mode MPA based applications, modelling electro-mechanical coupled behaviours of d31-mode MPA, which can be used to predict their performance, plays a vital role in their design, manufacture and optimization. A finite element model is often applied for computation and analysis, when d31-mode MPA is used in a complex structure (Xu et al 2011; Tolliver et al 2013). For direct finite element modelling of d31-mode MPA( Tolliver et al 2013), the stacked configuration makes model defining

process cumbersome and the electro-mechanical coupled elements of piezo material consumes large computational efforts, thus inducing a long model solving time.

In another paper of authors (Zhang and Lu 2016), simple equivalent finite element models of d33-mode MPA, which are based on the uniform-electric-field approximation, were presented. The presented finite element models consider d33-mode MPA as an equivalent homogenous bulk which could be simply meshed with pure-solid elements and consider the inverse piezoelectric effect of the applied voltage with equivalent external forces, which greatly facilitates the modelling processes and greatly cuts down the computational effort. Inspired by simple equivalent finite element models of d33-mode MPA, this paper develops simple equivalent finite element models for d31-mode MPA, which could facilitate the modelling processes and reduce the computational effort with little compromise of effectiveness for modelling d31-mode MPA.

## 2. Model Formulation

Based on the IEEE standards on piezoelectricity (Meitzler, Tiersten et al 1988), the 3-D piezoelectric constitutive equations of piezoelectricity can be shown below:

$$
\begin{Bmatrix} T_1 \\ T_2 \\ T_3 \\ T_4 \\ T_5 \\ T_6 \end{Bmatrix} = \begin{bmatrix} c_{11}^E & c_{12}^E & c_{13}^E & 0 & 0 & 0 \\ c_{12}^E & c_{22}^E & c_{23}^E & 0 & 0 & 0 \\ c_{13}^E & c_{23}^E & c_{33}^E & 0 & 0 & 0 \\ 0 & 0 & 0 & c_{44}^E & 0 & 0 \\ 0 & 0 & 0 & 0 & c_{55}^E & 0 \\ 0 & 0 & 0 & 0 & 0 & c_{66}^E \end{bmatrix} \begin{Bmatrix} S_1 \\ S_2 \\ S_3 \\ S_4 \\ S_5 \\ S_6 \end{Bmatrix} + \begin{bmatrix} 0 & 0 & e_{31} \\ 0 & 0 & e_{32} \\ 0 & 0 & e_{33} \\ 0 & e_{24} & 0 \\ e_{15} & 0 & 0 \\ 0 & 0 & 0 \end{bmatrix} \begin{Bmatrix} E_1 \\ E_2 \\ E_3 \end{Bmatrix}, \qquad (1.a)
$$

$$
\begin{Bmatrix} D_1 \\ D_2 \\ D_3 \end{Bmatrix} = \begin{bmatrix} 0 & 0 & 0 & 0 & e_{15} & 0 \\ 0 & 0 & 0 & e_{24} & 0 & 0 \\ e_{31} & e_{32} & e_{33} & 0 & 0 & 0 \end{bmatrix} \begin{Bmatrix} S_1 \\ S_2 \\ S_3 \\ S_4 \\ S_5 \\ S_6 \end{Bmatrix} + \begin{bmatrix} \varepsilon_{11}^s & 0 & 0 \\ 0 & \varepsilon_{22}^s & 0 \\ 0 & 0 & \varepsilon_{33}^s \end{bmatrix} \begin{Bmatrix} E_1 \\ E_2 \\ E_3 \end{Bmatrix}, \qquad (1.b)
$$

where $S_q, T_p, E_k$, and $D_i$ ($q, p = 1, 2, 3, 4, 5, 6$ and $k, i = 1, 2, 3$) are respectively the components of strain tensor $S$, stress tensor $T$, electric field tensor $E$ and electric displacement tensor $D$. $c_{pq}^E$, $e_{kp}$, $\varepsilon_{ik}^S$ are respectively the components of elastic stiffness

matrix $c^E$ measured at constant electric fields, piezoelectric stress matrix $e$ measured at constant strains and dielectric coefficients $\varepsilon^S$ measured at constant strains. The subscript notation follows the IEEE standards (Meitzler, Tiersten et al. 1988) and the measurements of these coefficients are also standardized there.
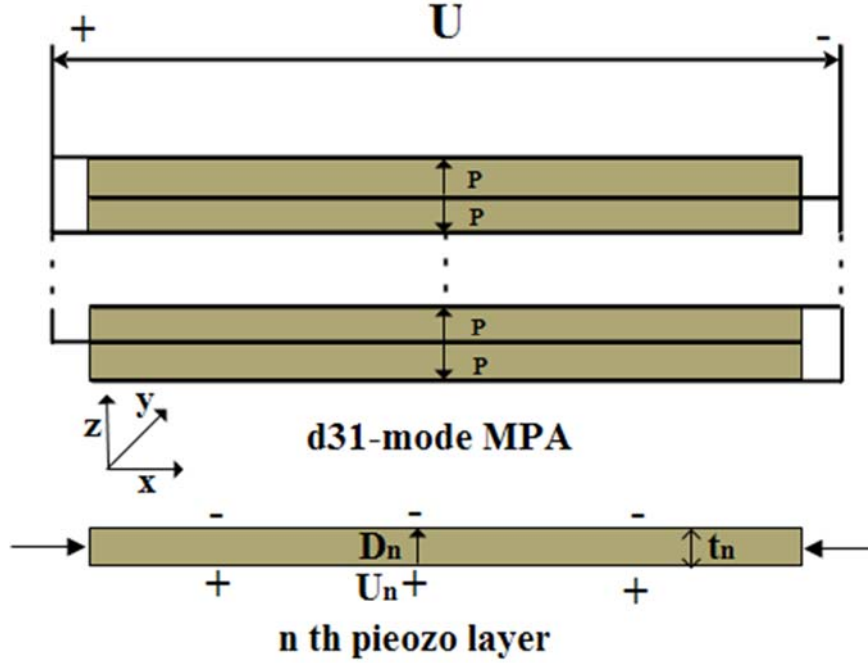


**Figure 2 The nth piezo layer of d31-mode MPA**

With reference to Figure 2, consider the $n$ th piezo layer at certain position $z_n$ of d31-mode MPA with thickness $t_n$ (where $n = 1, 2, 3 \ldots k$ and $k$ is the number of piezo layers stacked in d31-mode MPA).

The third row of Equation (1.b) gives:

$$D_3 = e_{31} S_1 + e_{32} S_2 + e_{33} S_3. \tag{2}$$

The charge balance in the $z$ direction gives:

$$\frac{\partial D_3}{\partial z} = 0. \tag{3}$$

Substituting Equation (2) into Equation (3) gives:

$$e_{31} \frac{\partial^2 u(x,t)}{\partial x \partial z} + e_{32} \frac{\partial^2 u(y,t)}{\partial y \partial z} + e_{33} \frac{\partial^2 u(z,t)}{\partial^2 z} - \varepsilon_{33}^s \frac{\partial^2 \varphi(z,t)}{\partial^2 z} = 0. \tag{4}$$

As $\dfrac{\partial^2 u(x,t)}{\partial x \partial z} = 0$ and $\dfrac{\partial^2 u(y,t)}{\partial y \partial z} = 0$, Equation (4) can becomes:

$$\frac{\partial^2 \varphi(z,t)}{\partial^2 z} = \frac{e_{33}}{\varepsilon_{33}^s} \frac{\partial^2 u(z,t)}{\partial^2 z}, \tag{5}$$

Integrating Equation (5) with regard to $z$ yields:

$$E_3 = -\frac{e_{33}}{\varepsilon_{33}^s} S_3 + B_1, \tag{6}$$

where $B_1$ is an integration constant.

As d31-mode MPA is designed for longitudinal deformation and vibration in $x$ direction (denoted by subscript '1'), the excitation frequency band of interest is well below the lowest resonant frequency in lateral $z$ direction (denoted by subscript '3'). So, the distribution of the deformation $u(z,t)$ in lateral $z$ direction can be seen to be uniform along lateral $z$ direction (i.e. $S_3$ can be seen as a constant). Then, based on Equation (6), $E_3 = -\dfrac{\partial \varphi(z,t)}{\partial z}$ can be seen as a constant, which gives:

$$E_3 = -\frac{\partial \varphi(z)}{\partial z} = -\frac{\varphi(z_p + t_n) - \varphi(z_p)}{t_n} = \frac{U_n(t)}{t_n}. \tag{7}$$

From the analysis justified above, it can be seen that the uniform-electric-field-approximation is valid under the condition that the frequency band of interest is well below the lowest resonance frequency in $z$ direction. As d31-mode MPA is designed for longitudinal deformation and vibration in $x$ direction and the excitation frequency band of interest is well below the lowest resonant frequency in lateral $z$ direction, the uniform-electric-field-approximation is perfectly all right for modelling d31-mode MPA. Note, the rationale behind the uniform-electric-field approximation together with the scope and limitation for effectively modelling d31-mode MPA is different in nature to that for effectively modelling d33-mode MPA(Zhang and Lu 2016).

With reference to Figure 2, the electrical configuration of d31-mode MPA gives $E_1 = E_2 = 0$.

By substituting $E_1, E_2$ and $E_3$ into Equation (1.a), the constitutive Equation for the $n$ the piezo layer of d31-mode MPA can be derived shown in Equation (8).

$$
\begin{Bmatrix} T_1 \\ T_2 \\ T_3 \\ T_4 \\ T_5 \\ T_6 \end{Bmatrix} = \begin{bmatrix} c_{11}^E & c_{12}^E & c_{13}^E & 0 & 0 & 0 \\ c_{12}^E & c_{22}^E & c_{23}^E & 0 & 0 & 0 \\ c_{13}^E & c_{23}^E & c_{33}^E & 0 & 0 & 0 \\ 0 & 0 & 0 & c_{44}^E & 0 & 0 \\ 0 & 0 & 0 & 0 & c_{55}^E & 0 \\ 0 & 0 & 0 & 0 & 0 & c_{66}^E \end{bmatrix} \begin{Bmatrix} S_1 \\ S_2 \\ S_3 \\ S_4 \\ S_5 \\ S_6 \end{Bmatrix} + \begin{bmatrix} e_{31} \dfrac{U_n}{t_n} \\ e_{32} \dfrac{U_n}{t_n} \\ e_{33} \dfrac{U_n}{t_n} \\ 0 \\ 0 \\ 0 \end{bmatrix},
\tag{8}
$$

Assuming negligible thickness of electrode layers and considering that each piezo layer in MPA has the same material properties, thickness ($t_n = t_p$) and the same applied voltage ($U_n(t) = U(t)$) due to the electrically parallel connected structure, it is effective to consider Equation (8) as the constitutive equation for the whole d31-mode MPA, which can be written in the form:

$$
\begin{Bmatrix} T_1 \\ T_2 \\ T_3 \\ T_4 \\ T_5 \\ T_6 \end{Bmatrix} = \begin{bmatrix} c_{11}^E & c_{12}^E & c_{13}^E & 0 & 0 & 0 \\ c_{12}^E & c_{22}^E & c_{23}^E & 0 & 0 & 0 \\ c_{13}^E & c_{23}^E & c_{33}^E & 0 & 0 & 0 \\ 0 & 0 & 0 & c_{44}^E & 0 & 0 \\ 0 & 0 & 0 & 0 & c_{55}^E & 0 \\ 0 & 0 & 0 & 0 & 0 & c_{66}^E \end{bmatrix} \begin{Bmatrix} S_1 \\ S_2 \\ S_3 \\ S_4 \\ S_5 \\ S_6 \end{Bmatrix} + \begin{bmatrix} p_1 \\ p_2 \\ p_3 \\ 0 \\ 0 \\ 0 \end{bmatrix},
\tag{9}
$$

Where $p_1 = e_{31} \dfrac{U(t)}{t_p}$ , $p_2 = e_{32} \dfrac{U(t)}{t_p}$ and $p_3 = e_{33} \dfrac{U(t)}{t_p}$ .

Therefore, based on Equation (9), the electro-mechanical coupled and multi-layer finite element model of d31-mode MPA can be simply considered as an equivalent homogeneous bulk meshed with pure-solid elements of elastic stiffness matrix $c^E$ and the effect of voltage can be equivalent to external forces $F_i = p_i \cdot A_i = e_{3i} \dfrac{U(t)}{t_p} A_i$ ($i = 1, 2, 3$ which denote x, y and z axis respectively), shown in Figure 3. This is the proposed model 1.

The proposed model 1 can be further simplified into the proposed model 2 shown as follows.

Equation (9) can be transformed into the following form:

$$
\begin{Bmatrix} S_1 \\ S_2 \\ S_3 \\ S_4 \\ S_5 \\ S_6 \end{Bmatrix} = \begin{bmatrix} s_{11}^E & s_{12}^E & s_{13}^E & 0 & 0 & 0 \\ s_{12}^E & s_{22}^E & s_{23}^E & 0 & 0 & 0 \\ s_{13}^E & s_{23}^E & s_{33}^E & 0 & 0 & 0 \\ 0 & 0 & 0 & s_{44}^E & 0 & 0 \\ 0 & 0 & 0 & 0 & s_{55}^E & 0 \\ 0 & 0 & 0 & 0 & 0 & s_{66}^E \end{bmatrix} \begin{Bmatrix} T_1 + p_1 \\ T_2 + p_2 \\ T_3 + p_3 \\ T_4 \\ T_5 \\ T_6 \end{Bmatrix},
\tag{10}
$$

where the compliance matrix $s^E$ is the inverse matrix of matrix $c^E$ (i.e. $s^E = (c^E)^{-1}$ ).

For applications of d31-mode MPA, the deformation along the $x$ axis is of interest and the deformation along $y$ axis and $z$ axis is of little importance. Based on the equivalent deformation on $x$ axis, $p_1$, $p_2$ and $p_3$ can be further equivalent to $p_1^{'}$ ( $p_2^{'} = p_3^{'} = 0$ )by using the first row of Equation (10):

$$
s_{11}^E p_1 + s_{12}^E p_2 + s_{13}^E p_3 = s_{11}^E p_1^{'}
\tag{11}
$$

Solving Equation (11) gives $p_1^{'} = \dfrac{e_{31} s_{11}^E + e_{32} s_{12}^E + e_{33} s_{13}^E}{s_{11}^E t_p} \cdot U(t)$ ( $p_2^{'} = p_3^{'} = 0$ ).

So, the effect of voltage can be also equivalent to external forces $F_1^{'} = p_1^{'} \cdot A_1 = \dfrac{e_{31} s_{11}^E + e_{32} s_{12}^E + e_{33} s_{13}^E}{s_{11}^E t_p} A_1 \cdot U(t)$ shown in Figure 4. This is the proposed model 2.

Note, the two proposed equivalent finite element models of d31-mode MPA are both based on the uniform-electric-field approximation. So, the proposed two models are valid also under the condition that the frequency band of interest is well below the lowest resonance frequency in $z$ direction. As d31-mode MPA is designed for longitudinal deformation and vibration (i.e. $x$ direction) and the excitation frequency band of interest is well below the lowest resonant frequency in lateral $z$ direction, the proposed two equivalent finite element models are perfectly all right for modelling d31-mode MPA. Besides, with a larger aspect ratio, more longitudinal vibration modes can be free of lateral effects and thus can be captured by the proposed models.
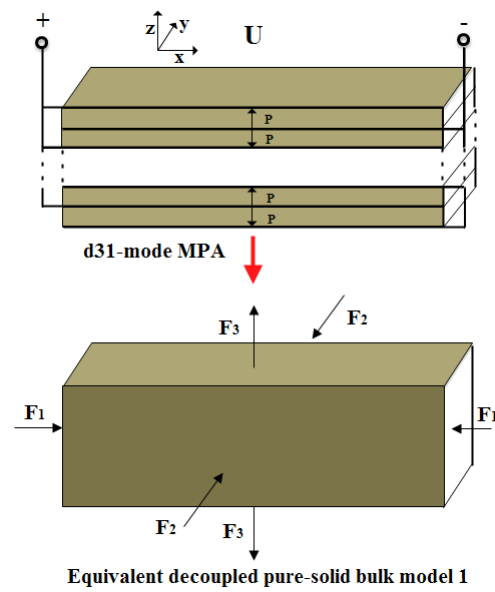
**Figure 3 Equivalent decoupled pure-sold bulk model 1 of d31-mode MPA**
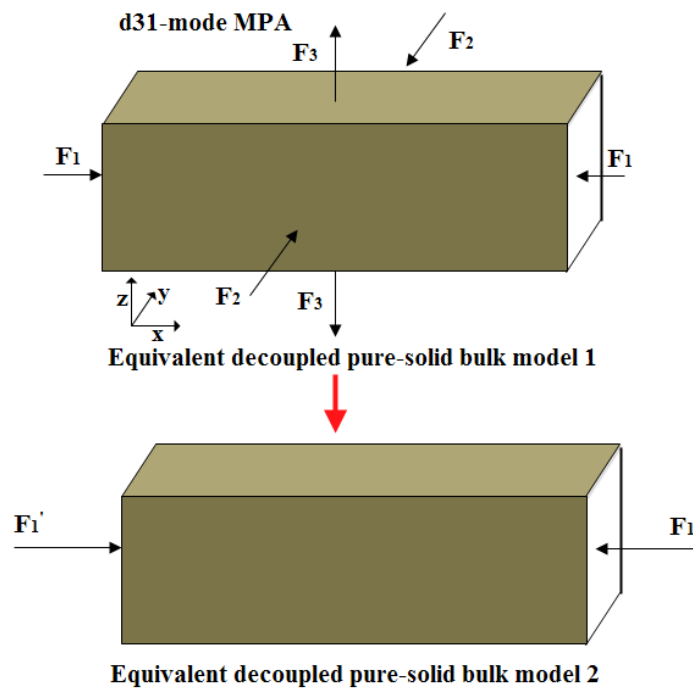


**Figure 4 Equivalent decoupled pure-sold bulk model 2 of d31-mode MPA**

## 3. Validation and Discussion

For validation and discussion, a case study is carried out in this section. Frequency responses of free-end displacement for a free-free vibration of d31-mode MPA are

simulated for comparisons between electro-mechanical coupled and multi-layer finite element model and the proposed equivalent models.

With reference to the right part of Figure 1, a d31-mode MPA stacked by 5 piezo layer ($k = 5$, $L = 0.02m$, $W = 0.002m$, $H = 0.002m$ and $t_p = \dfrac{H}{k} = 0.0004m$) and a d31-mode MPA with 1 piezo layer ($k = 1$, $L = 0.02m$, $W = 0.002m$, $H = 0.002m$ and $t_p = \dfrac{H}{1} = 0.002m$) are respectively investigated. The materials properties of MPS are with reference to PZT-5H (Arevalo and Foulds 2013).

The related finite element models are implemented on the commercial software ANSYS. To obtain the frequency response, the 'Harmonic Response' module in ANSYS is performed. To implement the electro-mechanical coupled and multi-layer finite element model, the extension package 'Piezo Extension_R150_v8'(ANSYS 2015) is used to allow analysing electro-mechanical coupled behaviours. A multi-layer configuration of d31-mode MPA is build and then meshed with electro-mechanical coupled elements and actuated with the voltage applied at two ends of each piezo layer. The meshed electro-mechanical coupled and multi-layer finite element model of d31-mode MPA stacked by 5 piezo layers is shown in Figure 5. To implement the proposed two equivalent models, a bulk model is simply built and simply meshed with pure-solid elements shown in Figure 6 and then actuated with equivalent forces as shown in Figure 3 and Figure 4.
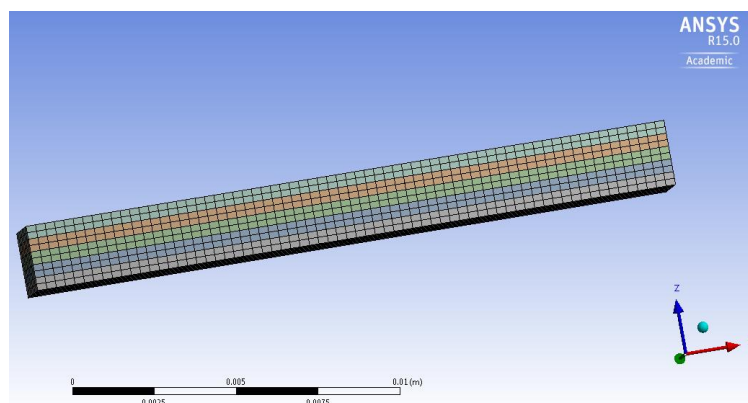


**Figure 5 Meshed electro-mechanical coupled and multi-layer model of d31-mode MPA (k=5)**
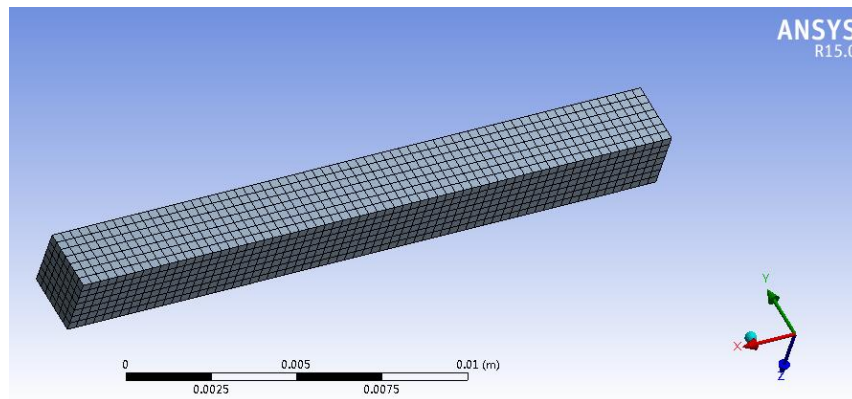
**Figure 6 Meshed equivalent pure-solid bulk model of d31-mode MPA**

The simulation results for the one stacked by 5 piezo layer and the one with 1 piezo layer are respectively shown in Figure 7 and Figure 8. The results simulated by the proposed model 2 almost overlap with those simulated by the model 1 for the first four resonant modes, which validates their equivalence in modelling along the x axis. The deviations between the proposed two models for modelling higher frequency are induced by lateral resonance (deformation along y axis and z axis) for modelling which the proposed model 2 is not equivalent to the proposed model 1. Compared with the electro-mechanical coupled and multi-layer finite element model, both the proposed models show good match until the frequency rises to the fourth resonant mode. The derivation from the fourth resonant mode is expected. As justified before, the proposed two models are valid under the condition that the frequency band of interest is well below the lowest resonance frequency in $z$ direction. The $4^{th}$ resonant frequency, which is approaching to the $1^{st}$ lateral resonance frequency, compromise the effectiveness of the proposed model.

Comparing the results shown in Figure 8 for a d31-mode MPA with 1 piezo layer ($k = 1$, $L = 0.02m$, $W = 0.002m$, $H = 0.002m$ and $t_p = \dfrac{H}{1} = 0.002m$) with the results shown in Figure 9 for a d31-mode MPA with 1 piezo layer ($k = 1$, $L = 0.01m$, $W = 0.002m$, $H = 0.002m$ and $t_p = \dfrac{H}{1} = 0.002m$) validates the justified analysis that, with a larger aspect ratio, more longitudinal vibration modes can be free of lateral effects and thus can be captured by the proposed models.

free-end displacement under 100V excitaiton voltage
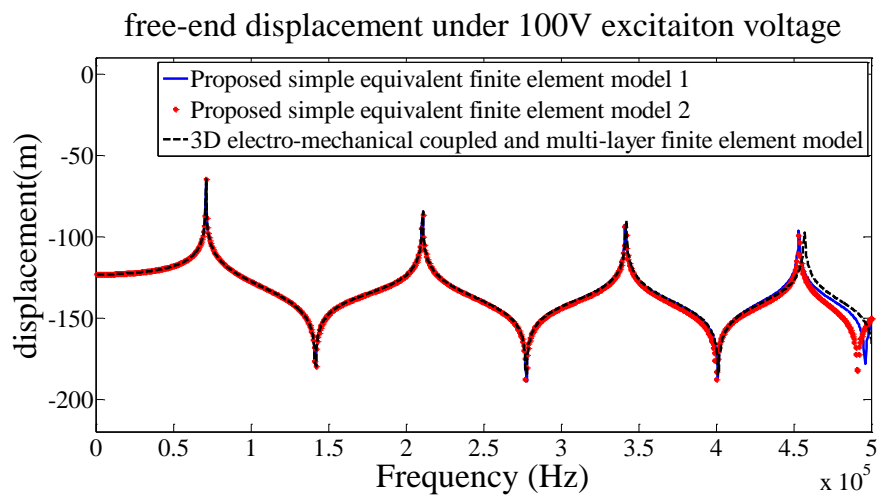


**Figure 7 Simulation results for d31-mode MPA stacked by 5 piezo layers ( $L = 0.02m$ )**
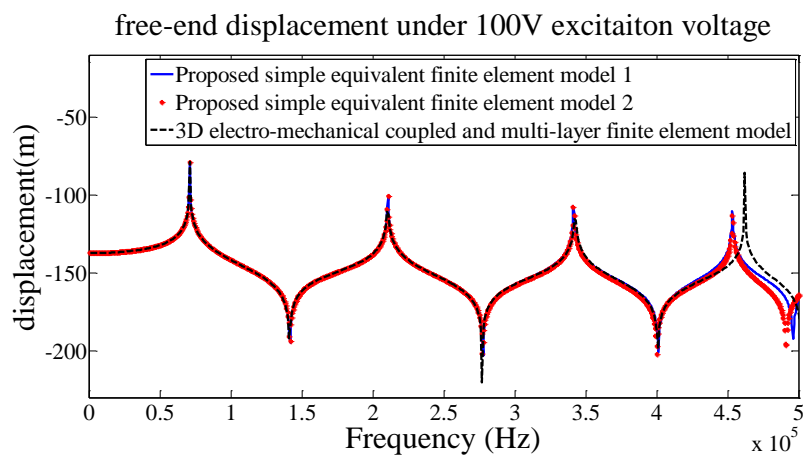
free-end displacement under 100V excitaiton voltage



**Figure 8 Simulation results for d31-mode MPA with 1 piezo layer ( $L = 0.02m$ )**

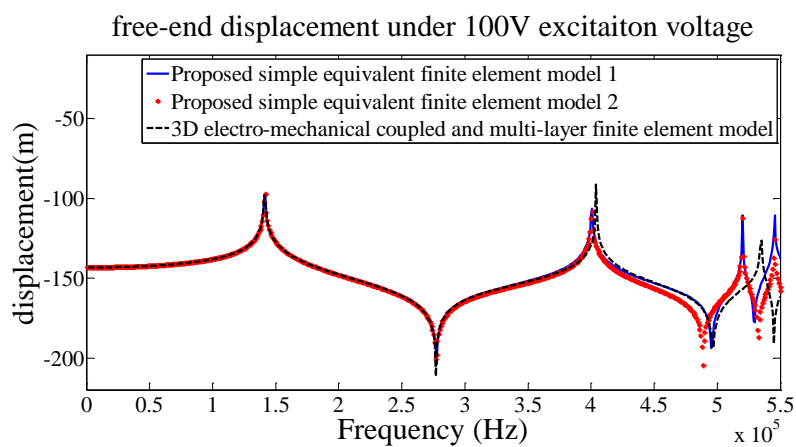free-end displacement under 100V excitaiton voltage



**Figure 9 Simulation results for d31-mode MPA with 1 piezo layer ( $L = 0.01m$ )**

125

## 4. Conclusion

In conclusion, two simple equivalent finite element models of d31-mode MPA, which consider d31-mode MPA as a simple homogenous pure-solid bulk model actuated with equivalent external forces, are proposed. Compared with direct finite element modelling of d31-mode by using an electro-mechanical coupled and multi-layer model, the proposed equivalent modelling method could greatly facilitate the modelling processes and reduce the computational effort with little compromise of effectiveness. Based on the IEEE standard 3D constitutive relations of piezoelectricity, the rationale behind the proposed equivalent models together with the scope and limitation, which is different in nature to d31-mode MPA, are presented. The related equivalent forces and other equivalent parameters are derived in terms of the standard 3D piezoelectric coefficients. The two proposed equivalent finite element models of d31-mode MPA are valid under the condition that the frequency band of interest is well below the lowest resonance frequency in $z$ direction. However, this limitation is of little importance, as d31-mode MPA is designed for longitudinal deformation and vibration (i.e. $x$ direction) and the excitation frequency band of interest is well below the lowest resonant frequency in lateral $z$ direction.

## References

ANSYS (2015) Piezo extension_R150_v8. Available at: https://support.ansys.com/portal/site/AnsysCustomerPortal

Arevalo A and Foulds IG (2013) Parametric Study of Polyimide-Lead Zirconate Titanate Thin Film Cantilevers for Transducer Applications. *In 2013 COMSOL Conference, Rotterdam, Holland*.

Meitzler A, Tiersten H, Warner AW, et al. (1988) 176-1987 -IEEE Standard on Piezoelectricity. IEEE Ultrasonics, Ferroelectrics, and Frequency Control Society INSPEC Accession Number: 3237638. DOI:10.1109/IEEESTD.1988.79638

Tolliver L, Xu T-B and Jiang X (2013) Finite element analysis of the piezoelectric stacked-HYBATS transducer. *Smart Materials and Structures*,22(3), 035015.

Uchino K and Giniewicz J (2003) *Micromechatronics* (Boca Raton, FL: Taylor & Francis) Page 383

Xu T-B, Jiang X and Su J (2011) A piezoelectric multilayer-stacked hybrid actuation/transduction system. A*pplied Physics Letters*, 98(24), 243503.

Zhang YK and Lu T-F (2016) Simple equivalent finite element models of d33-mode multi-layer piezoelectric actuator, submitted to *Smart Materials and Structures*, SMS-103187.

# Chapter 9

# CONCLUSIONS AND RECOMMENDATIONS FOR FUTURE WORK

# CHAPTER 9

# CONCLUSIONS AND RECOMMENDATIONS FOR FUTURE WORK

Section 9.1 draws conclusions from the research presented in this thesis, while recommended future work is presented in Section 9.2.

## 9.1 Conclusions

Longitudinal piezoelectric transducers (LPT), which collectively refer to piezoelectric actuators, vibrators, sensors and actuators designed for longitudinal deformations or vibrations, are the most widely used piezoelectric devices. Compared with other types of piezoelectric transducers such as bending and shear piezoelectric transducers, LPT provides a larger stiffness, a larger operation bandwidth, more simple and compact structure and more direct energy conversion.

LPT model, which can be used to predict the behavior or performance in time/frequency domain, plays a vital role in the design and optimization of these LPT-based applications. However, existing models which can be used for dynamic behavior prediction, are based on the complex electro-mechanical coupled fundamentals of piezoelectricity, which involves a complex position-varying electric field. Solving these models for design and optimization of LPT-based applications is very computationally inefficient.

LPT can, in principle, be divided into d33-mode LPT and d31-mode LPT. After extensive investigations of literature, it is found that the complex fundamentals for either d33-mode LPT or d31-mode LPT could be greatly simplified by applying the uniform-electric-field approximation. The uniform-electric-field approximation is widely made for static case of d33-mode LPT and d31-mode LPT in literature. However, whether this approximation is applicable to dynamic cases, what is the rationale behind the approximation for modelling d33-mode LPT and d31-mode LPT, what is the scope and limitations of the approximation, and how this approximation could simplify and facilitate the analysis and calculation of d33-mode LPT and d31-mode LPT, have not been well explored in literature. Therefore, the aim of this research is to study the

uniform-electric-field approximation in simplifying the analysis, modelling and calculations of LPT for facilitating design and optimization of the LPT-based applications.

In this thesis work, the rationale behind the uniform-electric-field approximation for modelling d33-mode LPT together with its scope and limitations is first investigated and presented. It is found that, for d33-mode LPT, when the thickness of a piezo layer in d33-mode LPT is well less than quarter wavelength of a longitudinal vibration mode, the uniform-electric-field approximation can mathematically prove effective. Therefore, this condition limits the frequency range of the approximation from DC to certain longitudinal vibration mode whose corresponding quarter wavelengths are far larger than the thickness of piezo layer. However, as the thin piezo layer in d33-mode LPT is often used in a stack configuration or joined with other propagating medium in the propagation direction, the longitudinal propagation length of d33-mode LPT is often far larger than the thickness of a piezo layer, thus resulting in a relatively large quarter wavelength and enabling a sufficient effective frequency range for applications. Therefore, the limitation of the approximation is often of minor importance for modelling d33-mode LPT.

Then, based on the approximation, simplified fundamentals of both simple-layer-type and stack-type d33-mode LPT are formulated. It is interestingly found that, by applying the uniform-electric-field-approximation, the multi-layer stack configuration of stack-type d33-mode LPT can be effectively modeled as a whole. It greatly simplifies and facilitates the modelling of the stack-type d33-mode LPT, which could provide very simple analytical solutions.

To facilitate the modelling of free and loaded vibration of d33-mode LPT in a straightforward way, the simplified fundamentals of d33-mode LPT is wrapped into a simple three-port equivalent circuit. Compared with existing equivalent circuits, the proposed circuit of d33-mode LPT has a simpler structure and can be extended to any electrical and mechanical condition. Besides, as the proposed circuit elements are explicitly and exactly derived in terms of material and dimension information rather than determined from measured information, the proposed circuit model allows one to predict behaviors with material properties and structural dimension prior to experiments.

In many LPT-based applications, LPT are joined with other layers, such as backing layers and propagating layers. For the calculations and analysis of a multilayer structure, a transfer matrix method is always used. Therefore, to further facilitate the calculation when d33-mode LPT is joined with other layers, the simplified fundamentals of d33-mode LPT is wrapped into a transfer matrix form. For modelling stack-type d33-mode LPT, compared with using the transfer matrix proposed in literature, which is subjected to individual piezo layer in stack-type d33-mode LPT, the proposed simplified transfer matrix, which considers the whole stack-type d33-mode LPT to be an equivalent homogenous bulk, contributes to a much simpler form of analytical solution and greatly cut down the computational effort. Note, although the proposed transfer matrix is aimed at stack-type, it can be also applied to single-type LPT simply by letting the number of piezo layer equal 1. Even for modelling individual piezo layer, the proposed transfer matrix based on the simplified fundamentals is simpler and more computationally efficient than the transfer matrix formulated in literature on the basis of the complex fundamentals.

When LPT are used in a complex structure, a finite element model is widely applied for computation and analysis. Based on the uniform-electric-field-approximation, two simple equivalent finite element models of d33-mode LPT are proposed and developed. The proposed finite element models consider multi-layer d33-mode LPT as equivalent homogenous bulk which could simply meshed with pure-solid and consider the inverse piezoelectric effect of the applied voltage with equivalent external forces. Compared with direct finite element modeling of stack-type d33-mode LPT by using an electro-mechanical coupled and multi-layer model, the proposed finite element models greatly facilitate the modelling processes and cut down the computational effort. Based on the IEEE standard 3D constitutive relations of piezoelectricity, the rationale behind the proposed equivalent models together with the scope and limitation are presented. Also, the related equivalent forces and other equivalent parameters are derived in terms of the standard 3D piezoelectric coefficients.

After exploring the effectiveness of the uniform-electric-field approximation in modeling d33-mode LPT, the rationale behind the uniform-electric-field approximation for d31-mode together with its scope and limitations is investigated. Differently to d33-mdoe LPT, the voltage is excited in lateral direction for d31-mode. It is found that, for

d31-mode LPT, the electric field is coupled with its normal strain in the lateral direction. So, the electric field can be approximated to be uniform under the condition that the normal strain in the lateral direction can be approximated to be uniform. The normal strain in the lateral direction can be approximated to be uniform when the excitation frequency is well below (around three time less) than the lowest lateral resonance frequency. As the d31-LPT is designed for longitudinal deformations or vibrations, the frequency band of interest for longitudinal vibration is well below the lowest lateral resonance frequency. Therefore, the uniform-electric-field-approximation is perfectly all right for modelling d31-LPT.

Then, based on the approximation, simplified fundamentals of d31-mode LPT are derived. Besides, a simple equivalent mixing method, which can flexibly consider the electrode layers and adhesive layers, is proposed. Then, a simple 1D equivalent homogenous analytical model of D31-LPT is formulated. Also, inspired by d33-mode, the related the related equivalent circuit and transfer matrix of d31-mode LPT are formulated. The advantages of the equivalent circuit and the transfer matrix form of d31-mode LPT is the same to those of d33-mode LPT.

Based on the uniform-electric-approximation and inspired by d33-mode, two simple equivalent finite element models of d31-mode LPT are proposed and developed. The proposed finite element models consider multi-layer d31-mode LPT as equivalent homogenous bulk which could simply meshed with pure-solid and consider the inverse piezoelectric effect of the applied voltage with equivalent external forces. Based on the IEEE standard 3D constitutive relations of piezoelectricity, the rationale behind the proposed equivalent models of d31-mode LPT together with the limitation and scope, which are different in nature to d33-mode LPT, are presented. Also, the related equivalent forces and other equivalent parameters are derived in terms of the standard 3D piezoelectric coefficients. Compared with direct finite element modelling of stack-type d31-mode LPT by using an electro-mechanical coupled and multi-layer model, the proposed equivalent modelling method could greatly facilitate the modelling processes and reduce the computational effort with little compromise of effectiveness.

The research satisfied the aim of studying the uniform-electric-field approximation in simplifying the analysis, modelling and calculations of LPT to facilitate design and optimization of the LPT-based applications.

## 9.2 Recommendations for future work

It is recommended that further research be undertaken in the following areas:

- Based on the simplified models of LPT developed in this research, explore the non-linear behaviors of LDT (for example, the non-linearity to the frequency shift of the vibration modes).

- Investigate the effectiveness of the uniform-electric-field approximation in other piezoelectric transducers (such as bending mode and shear mode

# Appendix A

**Conference Paper-1**

*Full citation*: Yangkun Zhang and Tien-Fu Lu 2014, 'Investigation on the Uniform-Electrical-Field Assumption for Modeling multi-layer piezoelectric actuators', *8ᵗʰ Asia International conference on Mathematical Modeling and computer simulation*, 23-25 September, Taipei, Taiwan, page 251-254

This paper is to investigate the uniform-electric-field approximation for d33-mode LPT at the early stage of this research.

Zhang, Y. & Lu, T.F. (2014). Investigation on the Uniform Electrical-Field Assumption for Modeling multi-layer piezoelectric actuators.
*8th Asia International conference on Mathematical Modeling and computer simulation*, 23-25 September, Taipei, Taiwan, page 251-254.

# Appendix B

**Conference Paper-2**

*Full citation*: Conference-2 Yangkun Zhang and Tien-Fu Lu 2014, 'A Simple Distributed Parameter Analytical Model of Multi-layer Piezoelectric Actuator', *8th Asia International conference on Mathematical Modeling and computer simulation*, 23-25 September, Taipei, Taiwan, page 247-250

This conference paper is to demonstrate how the uniform-electric-field approximation could simplify and facilitate the modelling of stack-type d33-mode LPT at the early stage of the research.

Zhang, Y. & Lu, T.F. (2014). A Simple Distributed Parameter Analytical Model of Multi-layer Piezoelectric Actuator.
*8th Asia International conference on Mathematical Modeling and computer simulation*, 23-25 September, Taipei, Taiwan, page 247-250.